Enhanced Aqueous Solubility and Photodimerization of Polycyclic Aromatics Mediated by γ-Cyclodextrin Derivatives

Dissertation

zur Erlangung des Grades des
Doktors der Naturwissenschaften
der Naturwissenschaftlich-Technischen-Fakultät III
Chemie, Pharmazie, Bio- und Werkstoffwissenschaften
der Universität des Saarlandes

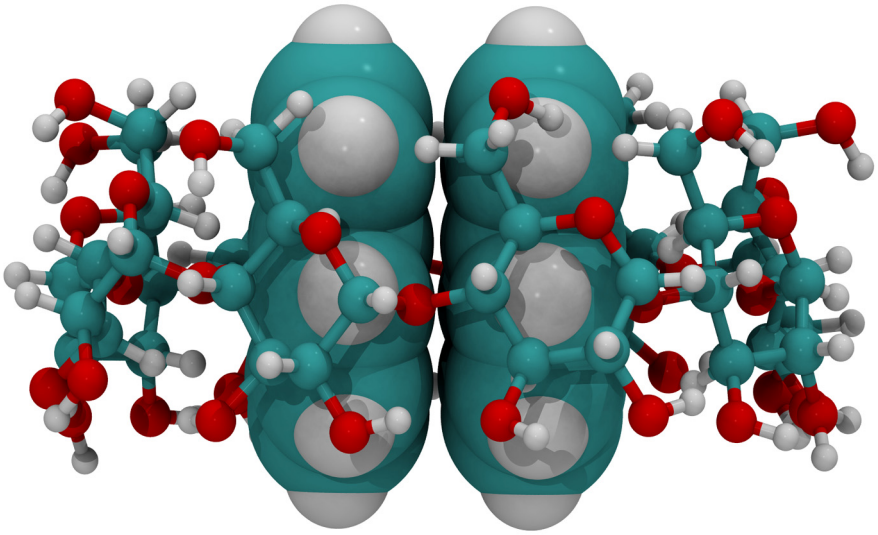

von

Hai Ming Wang

Saarbrücken, 2012

Enhanced Aqueous Solubility and Photodimerization of Polycyclic Aromatics Mediated by *γ*-Cyclodextrin Derivatives

Dissertation
zur Erlangung des Grades des
Doktors der Naturwissenschaften
der Naturwissenschaftlich-Technischen-Fakultät III
Chemie, Pharmazie, Bio- und Werkstoffwissenschaften
der Universität des Saarlandes

von

Hai Ming Wang
Saarbrücken
2012

Tag des Kolloquiums:	20. April 2012
Dekan:	Prof. Dr. Wilhelm F. Maier
Berichterstatter:	Prof. Dr. Gerhard Wenz
	Prof. Dr. Gregor Jung
Vorsitz:	Prof. Dr. Kaspar Hegetschweiler
Akad. Mitarbeiter:	Dr. Yi Dong

Die vorliegende Arbeit wurde in der Zeit von September 2008 bis April 2012 am Institut für Organische Makromolekulare Chemie an der Universität des Saarlandes unter Leitung von Prof. Dr. Gerhard Wenz angefertigt.

Table of Contents

Summary

A series of hydrophilic *γ*-cyclodextrin (CD) thioethers were synthesized and selected as hosts. They were able to solubilize polycyclic aromatic guests in water to much higher extents than native CDs. The results of experimental (phase-solubility method and fluorescence spectroscopy) and theoretical (quantum mechanical and space-filling calculations) investigations confirmed the formation of 1:2 CD-guest complexes in aqueous solution.

True molecular solutions of C_{60} were obtained by dissolving C_{60} in aqueous solutions of *γ*-CD thioethers and confirmed by using dynamic light scattering method. We also succeed to obtain stable aqueous dispersions of C_{60}, by employing the methods based on solvent exchange in presence of *γ*-CD thioethers.

γ-CD thioether acted as a supramolecular catalytic nano-reaction vessel and facilitates the photodimerization of the aromatic guests in aqueous medium. High quantum yields of the photodimerizations in presence of *γ*-CD thioethers were obtained when compared to those of the aromatic guests in host-free solutions. The orientation of two molecules of acenaphthylene when bound to CD led to the selective formation of the *trans* product upon irradiation in quantitative yield for the first time. Excitation of the 1:2 CD–guest inclusion complex of coumarin in water resulted in an increased yield of *syn* head-to-head dimer. Other photoproducts of coumarin which typically produced in the absence of the template were remarkably suppressed by salting out effect.

Zusammenfassung

Eine Reihe von hydrophilen *γ*-Cyclodextrin (CD) Thioethern wurden in der vorliegenden Dissertation synthetisiert. Im Vergleiche zu nativen CDs konnten sie polyzyklische aromatische Gäste in Wasser besser solubilisieren. Durch experimentelle und theoretische Untersuchungen wurde die Bildung von 1:2 CD–Gast Komplexen in wässriger Lösung bestätigt.

Durch Verwendung von *γ*-CD Thioethern wurden wässrige Lösungen von C_{60} erhalten. Dies wurde mittels Dynamischer Lichtstreuung belegt. Mit Methoden auf der Grundlage des Lösungsmittelsaustausches haben wir in gegenwart von *γ*-CD Thioethern beständige wässrige Dispersionen mit C_{60} erfolgreich hergestellt.

γ-CD Thioether werden als supramolekulare katalytische Nano-Reaktionsgefäße angesehen und ermöglichen die Photodimerisierung von aromatischen Gästen im wässrigem Medium. Hohe Quantenausbeuten wurden bei der Photodimerisierung von aromatischen Gästen in gegenwart von *γ*-CD Thioethern erhalten, im Vergleich zu Gast freien Lösungen. Durch Bestrahlung wurde aufgrund der Orientierung von Acenaphthylen im CD zum ersten Mal selektiv in quantitativer Ausbeute das *trans* Produkt erhalten. Durch Anregung von 1:2 CD–Cumarin Wirts–Gast–Verbindungen in Wasser wurde eine höhere Ausbeute von *syn* head-to-head Dimeren erreicht. Weitere Photoprodukte von Cumarin die typischerweise in Abwesenheit von Templaten entstehen konnten bemerkenswerterweise durch Aussalzeffekte unterdrückt werden.

1 Introduction and Literature Review

1.1 Supramolecular Chemistry

Supramolecular chemistry is a concept and term defined by J. M. Lehn in 1970's.[1-3] It is a highly interdisciplinary field of science and covers the chemical, physical, and biological features of the chemical species of greater complexity than molecules themselves, that result from the association of two or more chemical species held together and organized by means of intermolecular (non-covalent) interactions.[4-7]

Early works in supramolecular chemistry focused mainly on the interactions between simple organic host and guest molecules. At present, supramolecular chemistry has become a comprehensive diverse subject including crystal engineering, solid-state inclusion chemistry, molecular recognition and material science.[4,8-11]

Several types of non-covalent interactions are present in supramolecular species in various of strength, depending on distance and directionality such as the Coulombic forces, hydrogen bonding interactions, van der Waals interactions, dipole-dipole interactions, charge transfer, π–π stacking interactions, and so on.[12] Consequently, supermolecules which are held together mainly driven by non-covalent interactions are thermodynamically less stable and dynamically more flexible than "normal" molecules since intermolecular interactions are in general weaker than covalent bonds.

The complicated non-bonding interactions involved in molecular recognition have been the subject of numerous experimental and theoretical studies for many years.[13] The term "molecular recognition" describes structure-based selectivity or intermolecular interactions between two or more molecular

moieties. Molecular recognition, as defined by Lehn,[3] is a process involving binding and selection of a substrate by a receptor molecule. Current thinking attributes the ability of two molecules to recognize one another to the geometric complementarity between the molecules. In other words, a substrate must spatially "fit" in order to bind specifically and interact with the receptor.[14-16]

1.2 Host Molecules

Host molecules are organic molecules which are able to selectively bind organic or ionic molecules (or both) by means of various intermolecular interactions, resulting to the assembly of two or more species.[17-20] The most widely used host molecules are cyclodextrins (CDs), cucurbiturils (CB[*n*]), calixarenes, and crown ethers, *etc*. These hosts which possess macropolycyclic structures are of special interest since they have cavities with appropriate size and shape, and possess numerous branches, bridges, and connections, and consequently allow selective molecular recognition between host and guest molecules.

1.2.1 Cyclodextrins

CDs (Scheme 1.1), produced from starch by the action of the glucosyltransferase enzyme, are chiral, cyclic oligosaccharides consisting of glucose subunits connected through glycosidic α-1,4 bond, forming a structure as a hollow truncate cone with one ring wider than the other.[16,21-22] Those CDs, composed of six, seven, and eight glucose units, are produced in industrial scales and called α-, β-, and γ-CD, respectively. CDs are the most widely used receptors in host–guest inclusion chemistry, with a broad range of utilizations in different applications because of their inclusion properties, for instance, they are used in the food and cosmetics industries and the pharmaceutical sector as stabilizing agents, and for the slow release of drugs.[23-28]

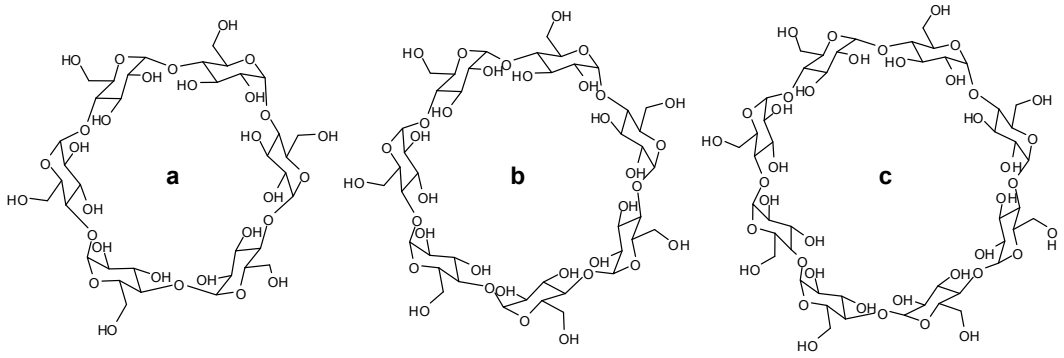

Scheme 1.1 Schematic representations of CDs. (a) α-CD, (b) β-CD, and (c) γ-CD contain 6, 7, and 8 glucopyranoside units, respectively.

CDs contain two kinds of free hydroxyl groups: the primary 6-OH groups are situated around the circumference of the narrower "primary face", and the secondary 2- and 3-OH groups are located on the circumference of the wider "secondary face". The interior of the CD molecule is lined with ether oxygen and hydrogen atoms, resulting in a hydrophobic torus where small organic and inorganic guest molecules can be encapsulated, forming a host–guest inclusion complex in aqueous solutions.[29-34]

Inclusion complexes are molecules comprising two or more molecules, in which the hosts include the guests *via* the non-covalent interaction. CDs are typical host molecules and may include a great variety of molecules with various sizes from small guest like benzene to large molecules like steroids, to form crystalline inclusion complexes. The inclusion of a guest in CD cavity is a process that the less polar guest substituted the water molecules in CDs' cavity. This process involves both entropy and enthalpy changes.[35-36] Various effects are known to play crucial roles in complexation. The major effect is the substitution of energetically unfavorable polar-apolar interactions by more favoured apolar-apolar and polar-polar interactions. CD-ring strain release, van der Waals interactions and hydrogen bonding between the host and guest also contribute to the complexation.

Table 1.1 lists the structural features of CDs, as well as some of the important physical properties of three native CDs.

Table 1.1 Characteristics of α-, β-, and γ-CDs.[15-16]

Properties	α-CD	β-CD	γ-CD
Molar weight	972	1135	1297
Solubility in water[a]	14.5	1.85	23.2
Cavity diameter, Å	4.7 — 5.3	6.0 — 6.5	7.5 — 8.3
Height of torus, Å	7.9 ± 0.1	7.9 ± 0.1	7.9 ± 0.1
Approx volume of cavity, Å^3	174	262	427
Crystal water, wt %	10.2	13.2 — 14.5	8.13 — 17.7

[a] g in100 mL at room temperature

CDs can easily be derivatised by modification of the hydroxyl groups and thus the physical properties of CDs can be altered. There are a large number of CD derivatives in the literature, containing groups such as alkyl, hydroxyalkyl, carboxyalkyl, amino, thiol and tosyl, which often contain ether or ester linkages.[37-39] Modifications on the free hydroxyl groups of native CDs with appropriate function groups[40-42] may not only significantly increase the water solubility of CDs, but also greatly increase the ability of CDs to form inclusion complexes with guest molecules.

The use of CDs as nano-vessels to perform chemical reactions has attracted the interest of chemists since the 1960s.[43] The effects of CDs on the organic reactions are divided mainly into two categories. The first is “enzyme model”. CD and the reactant initially form a CD-reactant reaction intermediate involving a covalent bond which finally leads to the product. The second effect does not involve a covalent bond. The hydrophobic cavity of the CD gives the reactant access to a new reaction environment, *i.e.*, an “extra reaction field” in which the reactivity changes.[44]

There are specific interactions between the CD and the reactant. The microenvironment around the reactant in the CD cavity is different from that in the reaction media. Three distinct microenvironmental effects are expected: microsolvent effects, the protection of unstable intermediates or products, and the solubilization of the reactant. In addition, conformational effects which include

the control of reactant conformation, control of the orientation between reactants, and control of the reactant size can also be expected. A combination of several of these effects are evident for organic reactions.[44]

1.2.2 Other Receptors

Cucurbiturils are a class of host molecules which are able to form inclusion complexes with small guest molecules in water like CDs. The cucurbit[*n*]urils (CB[*n*], see **Scheme 1.2**), a family of pumpkin-like macrocyclic hosts with five, six, seven, eight or more methylene-bridged glycoluril units, feature a well defined hydrophobic nano-cavity similar to those of CDs and polar carbonyl groups surrounding the portals.[45-50] Cucurbiturils are synthesized by an acid-catalyzed condensation reaction of glycoluril and formaldehyde.[31]

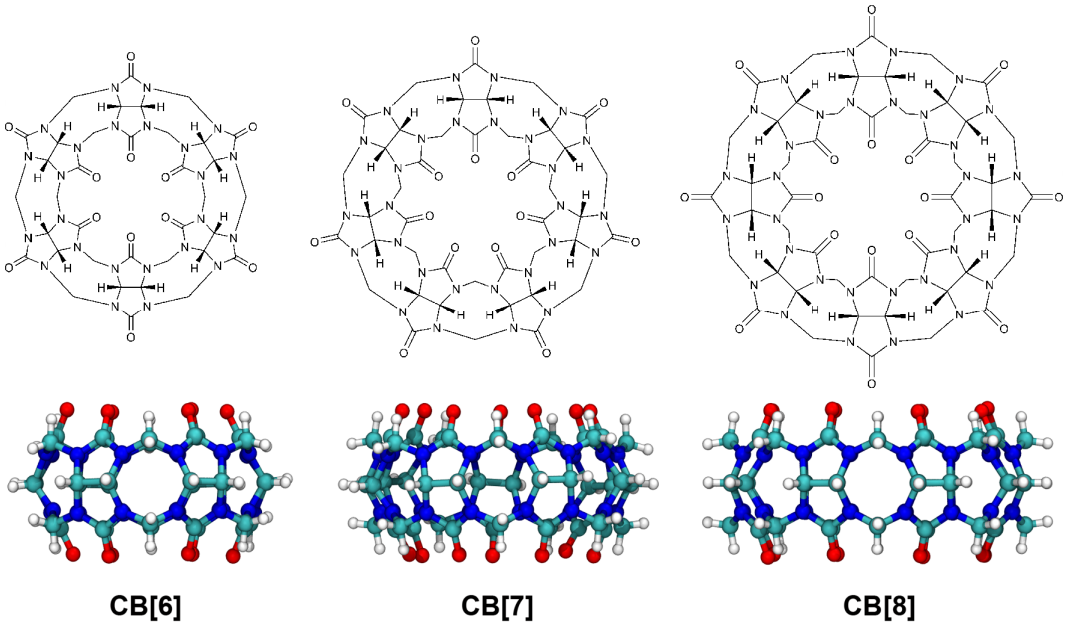

Scheme 1.2 Schematic representation of the structures of CB[6], CB[7] and CB[8], which were constructed with the available crystallographic data.[51-52] The rendering was performed with VMD 1.8.7.[53]

The cavity volume of CBs depends on the number of glycoluril units. On going from CB[6] to CB[8], the mean diameter of the internal cavity increases progressively from 5.8 to 8.8 Å. In terms of cavity size, CB[6], CB[7], and CB[8] are

similar to α-, β-, and γ-CD, respectively.[31,48]

CBs attracted our attention because the varying cavity of CB[*n*] showed remarkable affinity and selectivity towards hydrophobic or/and cationic species via hydrophobic interaction or cation-dipole interaction. CBs have also been shown to be effective in manipulating photochemical reactions.

1.3 Investigation on the Solubility Enhancement

1.3.1 Methods for Solubilizing Poorly Soluble Guests

Solubility enhancement of the poorly soluble organic molecules in aqueous solution has attracted a lot of interest especially for those poorly water-soluble drugs, as it was often necessary to deliver the desired dose in a specified volume of aqueous liquid.[25,54-57] Over the years a variety of solubilization techniques have been developed and widely used including high speed vibration milling, pH adjustment, cosolvent addition, surfactant addition, and host molecules (CDs, CB[*n*], crown ethers and calixarenes) addition.[54,58]

Among these techniques, addition of proper hosts into solvents is highly effective for the solubilization of nonpolar solutes. The nonpolar guest molecules are partially or completely included in the cavity of the supramolecular host, *i.e.*, forming an inclusion complex with acceptable water solubility. Such a host-guest complex has a rigid structure and a definite stoichiometry, usually 1:1 at low guest concentrations in water.

1.3.2 Phase-Solubility Method

The most widely used approach to study the relationship between the increased solubility of substrate (guest) and the increased concentration of ligand (host) in solution is the phase-solubility method, which is described by Higuchi and Connors.[59] A phase-solubility diagram is obtained by plotting the observed concentration of dissolved guest versus the total concentration of

host in solution.

All of the types of the phase solubility diagrams are shown in **Figure 1.1**. According to Higuchi and Connors, they are divided into two main categories, type A and B.[59] Type-A curves, which indicate the formation of soluble inclusion complexes, are obtained when the solubility of the guest increases with increasing host concentration over the entire concentration range. Type-A curves is subdivided into three categories: A_L (linear increases of guest solubility as a function of host's concentration, interpreted as the formation of a complex with *m*:1 stoichiometry), A_P (positively deviating isotherms, usually interpreted as *m*:*n* complex) and A_N (negative deviation from linearity with no reasonable explanation) subtypes. Type-B diagram suggests the formation of inclusion complexes with poor solubility, where B_s-type and B_I-type phase-solubility diagrams represent the formation of complex with limited solubility and insoluble complex, respectively.[55,60]

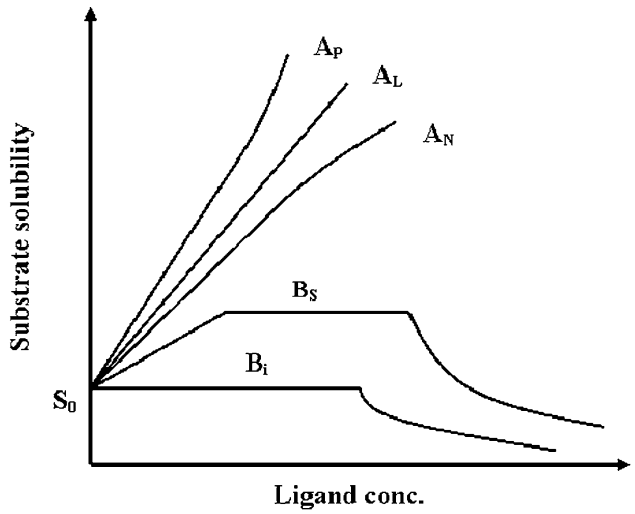

Figure 1.1 Types of phase solubility diagrams suggested by Higuchi and Connors.[59] (Figure taken from Ref [60])

β-CD often gives rise to B type curves due to its poor water solubility and also because of the formation of poorly soluble inclusion complex. With respect to *γ*-CD and the chemically modified CDs like HP-*β*-CD, they usually produce

soluble complexes and thus give A type systems.

1.3.3 Enhanced Aqueous Solubility by Cyclodextrin Derivatives

The polarity of the cavity has been estimated to be similar to that of aqueous ethanolic solution.[61] Consequently, CDs provide a lipophilic microenvironment for suitably sized hydrophobic molecules and thus solubilize hydrophobic organic compounds through the formation of water-soluble inclusion complexes mainly driven by hydrophobic interaction.[25]

Table 1.2 Solubility of drugs in different CD solutions.[25]

Drug	CDs[a]	Concentration[b]	Solubility enhancement factor[c]	Refs
Hydrocortisone	HE-*β*-CD	10	48.6	[62]
	HP-*β*-CD	10	33.9	[62]
	RM-*γ*-CD	10	55.2	[63]
Paclitaxel	*β*-CD	1.5	13	[64]
	HE-*β*-CD	50	2285	[64]
	HP-*β*-CD	50	2140	[64]
	DM-*β*-CD	50	99000	[64]
	γ-CD	15	50	[64]
	HP-*γ*-CD	50	200	[64]
Pancratistatin	HE-*β*-CD	10	5.2	[65]
	HP-*β*-CD	10	6.3	[65]
	DM-*β*-CD	10	7.5	[65]
	γ-CD	10	5.0	[65]
	HP-*γ*-CD	10	5.2	[65]

[a] HP-*β*-CD: (2-hydroxypropyl)-*β*-CD. HE-*β*-CD: (hydroxyethyl)-*β*-CD. DM-*β*-CD: 2,6-O-dimethyl-*β*-CD. RM-*γ*-CD: randomly methylated *γ*-CD. HP-*γ*-CD: (2-hydroxypropyl)-*γ*-CD. [b] Concentration of the aqueous CD solution, unit in % w/v. [c] The solubility in the aqueous CD solution divided by the intrinsic solubility in water measured at pH 7.4, r.t.

CDs have been playing a very important role in solubilization poorly soluble

guests. There are indeed many reports on the solubility enhancements of hydrophobic or amphiphilic guests, including pharmaceutical drugs, by CDs in aqueous solution.[25,54-56,60] But, due to the limited water solubilities of native CDs, the solubility enhancements reached by native CDs are generally small. However, modifications on the free hydroxyl groups of native CDs with appropriate function groups[40-42] may not only significantly increase the water solubility of CDs, but also greatly increase the ability of CDs to form inclusion complexes with guest molecules.

The solubilizing effects of native CD and various CDs derivatives on three different poorly-soluble drugs are listed in **Table 1.2**. The alkylated and hydroxyalkylated CDs such like methylated and 2-hydroxypropyl-CD appear to be more suitable for the solubilization of the poorly soluble drugs than the non-substituted native CDs, because of their increased aqueous solubility, lack of toxicity and ability to alter the phase solubility behaviour in favor of isotherms of the A-type.[41,66] CD sulfonates[67] perform even better than the neutral derivatives especially for the solubilization of hydrophobic guests like naphthalene in water.[40]

Our previously work reported a new class of hydrophilic per-6-deoxy-thioethers of *β*-CD showed exceptionally high binding constants ($K > 10^6$ M^{-1}, equivalent to $\Delta G < -34$ kJ·mol^{-1}) for *p*-disubstituted benzene derivatives in water.[34] The water solubility of camptothecin was found to be remarkably enhanced by *β*-CD thioethers. Moreover, the stabilities of the camptothecin complexes were significantly higher than that of any other CD derivative known from literature.[32] The higher hydrophobicity of sulphur compared to oxygen, leading to an extension of the hydrophobic cavity, and additional Coulomb interactions, were made responsible for the observed high binding potentials of these hosts.[34,68]

Besides, the combined use of cosolvent and CDs molecules has also proved to be an effective method to control the solubility of guest molecules.[54] Zung *et al*. observed synergistic effects of cosolvent and complexation in solubilizing

pyrene by using a series of alcohols.[69] It was suggested that the cosolvent act as space-regulating so that the guest molecule can better fit into the CD cavity.[54]

1.4 Supramolecular Controlled Photodimerization

Photochemical reaction is an important tool in modern synthetic chemistry. They often lead to products virtually inaccessible by thermal reactions and proceed along the excited-state pathway.[70] However, it is difficult to predict and control the outcome of photochemical reactions in homogeneous solutions where molecules behave rather chaotically. Bias in the orientation during reaction, which will lead to the regio- or stereoselective chemical reaction, may come from the reacting partners themselves,[71] chiral auxiliaries,[72-73] selective reagents, or the transition-metal catalysts with sophisticated ligands.

A variety of photochemical reactions is influenced and enhanced by the presence of a host molecule, *i.e.*, a molecular flask which includes the guest or guests, thus preorganizing them advantageously for a desired photochemical reaction.[70] The supramolecular host protects the included guest molecule(s) from the surrounding environment and thus controls the course of a photochemical reaction.[70,74]

CDs are favorite template scaffolds because of their good availability, various sizes, and the inherent chirality which is used for enantioselective photochemical reactions. Other examples include self-assembled cages, CBs, and self-assembled cavitand. Among these host molecules, γ-CD and CB[8] are particularly attractive because they are able to accommodate two guest molecules within the cavity, forming a 1:2 complex with desired orientations. Accordingly, regio- and stereoselective photodimerizations between two substrates, both in solution and in the solid state, might be achieved in the presence of these nano-vessels.[70,75-78]

1.4.1 Stilbenes

Stilbenes (**1a-h**, see **Scheme 1.3**) exhibit an inefficient and unselective photochemical reactivity in solution in the absence of host molecules that includes reversible isomerization (**2a-h**), cyclization to phenanthrene (**3a-h**), and dimerization to yield tetraphenylcyclobutane products.[75,79] The (*Z*)-isomers or the subsequent cyclized isomers are obtained as the major products.[80] Stilbenes are most ideal candidates to demonstrate the modulation of photochemical reactivity by host/guest interactions for they readily form inclusion complexes with CDs and other kind of host molecules.

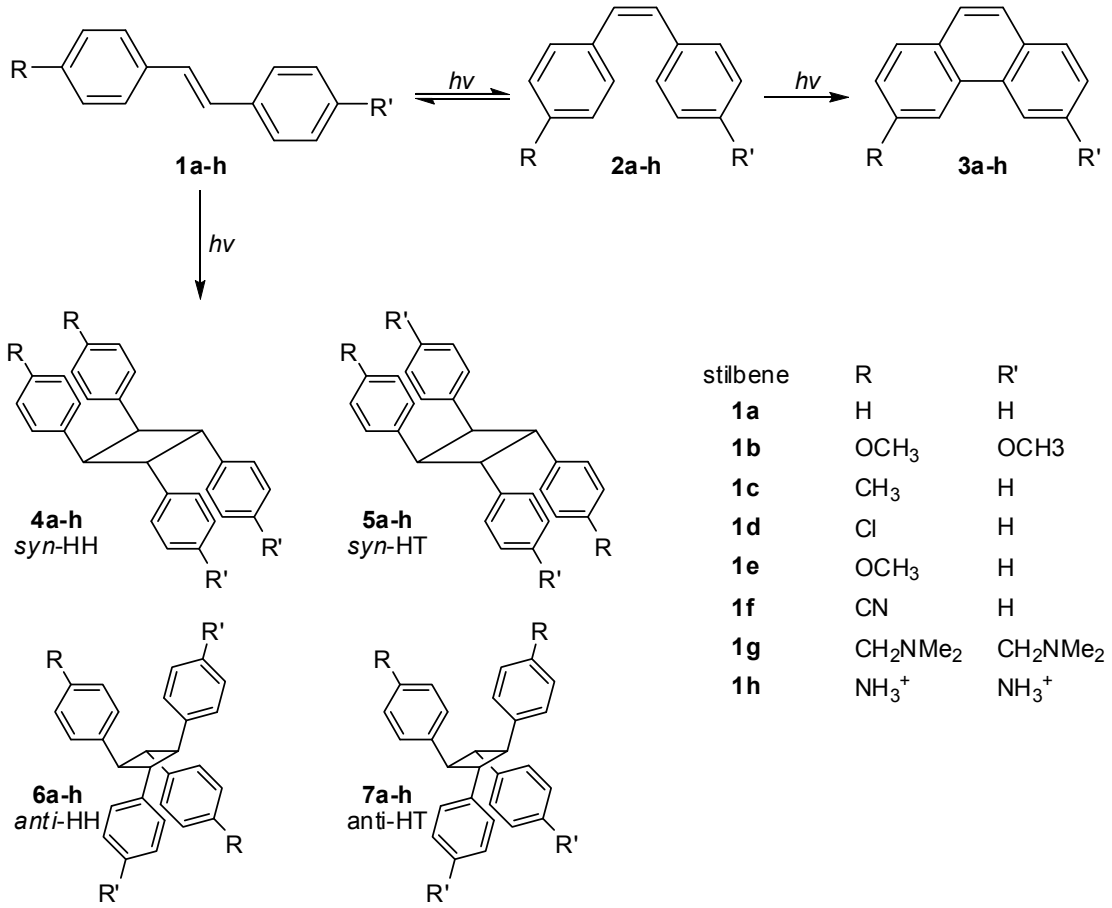

stilbene	R	R'
1a	H	H
1b	OCH_3	OCH3
1c	CH_3	H
1d	Cl	H
1e	OCH_3	H
1f	CN	H
1g	CH_2NMe_2	CH_2NMe_2
1h	NH_3^+	NH_3^+

Scheme 1.3 Reversible isomerization, cyclization, and photodimerization of stilbenes.

The influence of the ring size of a CD molecule on the photochemistry of a water-soluble stilbene (**1g**) was investigated.[81-83] The inclusion of stilbenes in α- or β-CD led to the prevention of the photo-dimerization, as only one guest molecule was able to be included in the cavity of α- or β-CD.[81-82] α- and β-CD

exerted a shielding effect on the guest molecule in water. The photodimerization of **1g** was significantly promoted in presence of γ-CD, selectively affording the *syn*-HH photodimer **4g** and *anti*-HH photodimer **7g** and in 19% and 79% yields, respectively. Moreover, the presence of γ-CD led to an increase of the rate of consumption of **1g**.[83]

Hubig *et al*. reported the effects of the crystalline γ-CD environment on the efficiency and stereoselectivity of the photodimerization of stilbenes **1a-f**.[75] Solid-state irradiation of the crystalline inclusion complex of stilbene **1a** in γ-CD yielded a single *syn*- dimer stereoselectively in high yield. Upon irradiation of the solid-state complexes of **1b-f** with γ-CD, the *syn*-HH **4b-f** and *syn*-HT **5b-f** isomers were exclusively formed over the *anti*- isomers in comparable yields (combine yield from 59% to 79%).

Complexation of stilbene **1h** with CB[8] in aqueous solution remarkably accelerated the rate of [2 + 2] photoreaction and significantly increased the stereoselectivity (*syn*-*anti* ratio > 95:5) of the photodimerization of stilbene **1h**.[46] The ability of CB[8] to include the two guest molecules with a parallel orientation of the olefinic groups in close proximity led to the high stereoselectivity of the photodimerization.

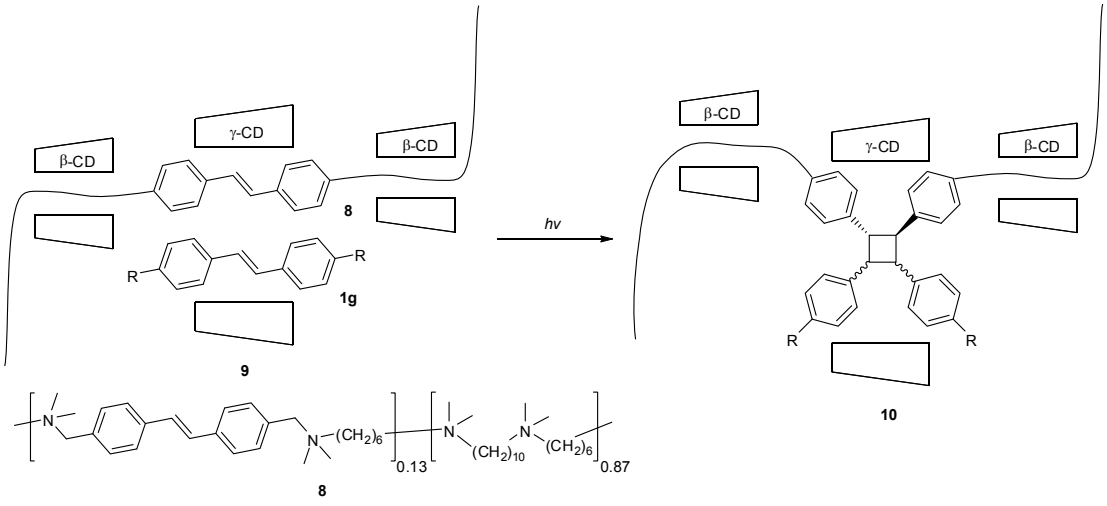

Scheme 1.4 Self-organization of the polymeric inclusion compound **9** and photochemical synthesis of polyrotaxane **10**.

Irradiation of the saturated aqueous solution of polymeric inclusion compound **9** (prepared by self-organization) with UV light afforded the polyrotaxane **10** as shown in **Scheme 1.4**. The additional inclusion of the monomeric stilbene **1g** in the inclusion compound of the polymeric stilbene **8** not only stabilized the supramolecular structure but also made possible further chemical modification. It was known as the first demonstration of the supramolecular catalysis of a polymer-analogous conversion, *i.e.*, a conversion of the repeating units without changing the chain length.[84]

1.4.2 Olefinic Compounds (Stilbene Analogs)

In presence of *α*- or *β*-CD, the photoisomerization of *trans*-2-styrylpyridine **18** in solid state was greatly suppressed, while the photodimerization was moderately facilitated with a low yield of the photodimers (< 6%). However, photolysis of the *γ*-CD complex of guest **18** in solid state led to the formation of the *syn*-head-to-tail dimer in fairly good yield.[85]

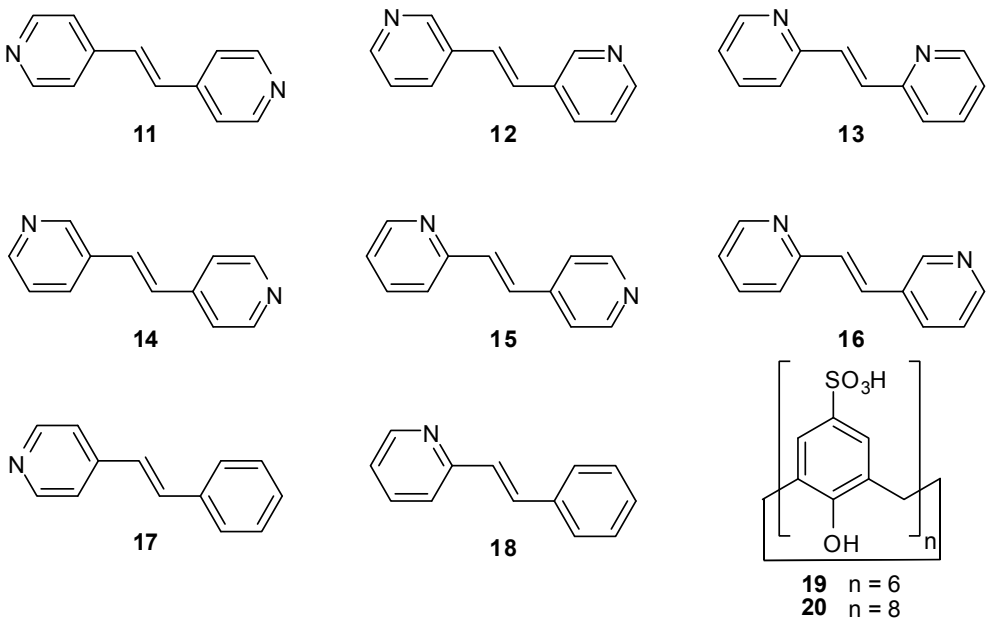

Scheme 1.5 Chemical structures of olefinic compounds.

The generality of CB[8] as a template to control the photodimerization of eight water-soluble hydrochloride salts of olefins (**Scheme 1.5**), namely, symmetrical

11–**13** and unsymmetrical bispyridyl ethylenes **14**–**16**, and stilbazoles **17**–**18**, had been investigated in an aqueous medium. In solution or in presence of CB[7], upon excitation all of the olefins yielded the products of geometric isomerization, cyclization, and hydration. In the presence of CB[8] the predominant product was photodimer of the guest. Moreover, predominantly a single dimer was obtained in each case instead of a mixture of dimers. The selective formation of the dimer was rationalized on the basis of the principles of best fit and minimization of electrostatic repulsion.[86]

The conformational flexibility of calixarenes obstructed their utility as reaction vessels for photoreaction. It was found that highly flexible calixarene **20** was rigidified to a single conformer in solution by dicationic guest molecules **14** and **15**.[87] Guest molecule assembled two hosts in an inverted cone capsular fashion. The photochemically active guests **14** and **15** became photo-inert due to the hindrance to the rotation of the C=C bond in the excited state from electrostatic interaction between the cationic sites of the guest and the anionic sites of the host.[87] Ramamurthy *et al.* reported that irradiation of the hydrochloride salt of guests **14**–**16**, in CB[8] aqueous media resulted in high yields of the *syn* photodimer.[88]

Nakamura *et al*. examined the photoirradiation products of **21a** derivatives having alkyl substituents on the phenyl group (**21b-f**). The effect of the alkyl substituent on the product distribution was rather limited for the photoreaction in MeOH solutions. Hydrochloride salts of guests upon irradiation in aqueous solution gave predominantly the *cis* isomer **22b-f** along with a mixture of dimers. However, the substituents had a distinct effect on the product distribution for the photoreaction of the inclusion complexes of hydrochloride salts of **21b-f** with CB[8] in aqueous solutions. Introducing an alkyl group at the 2- or 3-position of the phenyl group completely shifted the major product from the *syn*-HT dimer **24b-f** to the *syn*-HH dimer **25b-f**.[89]

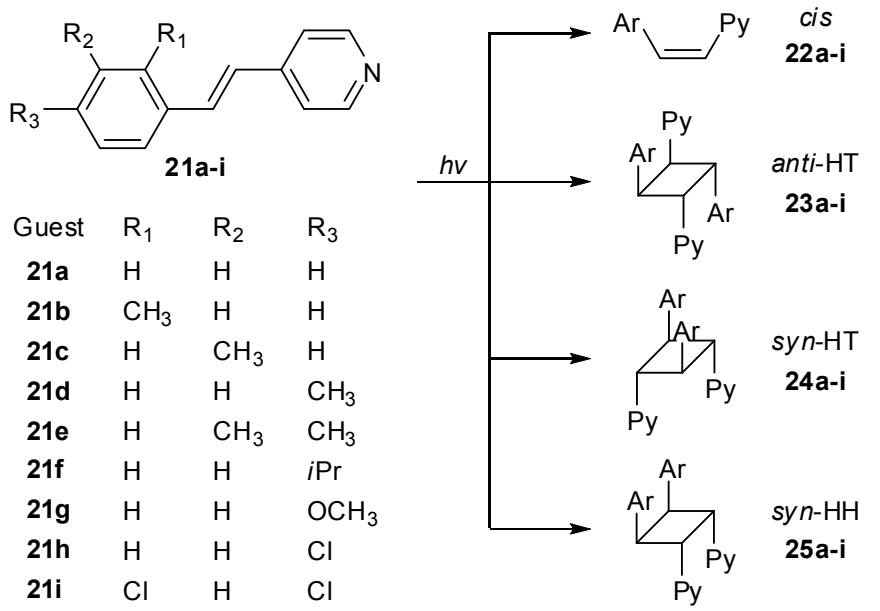

Guest	R_1	R_2	R_3
21a	H	H	H
21b	CH_3	H	H
21c	H	CH_3	H
21d	H	H	CH_3
21e	H	CH_3	CH_3
21f	H	H	*i*Pr
21g	H	H	OCH_3
21h	H	H	Cl
21i	Cl	H	Cl

Scheme 1.6 Chemical structures, photodimerization, and photoisomerization of trans-4-styrylpyridines.

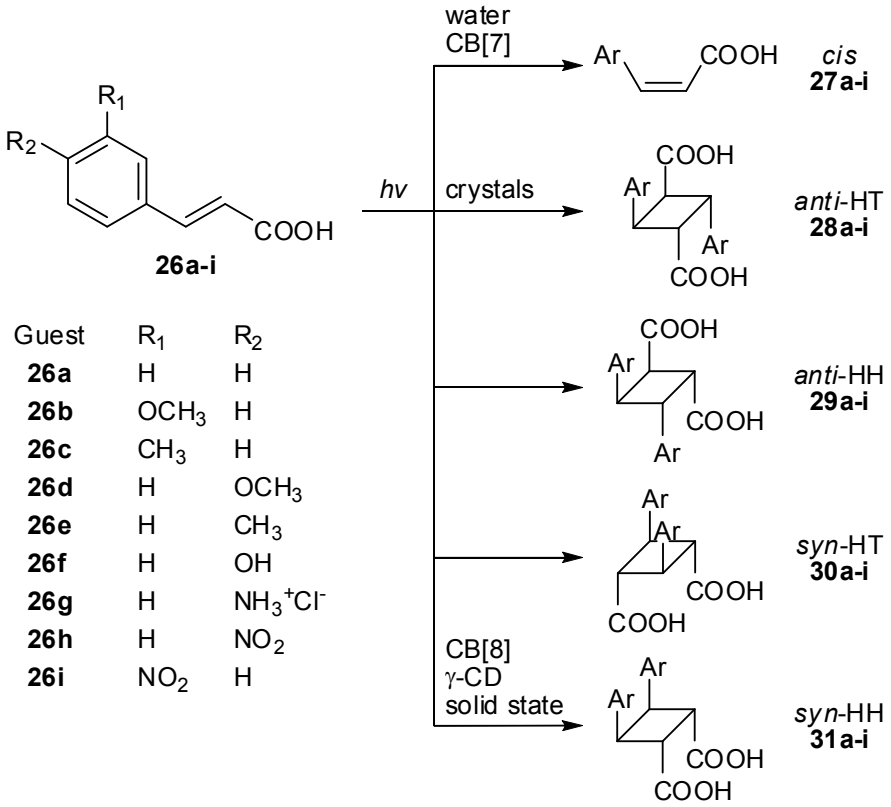

Guest	R_1	R_2
26a	H	H
26b	OCH_3	H
26c	CH_3	H
26d	H	OCH_3
26e	H	CH_3
26f	H	OH
26g	H	$NH_3^+Cl^-$
26h	H	NO_2
26i	NO_2	H

Scheme 1.7 Geometric isomerization and photodimerization of cinnamic acids **26a-i**.

Table 1.3 Product distributions (fractions of photodimers *syn*-HT and *anti*-HT and the geometric isomer *cis*) of the photoreaction of *trans*-cinnamic acids.[90]

Guest	Host	Guest/Host	Yield [%]		
			syn-HH	*anti*-HT	*cis*
26a	crystals	–	100		
	CB[8] solution	2:1		54	46
	CB[8] solid state	1:5	19	29	52
	CB[7] solid state	1:1	68		32
	γ-CD solid state	2:1		99	1
26b	CB[8] solution	2:1	72		28
	CB[8] solid state	1:1	78		22
	γ-CD solid state	2:1	96		4
26c	CB[8] solution	2:1	83		17
	CB[8] solid state	1:1	45		55
	γ-CD solid state	2:1	99		1
26d	CB[8] solution	2:1	72		28
	CB[8] solid state	1:1	48		52
	γ-CD solid state	2:1	100		
26e	crystals	–	100		
	CB[8] solid state	1:1	66	15	19
	CB[7] solid state	1:1	80		20
	γ-CD solid state	2:1		100	
26f	crystals	–	100		
	CB[8] solution	2:1		38	62
	CB[8] solid state	1:3	24	48	28
	γ-CD solid state	2:1		99	1
26g	crystals	–	100		
	CB[8] solution	1:2		88	12
	CB[8] solid state	1:1	68	14	18

Irradiations of the inclusion complexes of CB[8] with olefins **21a,d,g-i** produced predominantly the *anti*-HT dimer with only less than 5% *cis* isomer formation, possibly from uncomplexed olefin. The *syn*-HH dimer not formed in water or within CB[8] was one of the products during irradiation of **21a,d** with

γ-CD. *Anti*-HT dimer was obtained as the sole product of **21g** with γ-CD because of the charge transfer interaction between the electron-rich methoxy phenyl ring and electron deficient pyridinium ring of **21g**. As expected, the inclusion complexes of γ-CD with **21h** and **21i** produced the *syn*-HH dimer as the major product because of the existence of Cl–Cl interaction between guest molecules.[91]

The photochemical reactivity of *trans*-cinnamic acids **26a-i** had been investigated by utilizing CB[8] and γ-CD as reaction vessels.[90,92] Cinnamic acids **26a-i** upon irradiation in solution underwent geometric isomerization (**27a-i**), while dimerizing to different dimers in the crystalline state (see **Scheme 1.7** and **Table 1.3**). Irradiation of complexes of cinnamic acids **26a-i** with CB[7] resulted in only the corresponding *cis* isomers **27a-i**.[92] CB[8] and γ-CD had the ability to include two molecules of cinnamic acids **26a-g** and align them in a head-head fashion within their large cavities to yield a *syn*-HH **31a-g** dimer in nearly quantitative yields. The reported methodology worked with *trans*-cinnamic acids **26a-g** that did not dimerize either in solution or in the solid state.[90] More specifically, CB[8] functioned well both in solid state and aqueous solution, γ-CD worked best as solid complexes only.[90,92]

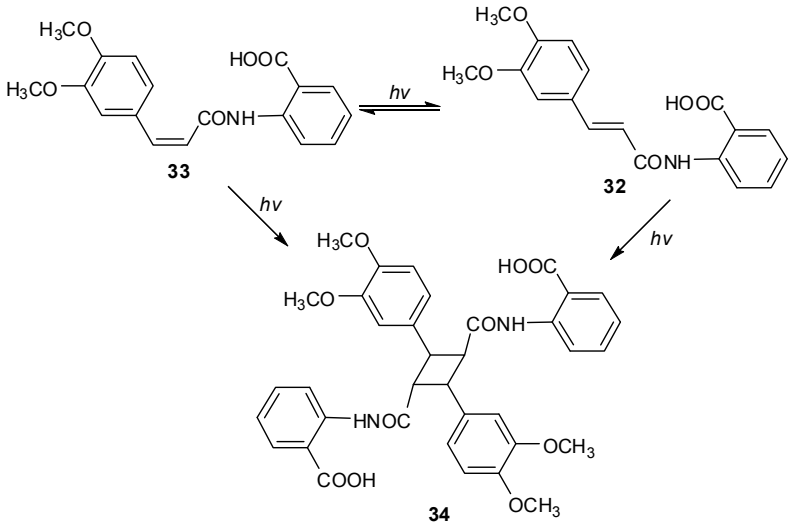

Scheme 1.8 Photoreaction pathway of tranilast **32**.

As shown in **Scheme 1.8**, *α*- and *β*-CD decelerated both the photoisomerization (**33**) and photodimerization (**34**) of the anti-allergic drug tranilast **32** due to the 1:1 complex formation. On the other hand, the photoisomerization of **32** was decelerated over the employed *γ*-CD concentration range. *γ*-CD accelerated the photodimerization of **32** at higher guest/*γ*-CD ratios by 5,500 times due to the formation of 1:2 host–guest inclusion complex. With increasing concentration *γ*-CD, the photodimerization rate significantly decreased. In particular, the dimerization was decelerated by 19,300 times when a 2:1 host–guest complex was formed at lower guest/*γ*-CD ratios. The results revealed clear evidence for the cavity-size and stoichiometry-dependent dimerization of **32** in CD complexes.[93-94]

1.4.3 Coumarins

As shown in **Scheme 1.9**, photodimerization of coumarin derivatives **35** led to four different dimers, *viz.*, *syn*-HH **36**, *syn*-HT **37**, *anti*-HH **38**, and *anti*-HT **39**.[95-100] The photodimerization of coumarins (**35a-i**) were found to proceed selectively in solid inclusion complexes with *β*- and *γ*-CD. **Table 1.4** summarizes the photochemical reactivities in solid complexes with *β*- and *γ*-CDs. Some substituted coumarins which were photochemically inert as neat solids, such as **35g** and **35h** and coumarin **35a** which behaved non-topochemically, gave high yields of photodimer when irradiated as CD complexes. Others (**35b**, **35e**, and **35f**), which dimerized readily in their neat solid state, were unreactive when precipitated with *β*-CD due to the enforced isolation of the coumarin molecules in their 1:1 host-guest complexes. *γ*-CD and coumarins **35** formed 1:2 complexes and yielded, in general, *syn*-dimers **36** and **37** upon irradiation.[76]

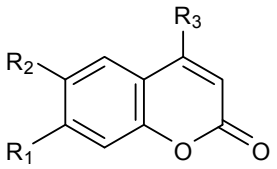

35a-n

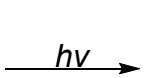

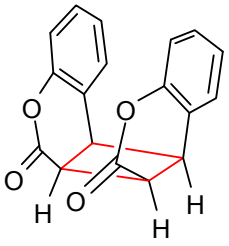

36a-n
syn-HH

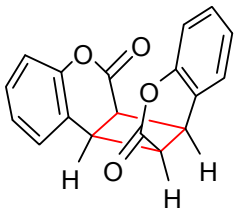

37a-n
syn-HT

coumarins	R_1	R_2	R_3
35a	H	H	H
35b	H	H	Cl
35c	H	H	OCH_3
35d	H	Cl	CH_3
35e	CH_3	H	H
35f	OCH_3	H	H
35g	CH_3	H	CH_3
35h	H	CH_3	CH_3
35i	OCH_3	H	CH_3
35j	H	CH_3	H
35k	AcO	H	H
35l	AcO	H	CH_3
35m	OH	H	CH_3
35n	NH_3^+	H	CH_3

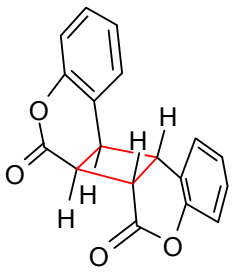

38a-n
anti-HH

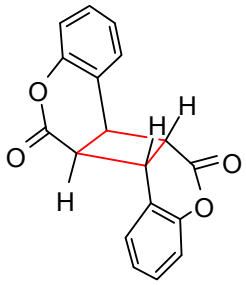

39a-n
anti-HT

Scheme 1.9 Chemical structures of coumarins and possible [2 + 2] photodimers produced upon irradiation.

Table 1.4 Product distributions (fractions of photodimers *syn*-HH, *syn*-HT, *anti*-HH, and *anti*-HT) of the photodimerization of coumarins in various media.[45,76]

Guest	Host	Host / Guest	Yield [%]			
			syn-HH	*syn*-HT	*anti*-HH	*anti*-HT
35a	*β*-CD solid state	1:2	64			
	CB[8] solution	1:1.7	43	57		
35b	*β*-CD solid state	1:1	[a]			
	γ-CD solid state	1:2	[a]			
35c	*β*-CD solid state	1:1	[a]			
35d	*β*-CD solid state	[b]				
	γ-CD solid state	[b]				
35e	*β*-CD solid state	1:1	[a]			
	γ-CD solid state	1:2	80			
	CB[8] solution	1:2	**> 99**			

35f	*β*-CD solid state	1:1	[a]			
	γ-CD solid state	1:2	65	35		
	CB[8] solution	[c]	30	70		
35g	*β*-CD solid state	2:2			94	
	γ-CD solid state	1:2	57	28		
	CB[8] solution	1:1.3	36		40	24
35h	*β*-CD solid state	2:2	48			
	γ-CD solid state	1:2	74			
	CB[8] solution	1:1	73		27	
35i	*β*-CD solid state	2:2	45	25		
	CB[8] solution	[c]	48		12	40
35j	CB[8] solution	1:1.6	31	69		
35k	CB[8] solution	1:1	22	78		
35l	CB[8] solution	[c]	32		22	46

[a] No dimers detected. [b] No solid complex isolated. [c] No complexation.

The formation of 2:2 inclusion complexes with *β*-CD rather facilitated the photodimerization and, in some circumstance, remarkably changed the stereoselectivity from that of *γ*-CD complexes. For instance, coumarin **35g** formed a crystalline 2:2 host–guest complex with *β*-CD and photo-dimerized in a reaction nano-vessel to form the *anti*-HT **39g** photodimer. The production of this dimer appeared to occur because of a preferential spatial fit of this product to the *β*-CD dimer cavity.[101] Coumarin **35m** with *β*-CD in solid state selectively dimerized to *anti*-HT dimer upon irradiation because of the formation of 2:2 inclusion complex.[102]

Moreover, the reactivity and selectivity of photodimerization of coumarins had been investigated by employing CB[8] in water.[45,103-104] CB[8] acted as a supramolecular catalytic nano-reaction vessel and effectively manipulated the photodimerization of both neutral (**35f, j, m**) and cationic (**35n**) coumarins derivatives.[103] Direct irradiation of these 1:2 host-guest complex in water gave HT adduct as the major product. Coumarins with non-polar substituents at the

6- or 7- position underwent photodimerization in presence of CB[8] in water, gave the *syn* dimer as the major products, as shown in **Table 1.4**.[45] The available free volume and the hydrophobic confined environment were responsible for the observed selectivity.[103] Guest induced shape change of the cavity was likely rate limiting in the supramolecular catalyzed photodimerization of coumarins mediated by CB[8].[105]

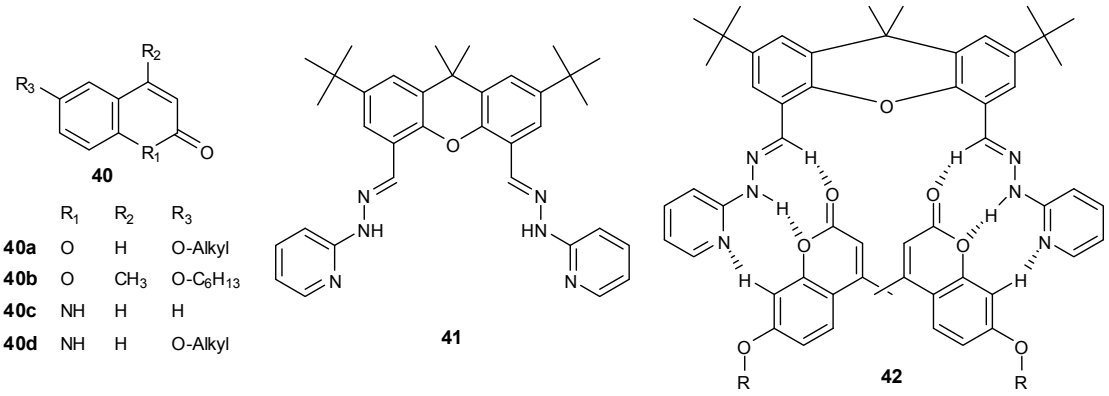

	R_1	R_2	R_3
40a	O	H	O-Alkyl
40b	O	CH_3	O-C_6H_{13}
40c	NH	H	H
40d	NH	H	O-Alkyl

Scheme 1.10 Chemical structures of coumarin analogs and the symmetric ditopic molecular receptor.

The photodimerization of coumarin **40a-d** in presence of a symmetric ditopic molecular receptor **41**, which were capable of binding substrates with complementary donor and acceptor sites to form a supramolecular complex through hydrogen bonding, were investigated. Irradiation of the 2:1 supramolecular complex **42** formed by host **41** with coumarin **40b** led to the selective formation of the *syn*-HH photoproduct. Other photoproducts typically produced in the absence of the template were suppressed.[106]

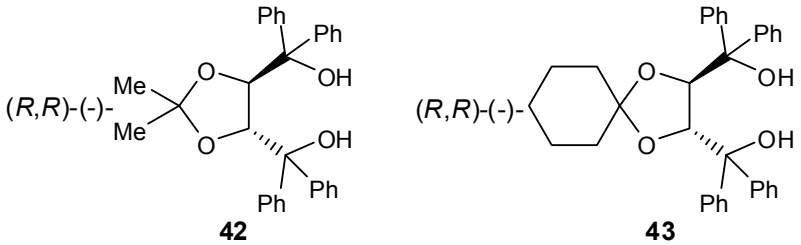

42 **43**

Scheme 1.11 Chemical structures of two optically active hosts.

Enantioselective photoreactions of coumarin in solution in presence of chiral hosts had been less studied. Tanaka *et al*. reported the photodimerization of coumarins (**35a**, **35j**) to the corresponding *anti*-HH dimers proceed efficiently in cyclohexane in presence of chiral hosts **42** and **43** (**Scheme 1.11**) in high enantioselectivity.[107]

1.4.4 Acenaphthylenes

The photochemical reactivities of **ACE** had been studied extensively in the past few decades as **ACE** dimer can be easily characterized by NMR spectroscopy as the proton resonances of individual dimers were well established in literature.[108-116] Irradiation of **ACE** in solution led to two isomeric cyclobutane dimers (*cis* and *trans*, **Scheme 1.12**) and the relative yields of the dimers strongly depended on the reaction medium used.[117-118] Cowan *et al*. reported that the ratio of *cis* to *trans* depended on the nature of the excited state from which the reaction originated.[111-112]

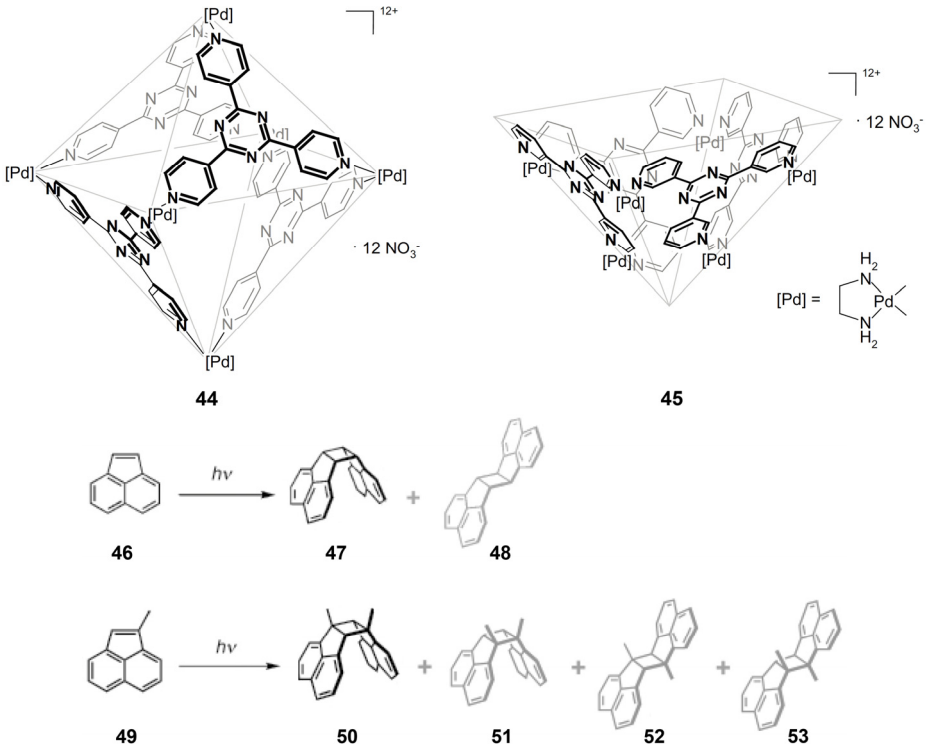

Scheme 1.12 Chemical structures of Pd-nanocage **44** and **45**, and photodimerizations of acenaphthylene **46** and **49**.

The photodimerizations of acenaphthylenes (**46** and **49**) within the Pd-nanocages (**Scheme 1.12**, **44** and **45**) were investigated.[119] The structurally well-defined coordination cages, which self-assembled from six metal ions and four tridentate ligands, selectively encapsulated acenaphthylene molecules at the fixed position of the nano-sized cavity, led to the quantitative formation of a *syn* dimer **47** of acenaphthylene **46** within cage **44** in an aqueous medium. The [2 + 2] photocycloaddition of asymmetrically substituted 1-methyl-acenaphthylene **49** was also found to be highly controlled by the Pd-nanocage **44**. Irradiation on the complex gave *syn*-HT isomer **50** in 98% yield.[119]

Interestingly, sensitized irradiation of acenaphthylene **46** in isotropic solvents yielded the *anti* dimer as the major product. The xanthene dye sensitized [2 + 2] triplet state photodimerization of acenaphthylene **46** encapsulated within Pd-nanocage yielded the *syn* dimer in quantitative yield. The absence of the *anti* dimer suggested that the cage did not favor reorientation of the pre-aligned *syn* configuration of the acenaphthylene molecules to the *anti* configuration within the lifetime of the triplet state. Thus the Pd-nanocage was able to yield the *syn* dimer as a single product even from the triplet state.[120]

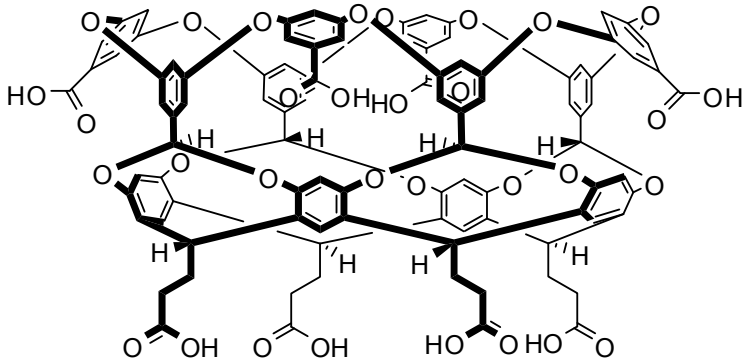

54

Scheme 1.13 Chemical structure of octa acid **54**.

Direct irradiation on acenaphthylene **46** included in a *syn* configuration within the water-soluble octa acid nano-capsule **54** (**Scheme 1.13**) preferentially

yielded a *syn* photodimer. By employing eosin Y as triplet sensitizer, *syn* and *anti* dimers were formed in the ratio of 60:40 when the aqueous solution of the acenaphthylene inclusion complex was irradiated. The mechanism of the formation of the *anti* dimer from the *syn* configuration of two acenaphthylene molecules was still an open question.[121]

1.4.5 Naphthalenes

The photodimerization of alkyl 2-naphthoate **55a-c** in water or in presence of CB[7] or CB[8] was investigated. Irradiation of saturated aqueous solution of **55a** did not resulted in any photodimer formation. CB[8] encapsulated two molecules of **55b** or **55c** and therefore facilitated the cubane-like photodimer **56** formation, see **Scheme 1.14**. Changes in either cavity size of CB[*n*] or size of alkyl substitutes could significantly modulate the interaction of CB[*n*] with guest **55a-c**, and thus afforded remarkable alterations in the photodimerization reactivities of guest molecules. [122]

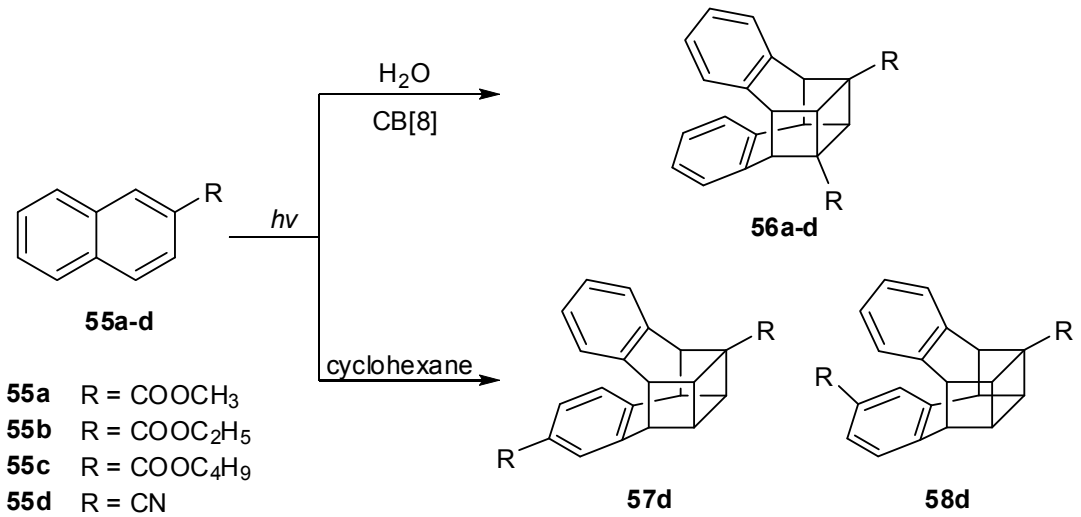

Scheme 1.14 Photodimerization of naphthalene derivatives **55a-d**.

A most recent paper by Wu *et al*. demonstrated that CB[8] can mediate the photodimerization of guest **55d** in aqueous solution. The product distribution revealed that the use of CB[8] as a nano reaction vessel inverted the product

selectivity from photodimers **57d** and **58d** in cyclohexane (see **Scheme 1.14**) to photodimer **56d** in quantitative yield (> 98%) with a large rate acceleration under ambient temperature and pressure.[49]

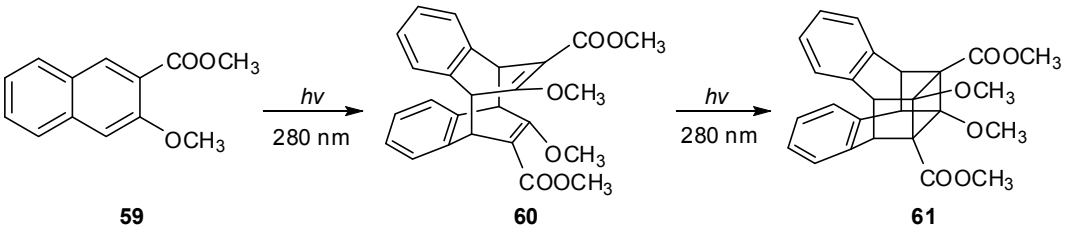

Scheme 1.15 Photodimerization of guest **59.**

Irradiation of naphthalene derivative **59** in methanol produced [4 + 4] intermediate **60** and *anti*-head-to-head cubane-like photocyclodimer **61** (**Scheme 1.15**). *γ*-CD formed a stable 2:1 inclusion complex with guest **59** both in aqueous solution and in solid state. Irradiation on the inclusion complex in which *γ*-CD performed as a chiral reaction vessel, resulted in the enantioselective photodimerization of **59** with ee values of 48% in aqueous solution and up to 34% in solid state for photodimer **61**, whereas no photodimer could be detected in host-free aqueous solution and the neat solids.[123-124]

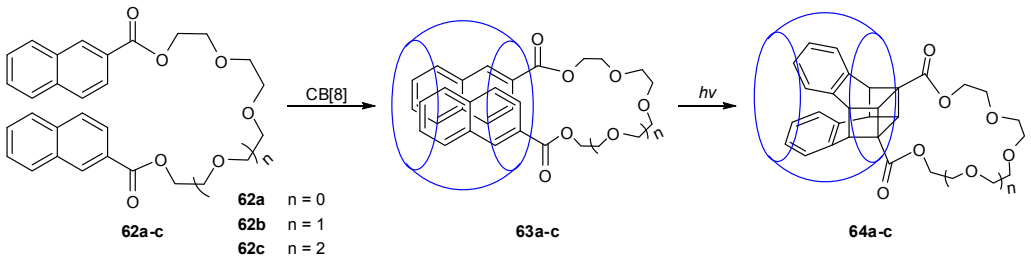

Scheme 1.16 CB[8] templated intramolecular photocycloaddition of molecule **62** in aqueous solution.

Interestingly, Wu *et al.* also reported a study on the photodimerization of a molecule with two reactive terminal aromatic groups separated by a long flexible chain (guests **62a-c**, see **Scheme 1.16**). Guest **62a-c** may undergo either intramolecular or intermolecular reactions. Owing to the hydrophilic

character of poly-ethylene glycol chain and the hydrophobic feature of the naphthalene terminal, CB[8] formed 1:1 inclusion complex with guest **62** like a molecular loop. Accordingly, irradiation on the inclusion complex in aqueous solution resulted in an exclusive formation of the intramolecular photodimer, whereas no photodimer of guest **62** could be detected in host-free solution.[125]

1.4.6 Anthracenes

The dimerization of anthracene and its derivatives is probably the best studied photochemical reaction in supramolecular molecular reaction vessels [70,77,120,126-131] such like Pd-nanocage **44**,[120] octa acid **54**,[132] CB[8][133] and so on.

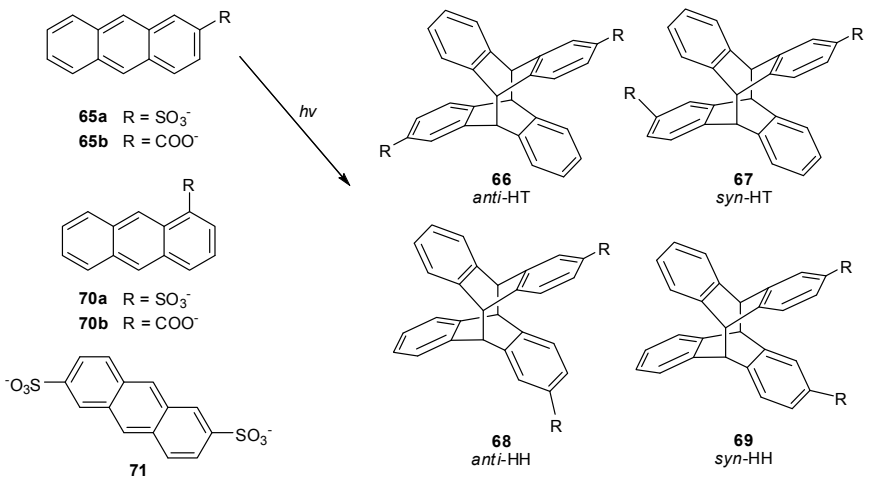

Scheme 1.17 Chemical structures and photodimerizations of anthracene derivatives.

Harada *et al*. synthesized polyrotaxanes containing *γ*-CDs by the photodimerization reactions of 9-anthryl groups at the ends of a polymer chain in the presence of *γ*-CDs.[134-135] Tamaki *et al*. reported that several water-soluble anthracene derivatives (**65**, **66**, and **67**, see **Scheme 1.17**) were included in aqueous solution by *β*- and *γ*-CD, resulted in 2:2 and 1:2 host-guest inclusion complexes, respectively.[127,136-137] The acceleration of the photodimerization by

γ-CD was most prominent for **65a**, **65b**, and **71**, slightly less for **70a**, and scarce for **70b** and **72c**. β-CD was also effectively accelerate the photodimerization of **65a** and **65b**, but inactive with the other anthracene derivatives. α-CD showed no interaction with all anthracene derivatives. Guests **65a,b** yielded four photodimers, *anti*-HT **66**, *syn*-HT **67**, *anti*-HH **68**, and *syn*-HH **69** upon irradiation. It was remarkable that the photodimerization of **65a,b** in the presence of β-CD quantitatively yielded the *anti*-HT **66** dimer, in contrast to the results of host-free or γ-CD-containing solutions. The reaction selectivities were explained in terms of the specific inclusion of anthracene into CDs. The quantum yield of photodimerization in presence of γ-CD (as high as 0.5) in aqueous solution was an order of magnitude greater than that in the absence of the host molecule.[136,138]

Investigation on the complexation and photodimerization of **65a** in presence of per-6-amino-CDs **72a-c** (see **Scheme 1.18**) showed that in neutral and alkaline media a 2:2 host-guest inclusion complex between **72b** and **65a** was formed in which two **65a** molecules orient anti-parallel to each other. Consequently, the dimeric complex underwent a rapid stereospecific photodimerization, giving rise to the *anti*-HT dimer, while HH dimer was not detected.[139]

Inoue *et al.* further investigated the photodimerization of anthracene **65b** in presence of γ-CD. The formation of a very stable 1:2 host-guest between γ-CD and **65b** inclusion complex was confirmed. The photoirradiation of **65b** solution in absence of γ-CD provided all isomers with a preference for the achiral isomer **66b**. In presence of γ-CD, irradiation on the complex gave a higher yield of isomer **67b**. A high ee value of the chiral dimer **67b** was obtained, and the value increased from 32% to 41% by lowering the temperature from 25 to 0 °C.[140]

A series of γ-CD derivatives (**73**-**92**) were synthesized and used as chiral hosts to manipulate the yield and stereochemical outcome of the photodimerization reactions of anthracene **65b** (**Scheme 1.18**). With γ-CD and γ-CD derivatives **73**, and **74a-d**, irradiation on anthracene **65b** in water led to the preferential

formation of HT dimers (**66b** and **67b**), while in solid-state, the formation of *syn*-HT **67b** was significantly suppressed.[141] Several secondary-face-substituted and skeleton-modified γ-CDs **75**-**80** did not significantly influence the relative yields of photodimers. The ee of *anti*-HH dimer **68b** was greatly enhanced in general with altroside-bearing γ-CDs **77**-**79**. An ee as high as 71% was obtained for dimer **67b** in the photodimerization mediated by CD **78** at 210 MPa and –21.5 °C.[142] By using a series of γ-CD derivatives possessing diamino side chain (**81**-**84**) as chiral hosts in presence and absence of $Cu(ClO_4)_2$ in aqueous solution, as high as 70% ee and 52% yield for dimer **68b** was achieved in aqueous solution at –50 °C. 43% ee for dimer **68b** can still be obtained by using even a 0.01 equiv of catalyst CuII·**82**.[143]

The yields of HH dimers were efficiently improved by the electrostatic interaction between diamino-γ-CDs **85a-d** and anthracene **65b**, and can be further enhanced by lowering the reaction temperature or solvent polarity. With increasing distance between the two amino groups on the CD primary rim (from CD **85a** to **85d**), the *anti*-to-*syn* ratio of the HH isomers gradually increased, reflecting the structure–function relationship in the supramolecular photoreaction system. The temperature- and solvent-controlled ee value inversion was the first example of a chirality inversion driven by entropy-related factors.[144] γ-CD **86** with a rigid cavity and a flexible dicationic sidearm switched the major products from HT dimers to the originally disfavored HH dimers, with an unprecedented enhancement of the ee of **68b** from 3% to 41% by maximizing the complex stability.[145]

When using mono- and bispyridinio-appended γ-CDs (**87** and **88a-d**) as chiral reaction vessels, γ-CD **88d** increased the ee more than 10-fold for the dimer **68b**, compared with native γ-CD.[146] No obvious difference in ee value of the isomer **67b** in presence of **88d** was observed compared to that done in unmodified γ-CD. Moreover, a slight difference in the position of the pyridinium cation of CD **88** also greatly affected the selectivity of relative yields and optical yields for the photodimerization of **65b**.[147]

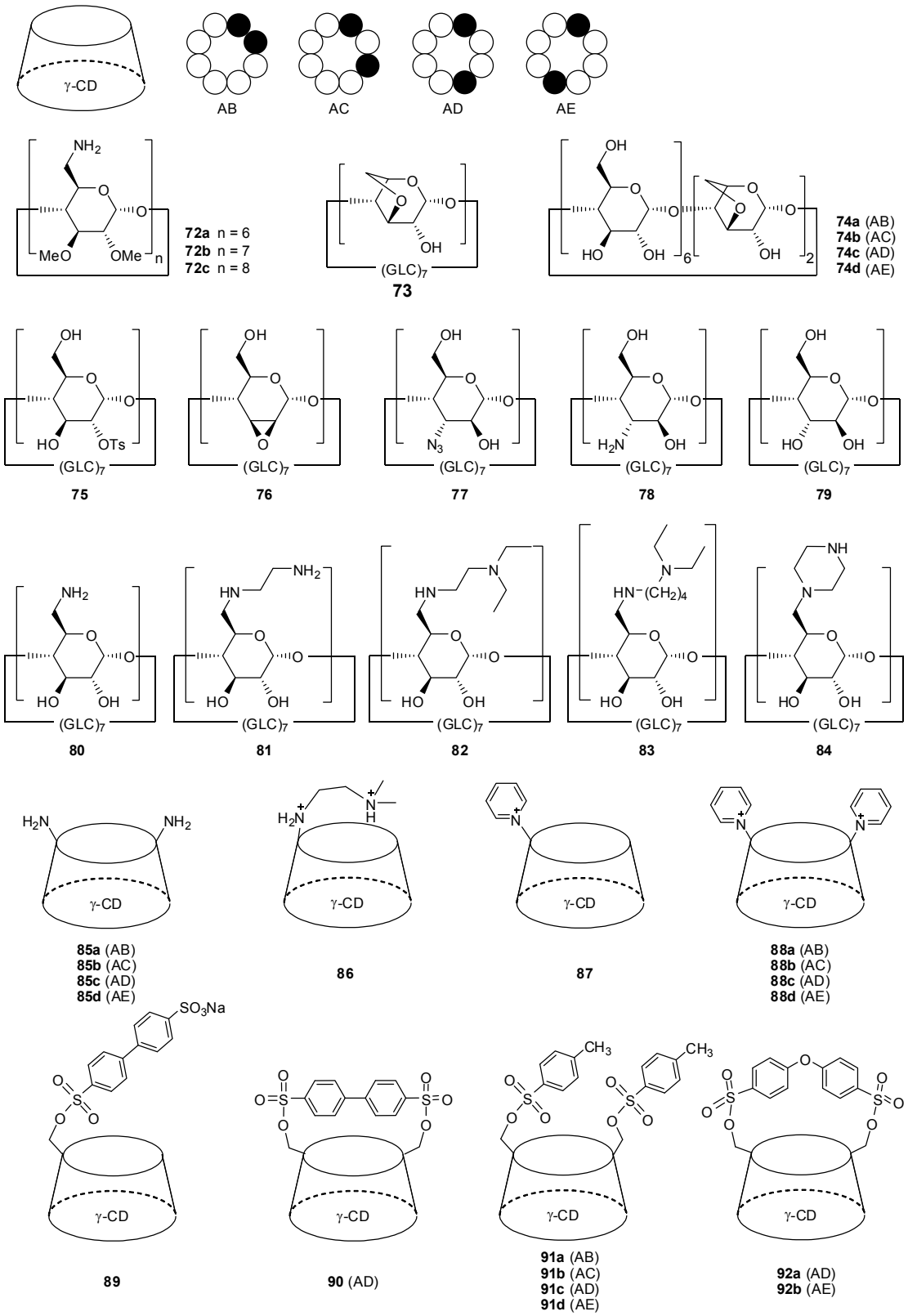

Scheme 1.18 Structures of CDs used as hosts for the photodimerization of anthracenes.

Other investigations studied the photodimerization reaction of **65b** mediated

by modified γ-CDs with a flexible (**89** and **91a-d**) or rigid cap (**90** and **92a-b**) in aqueous solution. [148-149] The use of capped γ-CDs considerably improved the yields of HH dimers, as compared with the results obtained with native γ-CD. The ee and the absolute configuration of dimer **67b** critically depended on the reaction temperature and the rigidity of capping. Thus, hosts **89** and **91c** afforded dimer **67b** in up to 40% ee in water at 0 °C and 24% ee in methanol-water at –45 °C whereas the product's chirality inverted, and an enhanced ee of –58 of the photodimer **67b** was obtained in presence of CD **90** with a rigid cap.[149] Much enhanced ee of –35% were consistently obtained for dimer **68b** by using any of the capped γ-CDs (**89**–**92**).[148]

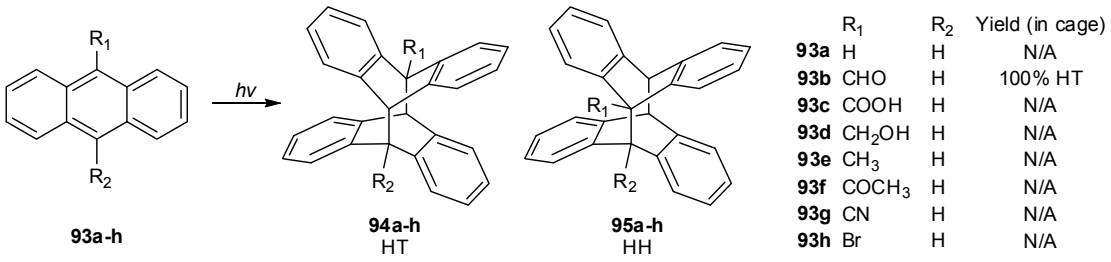

	R_1	R_2	Yield (in cage)
93a	H	H	N/A
93b	CHO	H	100% HT
93c	COOH	H	N/A
93d	CH_2OH	H	N/A
93e	CH_3	H	N/A
93f	$COCH_3$	H	N/A
93g	CN	H	N/A
93h	Br	H	N/A

Scheme 1.19 Structures of and photodimerization of anthracene derivatives **93a-h**.

Anthracenes **93a-h** were ideal candidates for undergoing photodimerization reaction inside the Pd-nanocage **44** since they had absorption above 330 nm. In isotropic solvents, irradiation on the 9-substituted anthracene derivatives **93b,c,f,g,h** led to the formation of HT **94** photodimer as the only product whereas anthracene derivatives **93d** and **93e** on irradiation yield both HT **94** and HH **95** photodimers in 40:60 and 25:75 ratios (**Scheme 1.19**), respectively.[120] Irradiation of the complex of anthracene-9-carbaldehyde **93b** with Pd-nanocage **44** in a ratio 2:1 led to selective formation of the photodimerization product 94b. Other 9-substituted anthracenes were photo-inactive inside the nanocage.

1.4.7 Other Guest Molecules

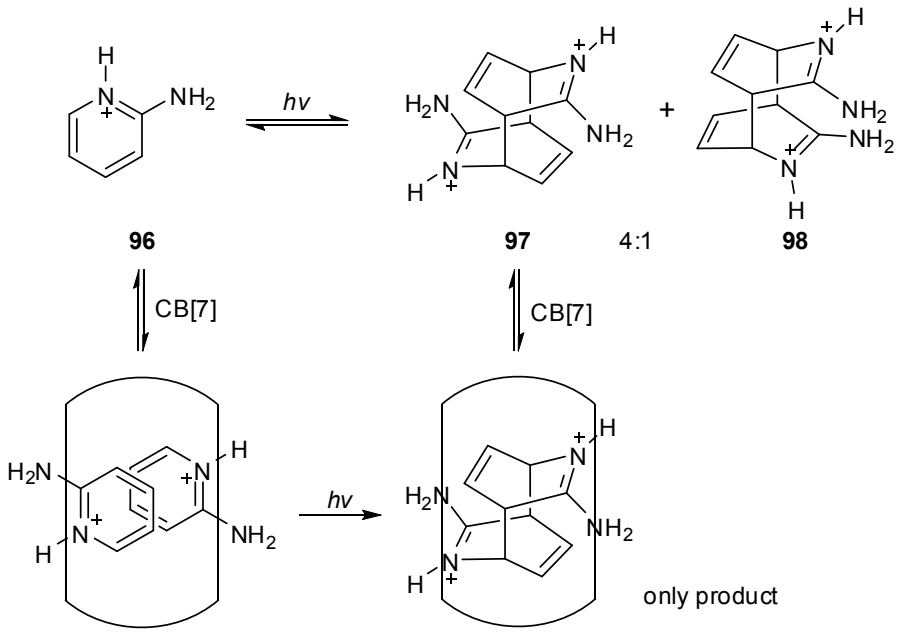

Scheme 1.20 CB[7] mediates the stereoselective photodimerization of 2-aminopyridine hydrochloride (**96**) in aqueous solution.

2-Aminopyridine hydrochloride **96** underwent a stereoselective photodimerization in aqueous solution in presence of CB[7], yielded exclusively the isomer **97** because of the formation of the 1:2 host-guest complex between **96** and CB[7], as shown in **Scheme 1.20**, whereas in the absence of CB[7], irradiation on the guests produced the isomers **97** and **98** in a 4:1 ratio.[150]

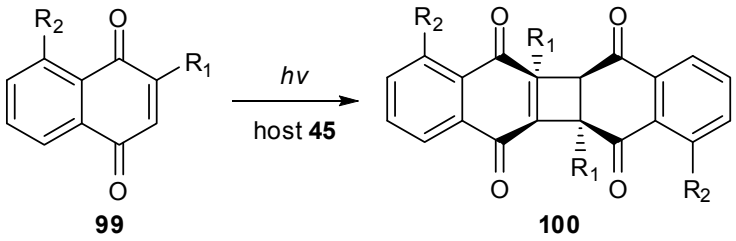

	R_1	R_2	Yield
99a	H	H	> 98%
99b	CH_3	H	78%
99c	H	OCH_3	79%

Scheme 1.21 Photodimerization of naphthoquinones **99a-c** in Pd-nanocage.

The photodimerization of naphthoquinones **99a-c** was most effectively controlled by Pd-nanocage **45**. Irradiation on the inclusion complex between host **45** and guest **99a** led to the quantitative formation of the dimer **100a** (yield > 98%, **Scheme 1.21**). The regioselectivity of the photodimerization of guest **99b**

was very high (96%) with Pd-nanocage **44** but only moderate (78%) with Pd-nanocage **45**. Photodimerization of **99c** afforded the isomer **100c** in 79% yield in presence of Pd-nanocage **45**. Irradiation of **99b** without the host did not afforded any dimerization product, while that of **99c** gave the *anti* dimer in 21% yield.[119]

1.5 Research Aims

As mentioned in the sections above, although the solubilization abilities of *β*-CD derivatives and the photodimerization of guest mediated by native *γ*-CD had been systematically studied, only few efforts had presently been made to evaluate the capabilities of modified *γ*-CD for solubility enhancements of guest molecules,[57,151-152] and the photochemical reactivities of the guests in presence of *γ*-CD derivatives were still lack of investigation.

Consequently, the aims of the present work were to design and synthesize a series of highly water-soluble hydrophilic per-6-thio-6-deoxy-*γ*-CDs with flexible neutral or ionic side arms in order to obtain a high ability of solubilization. Eight polycyclic aromatics of similar size: naphthalene, 2-naphthalene carboxylic acid, azulene, *trans*-stilbene, acenaphthylene, anthracene, phenanthrene, and tetracene were chosen as guest molecules. Solubilization of fullerene C_{60} in presence of these *γ*-CD thioethers were also discussed in this work.

It should be noted that some of the selected aromatic guests such as stilbene and anthracene can serve as candidates for photodimerization reactions. Accordingly, the photochemical reactivities of these guests in presence of *γ*-CD derivatives were also investigated.

1.6 References

[1] M. W. Hosseini, J. M. Lehn. Supramolecular catalysis of phosphoryl transfer - pyrophosphate synthesis from acetyl phosphate mediated by macrocyclic polyamines. *J. Am. Chem. Soc.* **1987**, *109*, 7047-7058.

[2] M. W. Hosseini, J. M. Lehn, L. Maggiora, K. B. Mertes, M. P. Mertes. Supramolecular catalysis in the hydrolysis of atp facilitated by macrocyclic polyamines - mechanistic studies. *J. Am. Chem. Soc.* **1987**, *109*, 537-544.

[3] J. M. Lehn. Supramolecular chemistry - scope and perspectives molecules, supermolecules, and molecular devices. *Angew. Chem. Int. Ed. Engl.* **1988**, *27*, 89-112.

[4] J. M. Lehn. Perspectives in supramolecular chemistry - from molecular recognition towards molecular information-processing and self-organization. *Angew. Chem. Int. Ed. Engl.* **1990**, *29*, 1304-1319.

[5] J. M. Lehn. Supramolecular chemistry - receptors, catalysts, and carriers. *Science* **1985**, *227*, 849-856.

[6] J. M. Lehn. Supramolecular chemistry. *Science* **1993**, *260*, 1762-1763.

[7] J. W. Steed, D. R. Turner, K. J. Wallace, *Core concepts in supramolecular chemistry and nanochemistry*, Wiley, **2007**.

[8] B. J. Holliday, C. A. Mirkin. Strategies for the construction of supramolecular compounds through coordination chemistry. *Angew. Chem. Int. Ed. Engl.* **2001**, *40*, 2022-2043.

[9] M. C. Daniel, D. Astruc. Gold nanoparticles: Assembly, supramolecular chemistry, quantum-size-related properties, and applications toward biology, catalysis, and nanotechnology. *Chem. Rev.* **2004**, *104*, 293-346.

[10] F. W. Zeng, S. C. Zimmerman. Dendrimers in supramolecular chemistry: From molecular recognition to self-assembly. *Chem. Rev.* **1997**, *97*, 1681-1712.

[11] J. M. Lehn. Toward complex matter: Supramolecular chemistry and self-organization. *Proc. Natl. Acad. Sci. USA* **2002**, *99*, 4763-4768.

[12] K. B. Lipkowitz. Applications of computational chemistry to the study of cyclodextrins. *Chem. Rev.* **1998**, *98*, 1829-1873.

[13] S. H. Gellman. Introduction: Molecular recognition. *Chem. Rev.* **1997**, *97*, 1231-1232.

[14] D. J. Cram. The benign of molecular hosts, guests, and their cenpleres. *Angew. Chem. Int. Ed. Engl.* **1988**, *27*, 1009-1020.

[15] V. T. D'Souza, K. B. Lipkowitz. Cyclodextrins: Introduction. *Chem. Rev.* **1998**, *98*, 1741-1742.

[16] J. Szejtli. Introduction and general overview of cyclodextrin chemistry. *Chem. Rev.*

1998, *98*, 1743-1753.

[17] H. J. Schneider. Mechanisms of molecular recognition - investigations of organic host guest complexes. *Angew. Chem. Int. Ed. Engl.* **1991**, *30*, 1417-1436.

[18] D. J. Cram. The design of molecular hosts, guests, and their complexes (nobel lecture). *Angew. Chem. Int. Ed. Engl.* **1988**, *27*, 1009-1020.

[19] T. Douglas, M. Young. Host-guest encapsulation of materials by assembled virus protein cages. *Nature* **1998**, *393*, 152-155.

[20] D. J. Cram, J. M. Cram. Host-guest chemistry. *Science* **1974**, *183*, 803-809.

[21] G. Wenz. Cyclodextrins as building-blocks for supramolecular structures and functional units. *Angew. Chem. Int. Ed. Engl.* **1994**, *33*, 803-822.

[22] G. Wenz. Cyclodextrin polyrotaxanes assembled from a molecular construction kit in aqueous solution. *J. Polym. Sci., Part A: Pol. Chem.* **2009**, *47*, 6333-6341.

[23] T. Irie, K. Uekama. Pharmaceutical applications of cyclodextrins. 3. Toxicological issues and safety evaluation. *J. Pharm. Sci.* **1997**, *86*, 147-162.

[24] R. A. Rajewski, V. J. Stella. Pharmaceutical applications of cyclodextrins. 2. In vivo drug delivery. *J. Pharm. Sci.* **1996**, *85*, 1142-1169.

[25] T. Loftsson, M. Brewster. Pharmaceutical applications of cyclodextrins. 1. Drug solubilization and stabilization. *J. Pharm. Sci.* **1996**, *85*, 1017-1025.

[26] K. Uekama, F. Hirayama, T. Irie. Cyclodextrin drug carrier systems. *Chem. Rev.* **1998**, *98*, 2045-2076.

[27] A. R. Hedges. Industrial applications of cyclodextrins. *Chem. Rev.* **1998**, *98*, 2035-2044.

[28] K. Kano, Y. Ishida. Supramolecular complex of cytochrome c with a polyanionic β-cyclodextrin. *Angew. Chem. Int. Ed. Engl.* **2007**, *46*, 727-730.

[29] W. Saenger, J. Jacob, K. Gessler, T. Steiner, D. Hoffmann, H. Sanbe, K. Koizumi, S. M. Smith, T. Takaha. Structures of the common cyclodextrins and their larger analogues - beyond the doughnut. *Chem. Rev.* **1998**, *98*, 1787-1802.

[30] K. A. Connors. The stability of cyclodextrin complexes in solution. *Chem. Rev.* **1997**, *97*, 1325-1357.

[31] E. Masson, X. Ling, R. Joseph, L. Kyeremeh-Mensah, X. Lu. Cucurbituril chemistry: A tale of supramolecular success. *RSC Advances* **2012**, *2*.

[32] A. Steffen, C. Thiele, S. Tietze, C. Strassnig, A. Kamper, T. Lengauer, G. Wenz, J.

Apostolakis. Improved cyclodextrin-based receptors for camptothecin by inverse virtual screening. *Chem. Eur. J.* **2007**, *13*, 6801-6809.

[33] G. Wenz, B. H. Han, A. Müller. Cyclodextrin rotaxanes and polyrotaxanes. *Chem. Rev.* **2006**, *106*, 782-817.

[34] G. Wenz, C. Strassnig, C. Thiele, A. Engelke, B. Morgenstern, K. Hegetschweiler. Recognition of ionic guests by ionic β-cyclodextrin derivatives. *Chem. Eur. J.* **2008**, *14*, 7202-7211.

[35] M. V. Rekharsky, Y. Inoue. Complexation thermodynamics of cyclodextrins. *Chem. Rev.* **1998**, *98*, 1875-1917.

[36] Y. Inoue, T. Hakushi, Y. Liu, L. Tong, B. Shen, D. Jin. Thermodynamics of molecular recognition by cyclodextrins. 1. Calorimetric titration of inclusion complexation of naphthalenesulfonates with α-, β-, and γ-cyclodextrins: Enthalpy-entropy compensation. *J. Am. Chem. Soc.* **1993**, *115*, 475-481.

[37] J. Boger, R. J. Corcoran, J. M. Lehn. Cyclodextrin chemistry. Selective modification of all primary hydroxyl groups of α- and β-cyclodextrins. *Helv. Chim. Acta* **1978**, *61*, 2190-2218.

[38] G. Gattuso, S. A. Nepogodiev, J. F. Stoddart. Synthetic cyclic oligosaccharides. *Chem. Rev.* **1998**, *98*, 1919-1958.

[39] A. R. Khan, P. Forgo, K. J. Stine, V. T. D'Souza. Methods for selective modifications of cyclodextrins. *Chem. Rev.* **1998**, *98*, 1977-1996.

[40] G. Wenz, T. Hofler. Synthesis of highly water-soluble cyclodextrin sulfonates by addition of hydrogen sulfite to cyclodextrin allyl ethers. *Carbohydr. Res.* **1999**, *322*, 153-165.

[41] T. Loftsson, D. Hreinsdottir, M. Masson. Evaluation of cyclodextrin solubilization of drugs. *Int. J. Pharm.* **2005**, *302*, 18-28.

[42] J. Pitha, J. Milecki, H. Fales, L. Pannell, K. Uekama. Hydroxypropyl-β-cyclodextrin - preparation and characterization - effects on solubility of drugs. *Int. J. Pharm.* **1986**, *29*, 73-82.

[43] R. Breslow, S. D. Dong. Biomimetic reactions catalyzed by cyclodextrins and their derivatives. *Chem. Rev.* **1998**, *98*, 1997-2011.

[44] K. Takahashi. Organic reactions mediated by cyclodextrins. *Chem. Rev.* **1998**, *98*, 2013-2033.

[45] N. Barooah, B. C. Pemberton, A. C. Johnson, J. Sivaguru. Photodimerization and complexation dynamics of coumarins in the presence of cucurbit[8]urils.

Photochem. Photobiol. Sci. **2008**, *7*, 1473-1479.

[46] S. Y. Jon, Y. H. Ko, S. H. Park, H. J. Kim, K. Kim. A facile, stereoselective [2+2] photoreaction mediated by cucurbit[8]uril. *Chem. Commun.* **2001**, 1938-1939.

[47] W. L. Mock, N. Y. Shih. Structure and selectivity in host guest complexes of cucurbituril. *J. Org. Chem.* **1986**, *51*, 4440-4446.

[48] J. W. Lee, S. Samal, N. Selvapalam, H. J. Kim, K. Kim. Cucurbituril homologues and derivatives: New opportunities in supramolecular chemistry. *Acc. Chem. Res.* **2003**, *36*, 621-630.

[49] B. Chen, S. F. Cheng, G. H. Liao, X. W. Li, L. P. Zhang, C. H. Tung, L. Z. Wu. Efficient and selective photodimerization of 2-naphthalenecarbonitrile mediated by cucurbit[8]uril in an aqueous solution. *Photochem. Photobiol. Sci.* **2011**, *10*, 1441-1444.

[50] C. A. Nijhuis, B. J. Ravoo, J. Huskens, D. N. Reinhoudt. Electrochemically controlled supramolecular systems. *Coordin. Chem. Rev.* **2007**, *251*, 1761-1780.

[51] J. Kim, I. S. Jung, S. Y. Kim, E. Lee, J. K. Kang, S. Sakamoto, K. Yamaguchi, K. Kim. New cucurbituril homologues: Syntheses, isolation, characterization, and X-ray crystal structures of cucurbit[n]uril (n = 5, 7, and 8). *J. Am. Chem. Soc.* **2000**, *122*, 540-541.

[52] Y. M. Jeon, H. Kim, D. Whang, K. Kim. Molecular container assembly capable of controlling binding and release of its guest molecules: Reversible encapsulation of organic molecules in sodium ion complexed cucurbituril. *J. Am. Chem. Soc.* **1996**, *118*, 9790-9791.

[53] W. Humphrey, A. Dalke, K. Schulten. VMD: Visual molecular dynamics. *J. Mol. Graph.* **1996**, *14*, 33-38.

[54] P. Li, L. W. Zhao, S. H. Yalkowsky. Combined effect of cosolvent and cyclodextrin on solubilization of nonpolar drugs. *J. Pharm. Sci.* **1999**, *88*, 1107-1111.

[55] M. E. Brewster, T. Loftsson. Cyclodextrins as pharmaccutical solubilizers. *Adv. Drug Deliver. Rev* **2007**, *59*, 645-666.

[56] X. J. Wang, M. L. Brusseau. Cyclopentanol-enhanced solubilization of polycyclic aromatic-hydrocarbons by cyclodextrins. *Environ. Sci. Technol.* **1995**, *29*, 2346-2351.

[57] X. Wang, M. Brusseau. Solubilization of some low-polarity organic compounds by hydroxypropyl-β-cyclodextrin. *Environ. Sci. Technol.* **1993**, *27*, 2821-2825.

[58] T. Braun, H. Rausch, L. P. Biro, E. Zsoldos, R. Ohmacht, L. Mark. The survivability of

polycrystalline C_{60} to high speed vibration milling. *Chem. Phys. Lett.* **2003**, *375*, 522-524.

[59] T. Higuchi, K. Connors. Phase-solubility techniques. *Adv. Anal. Chem. Instrum.* **1965**, *4*, 117-212.

[60] S. V. Kurkov, E. V. Ukhatskaya, T. Loftsson. Drug/cyclodextrin: Beyond inclusion complexation. *J. Inclusion Phenom. Macrocyclic Chem.* **2011**, *69*, 297-301.

[61] H. M. Wang, G. Wenz. Solubilization of polycyclic aromatics in water by γ-cyclodextrin derivatives. *Chem. Asian J.* **2011**, *6*, 2390-2399.

[62] T. Loftsson, H. Fridriksdottir, S. Thorisdottir, E. Stefansson. The effect of hydroxypropyl methylcellulose on the release of dexamethasone from aqueous 2-hydroxypropyl-β-cyclodextrin formulations. *Int. J. Pharm.* **1994**, *104*, 181-184.

[63] A. M. Siguroardottir, T. Loftsson. The effect of polyvinylpyrrolidone on cyclodextrin complexation of hydrocortisone and its diffusion through hairless mouse skin. *Int. J. Pharm.* **1995**, *126*, 73-78.

[64] U. S. Sharma, S. V. Balasubramanian, R. M. Straubinger. Pharmaceutical and physical-properties of paclitaxel (taxol) complexes with cyclodextrins. *J. Pharm. Sci.* **1995**, *84*, 1223-1230.

[65] J. J. Torres - Labandeira, P. Davignon, J. Pitha. Oversaturated solutions of drug in hydroxypropylcyclodextrins: Parenteral preparation of pancratistatin. *J. Pharm. Sci.* **1991**, *80*, 384-386.

[66] M. Linares, M. M. de Bertorello, M. Longhi. Solubilization of naphthoquinones by complexation with hydroxypropyl-β-cyclodextrin. *Int. J. Pharm.* **1997**, *159*, 13-18.

[67] V. Zia, R. A. Rajewski, V. J. Stella. Effect of cyclodextrin charge on complexation of neutral and charged substrates: Comparison of (SBE)(7M)-β-CD to HP-β-CD. *Pharm. Res.* **2001**, *18*, 667-673.

[68] K. Kano, Y. Ishida, K. Kitagawa, M. Yasuda, M. Watanabe. Heat-capacity changes in host-guest complexation by Coulomb interactions in aqueous solution. *Chem. Asian J.* **2007**, *2*, 1305-1313.

[69] J. B. Zung, A. Munoz de la Pena, T. T. Ndou, I. M. Warner. Influence of alcohol addition on the γ-CD: Pyrene complex. *J. Phys. Chem.* **1991**, *95*, 6701-6706.

[70] J. Svoboda, B. Konig. Templated photochemistry: Toward catalysts enhancing the efficiency and selectivity of photoreactions in homogeneous solutions. *Chem. Rev.* **2006**, *106*, 5413-5430.

[71] A. Mengel, O. Reiser. Around and beyond cram's rule. *Chem. Rev.* **1999**, *99*,

1191-1223.

[72] Y. Nishioka, T. Yamaguchi, M. Kawano, M. Fujita. Asymmetric [2+2] olefin cross photoaddition in a self-assembled host with remote chiral auxiliaries. *J. Am. Chem. Soc.* **2008**, *130*, 8160-8181.

[73] H. X. Xu, B. Chen, L. P. Zhang, L. Z. Wu, C. H. Tung. Diastereodifferentiating photodimerization of alkyl 2-naphthoates with chiral auxiliaries. *Tetrahedron Lett.* **2009**, *50*, 4965-4968.

[74] J. Svoboda. Flavin-based photocatalysts. **2008**.

[75] K. S. S. P. Rao, S. M. Hubig, J. N. Moorthy, J. K. Kochi. Stereoselective photodimerization of (*E*)-stilbenes in crystalline γ-cyclodextrin inclusion complexes. *J. Org. Chem.* **1999**, *64*, 8098-8104.

[76] J. N. Moorthy, K. Venkatesan, R. G. Weiss. Photodimerization of coumarins in solid cyclodextrin inclusion complexes. *J. Org. Chem.* **1992**, *57*, 3292-3297.

[77] H. Bouas-Laurent, A. Castellan, J. P. Desvergne, R. Lapouyade. Photodimerization of anthracenes in fluid solution: Structural aspects. *Chem. Soc. Rev.* **2000**, *29*, 43-55.

[78] G. Schmidt. Photodimerization in the solid state. *Pure Appl. Chem.* **1971**, *27*, 647–678.

[79] F. D. Lewis. Formation and reactions of stilbene exciplexes. *Acc. Chem. Res.* **1979**, *12*, 152-158.

[80] Y. Ito, T. Kajita, K. Kunimoto, T. Matsuura. Accelerated photodimerization of stilbenes in methanol and water. *J. Org. Chem.* **1989**, *54*, 587-591.

[81] M. S. Syamala, V. Ramamurthy. Consequences of hydrophobic association in photoreactions - photodimerization of stilbenes in water. *J. Org. Chem.* **1986**, *51*, 3712-3715.

[82] M. S. Syamala, S. Devanathan, V. Ramamurthy. Modification of the photochemical behavior of organic-molecules by cyclodextrin - geometric isomerization of stilbenes and alkyl cinnamates. *J. Photochem.* **1986**, *34*, 219-229.

[83] W. Herrmann, S. Wehrle, G. Wenz. Supramolecular control of the photochemistry of stilbenes by cyclodextrins. *Chem. Commun.* **1997**, 1709-1710.

[84] W. Herrmann, M. Schneider, G. Wenz. Photochemical synthesis of polyrotaxanes from stilbene polymers and cyclodextrins. *Angew. Chem. Int. Ed. Engl.* **1997**, *36*, 2511-2514.

[85] H. S. Banu, A. Lalitha, K. Pitchumani, C. Srinivasan. Modification of photochemical reactivity of trans-2-styrylpyridine: Effect of cyclodextrin complexation. *Chem. Commun.* **1999**, 607-608.

[86] M. Maddipatla, L. S. Kaanumalle, A. Natarajan, M. Pattabiraman, V. Ramamurthy. Preorientation of olefins toward a single photodimer: Cucurbituril-mediated photodimerization of protonated azastilbenes in water. *Langmuir* **2007**, *23*, 7545-7554.

[87] R. Kaliappan, Y. H. Ling, A. E. Kaifer, V. Ramamurthy. Sulfonatocalix[8]arene as a potential reaction cavity: Photo- and electro-active dicationic guests arrest conformational equilibrium. *Langmuir* **2009**, *25*, 8982-8992.

[88] M. Pattabiraman, A. Natarajan, R. Kaliappan, J. T. Mague, V. Ramamurthy. Template directed photodimerization of trans-1,2-bis(n-pyridyl)-ethylenes and stilbazoles in water. *Chem. Commun.* **2005**, 4542-4544.

[89] A. Nakamura, H. Irie, S. Hara, M. Sugawara, S. Yamada. Regiospecific [2+2] photocyclodimerization of trans-4-styrylpyridines templated by cucurbit[8]uril. *Photochem. Photobiol. Sci.* **2011**, *10*, 1496-1500.

[90] M. Pattabiraman, A. Natarajan, L. S. Kaanumalle, V. Ramamurthy. Templating photodimerization of trans-cinnamic acids with cucurbit[8]uril and γ-cyclodextrin. *Org. Lett.* **2005**, *7*, 529-532.

[91] R. Kaliappan, M. Maddipatla, L. S. Kaanumalle, V. Ramamurthy. Crystal engineering principles applied to solution photochemistry: Controlling the photodimerization of stilbazolium salts within γ-cyclodextrin and cucurbit[8]uril in water. *Photochem. Photobiol. Sci.* **2007**, *6*, 737-740.

[92] M. Pattabiraman, L. S. Kaanumalle, A. Natarajan, V. Ramamurthy. Regioselective photodimerization of cinnamic acids in water: Templation with cucurbiturils. *Langmuir* **2006**, *22*, 7605-7609.

[93] T. Utsuki, F. Hirayama, K. Uekama. Different photodimerization behavior of tranilast in α-cyclodextrin, β-cyclodextrin and γ-cyclodextrin complexes - cavity-size and stoichiometry dependence. *J. Chem. Soc., Perkin Trans. 2* **1993**, 109-114.

[94] F. Hirayama, T. Utsuki, K. Uekama. Stoichiometry-dependent photodimerization of tranilast in A γ-cyclodextrin inclusion complex. *Chem. Commun.* **1991**, 887-888.

[95] K. Muthuramu, V. Ramamurthy. Photo-dimerization of coumarin in aqueous and micellar media. *J. Org. Chem.* **1982**, *47*, 3976-3979.

[96] K. Muthuramu, N. Ramnath, V. Ramamurthy. Photo-dimerization of coumarins in

micelles - limitations of alignment effect. *J. Org. Chem.* **1983**, *48*, 1872-1876.

[97] X. L. Yu, D. Scheller, O. Rademacher, T. Wolff. Selectivity in the photodimerization of 6-alkylcoumarins. *J. Org. Chem.* **2003**, *68*, 7386-7399.

[98] T. Wolff, H. Gorner. Photodimerization of coumarin revisited: Effects of solvent polarity on the triplet reactivity and product pattern. *Phys. Chem. Chem. Phys.* **2004**, *6*, 368-376.

[99] Y. Tanaka, S. Sasaki, A. Kobayashi. Solid-state photoreaction on an inclusion compound of coumarin with β-cyclodextrin. *J. Inclusion Phenom. Macrocyclic Chem.* **1984**, *2*, 851-860.

[100] K. Tanaka, F. Toda, E. Mochizuki, N. Yasui, Y. Kai, I. Miyahara, K. Hirotsu. Enantioselective single-crystal-to-single-crystal photodimerization of coumarin and thiocoumarin in inclusion complexes with chiral host compounds. *Angew. Chem. Int. Ed. Engl.* **1999**, *38*, 3523-3525.

[101] T. J. Brett, J. M. Alexander, J. J. Stezowski. Chemical insight from crystallographic disorder-structural studies of supramolecular photochemical systems. Part 2. The β-cyclodextrin-4,7-dimethylcoumarin inclusion complex: A new β-cyclodextrin dimer packing type, unanticipated photoproduct formation, and an examination of guest influence on β-CD dimer packing. *J. Chem. Soc., Perkin Trans. 2* **2000**, *6*, 1095-1103.

[102] T. J. Brett, J. M. Alexander, J. J. Stezowski. Chemical insight from crystallographic disorder-structural studies of supramolecular photochemical systems. Part 3. The β-cyclodextrin-7-hydroxy-4-methylcoumarin inclusion complex: Direct observation of photodimerization by X-ray crystallography. *J. Chem. Soc., Perkin Trans. 2* **2000**, *6*, 1105-1111.

[103] N. Barooah, B. C. Pemberton, J. Sivaguru. Manipulating photochemical reactivity of coumarins within cucurbituril nanocavities. *Org. Lett.* **2008**, *10*, 3339-3342.

[104] B. C. Pemberton, N. Barooah, D. K. Srivatsava, J. Sivaguru. Supramolecular photocatalysis by confinement-photodimerization of coumarins within cucurbit[8]urils. *Chem. Commun.* **2010**, *46*, 225-227.

[105] B. C. Pemberton, R. K. Singh, A. C. Johnson, S. Jockusch, J. P. Da Silva, A. Ugrinov, N. J. Turro, D. K. Srivastava, J. Sivaguru. Supramolecular photocatalysis: Insights into cucurbit[8]uril catalyzed photodimerization of 6-methylcoumarin. *Chem. Commun.* **2011**, *47*, 6323-6325.

[106] W. G. Skene, E. Couzigne, J. M. Lehn. Supramolecular control of the template-induced selective photodimerization of 4-methyl-7-O-hexylcoumarin. *Chem. Eur. J.* **2003**, *9*, 5560-5566.

[107] K. Tanaka, T. Fujiwara. Enantioselective [2+2] photodimerization reactions of coumarins in solution. *Org. Lett.* **2005**, *7*, 1501-1503.

[108] S. Bhat, U. Maitra. Hydrogels as reaction vessels: Acenaphthylene dimerization in hydrogels derived from bile acid analogues. *Molecules* **2007**, *12*, 2181-2189.

[109] Livingst.R, K. S. Wei. Reversible photochemical dimerization of acenaphthylene. I. Reaction in liquid solutions. *J. Phys. Chem.* **1967**, *71*, 541-547.

[110] K. S. Wei, Livingst.R. Reversible photochemical dimerization of acenaphthylene. 2. Reaction in molten and crystalline phase. *J. Phys. Chem.* **1967**, *71*, 548-&.

[111] D. O. Cowan, R. L. E. Drisko. Photochimical reactions. 4. Photodimerization of acenaphthylene - mechanistic studies. *J. Am. Chem. Soc.* **1970**, *92*, 6286-6291.

[112] D. O. Cowan, R. L. E. Drisko. Photochemical reaction. 5. Photodimerization of acenaphthylene - heavy-atom solvent effects. *J. Am. Chem. Soc.* **1970**, *92*, 6281-6285.

[113] G. F. Koser, V. S. Liu. Heavy-atom effect on photo-dimerization of acenaphthylene - substituent analysis on efficiency of external aromatic perturbers. *J. Org. Chem.* **1978**, *43*, 478-481.

[114] N. Haga, H. Takayanagi, K. Tokumaru. Mechanism of photodimerization of acenaphthylene. *J. Org. Chem.* **1997**, *62*, 3734-3743.

[115] B. F. Plummer, M. J. B. Moore, J. Wright. Photochemical dimerization of acephenanthrylene and the heavy atom effect. *J. Org. Chem.* **2000**, *65*, 450-452.

[116] V. Ramamurthy. Synthetic chemistry: A perfect fit. *Nature* **2003**, *423*, 394-394.

[117] R. C. Santos, C. E. S. Bernardes, H. P. Diogo, A. F. M. Piedade, J. N. C. Lopes, M. E. M. da Piedade. Energetics of the thermal dimerization of acenaphthylene to heptacyclene. *J. Phys. Chem. A* **2006**, *110*, 2299-2307.

[118] V. Ramamurthy, S. Arumugam, L. S. Kaanumalle. Alkali ion exchanged nafion as a confining medium for photochemical reactions. *Photochem. Photobiol.* **2006**, *82*, 139-145.

[119] M. Yoshizawa, Y. Takeyama, T. Kusukawa, M. Fujita. Cavity-directed, highly stereoselective [2+2] photodimerization of olefins within self-assembled coordination cages. *Angew. Chem. Int. Ed. Engl.* **2002**, *41*, 1347-1349.

[120] S. Karthikeyan, V. Ramamurthy. Self-assembled coordination cage as a reaction vessel: Triplet sensitized [2+2] photodimerization of acenaphthylene, and [4+4] photodimerization of 9-anthraldehyde. *Tetrahedron Lett.* **2005**, *46*, 4495-4498.

[121] L. S. Kaanumalle, V. Ramamurthy. Photodimerization of acenaphthylene within a nanocapsule: Excited state lifetime dependent dimer selectivity. *Chem. Commun.* **2007**, 1062-1064.

[122] L. Lei, L. Luo, X. L. Wu, G. H. Liao, L. Z. Wu, C. H. Tung. Cucurbit[8]uril-mediated photo dimerization of alkyl 2-naphthoate in aqueous solution. *Tetrahedron Lett.* **2008**, *49*, 1502-1505.

[123] L. Luo, G. H. Liao, X. L. Wu, L. Lei, C. H. Tung, L. Z. Wu. γ-cyclodextrin-directed enantioselective photocyclodimerization of methyl 3-methoxyl-2-naphthoate. *J. Org. Chem.* **2009**, *74*, 3506-3515.

[124] L. Luo, S. F. Cheng, B. Chen, C. H. Tung, L. Z. Wu. Stepwise photochemical-chiral delivery in γ-cyclodextrin-directed enantioselective photocyclodimerization of methyl 3-methoxyl-2-naphthoate in aqueous solution. *Langmuir* **2010**, *26*, 782-785.

[125] X. L. Wu, L. Luo, L. Lei, G. H. Liao, L. Z. Wu, C. H. Tung. Highly efficient cucurbit[8]uril-templated intramolecular photocycloaddition of 2-naphthalene-labeled poly(ethylene glycol) in aqueous solution. *J. Org. Chem.* **2008**, *73*, 491-494.

[126] H. D. Becker. Unimolecular photochemistry of anthracenes. *Chem. Rev.* **1993**, *93*, 145-172.

[127] T. Tamaki, T. Kokubu. Acceleration of the photodimerization of water-soluble anthracenes included by β-and γ-cyclodextrins. *J. Inclusion Phenom. Macrocyclic Chem.* **1984**, *2*, 815-822.

[128] A. Ueno, F. Moriwaki, T. Osa, F. Hamada, K. Murai. Association, photodimerization, and induced-fit types of host-guest complexation of anthracene-appended γ-cyclodextrin derivatives. *J. Am. Chem. Soc.* **1988**, *110*, 4323-4328.

[129] A. Ueno, F. Moriwaki, Y. Iwama, I. Suzuki, T. Osa, T. Ohta, S. Nozoe. γ-cyclodextrin template method for controlling stereochemistry of bimolecular interactions and reactions. *J. Am. Chem. Soc.* **1991**, *113*, 7034-7036.

[130] J. Mizoguchi, Y. Kawanami, T. Wada, K. Kodama, K. Anzai, T. Yanagi, Y. Inoue. Enantiodifferentiating photocyclodimerization of 2-anthracenecarboxylic acid using a chiral n-(2-hydroxymethyl-4-pyrrolidinyl)benzamide template. *Org. Lett.* **2006**, *8*, 6051-6054.

[131] Y. Kawanami, T. C. S. Pace, J. Mizoguchi, T. Yanagi, M. Nishijima, T. Mori, T. Wada, C. Bohne, Y. Inoue. Supramolecular complexation and enantiodifferentiating photocyclodimerization of 2-anthracenecarboxylic acid with 4-aminoprolinol derivatives as chiral hydrogen-bonding templates. *J. Org. Chem.* **2009**, *74*, 7908-7921.

[132] L. S. Kaanumalle, C. L. D. Gibb, B. C. Gibb, V. Ramamurthy. A hydrophobic nanocapsule controls the photophysics of aromatic molecules by suppressing their favored solution pathways. *J. Am. Chem. Soc.* **2005**, *127*, 3674-3675.

[133] C. Yang, T. Mori, Y. Origane, Y. H. Ko, N. Selvapalam, K. Kim, Y. Inoue. Highly stereoselective photocyclodimerization of α-cyclodextrin-appended anthracene mediated by γ-cyclodextrin and cucurbit[8]uril: A dramatic steric effect operating outside the binding site. *J. Am. Chem. Soc.* **2008**, *130*, 8574-8575.

[134] M. Okada, Y. Takashima, A. Harada. One-pot synthesis of γ-cyclodextrin polyrotaxane: Trap of γ-cyclodextrin by photodimerization of anthracene-capped pseudo-polyrotaxane. *Macromolecules* **2004**, *37*, 7075-7077.

[135] M. Okada, A. Harada. Preparation of β-cyclodextrin polyrotaxane: Photodimerization of pseudo-polyrotaxane with 2-anthryl and triphenylmethyl groups at the ends of poly(propylene glycol). *Org. Lett.* **2004**, *6*, 361-364.

[136] T. Tamaki, T. Kokubu, K. Ichimura. Regioselective and stereoselective photodimerization of anthracene-derivatives included by cyclodextrins. *Tetrahedron* **1987**, *43*, 1485-1494.

[137] T. Tamaki. Reversible photodimerization of water-soluble anthracenes included in γ-cyclodextrin. *Chem. Lett.* **1984**, 53-56.

[138] T. Tamaki, Y. Kawanishi, T. Seki, M. Sakuragi. Triplet sensitization of anthracene photodimerization in γ-cyclodextrin. *J. Photoch. Photobio. A* **1992**, *65*, 313-320.

[139] S. Tamagaki, K. Fukuda, H. Maeda, N. Mimura, W. Tagaki. Complexation and photodimerization of anthracene-2-sulfonate in the presence of per-6-aminocyclodextrins. *J. Chem. Soc., Perkin Trans. 2* **1995**, 389-393.

[140] A. Nakamura, Y. Inoue. Supramolecular catalysis of the enantiodifferentiating [4+4] photocyclodimerization of 2-anthracenecarboxylate by γ-cyclodextrin. *J. Am. Chem. Soc.* **2003**, *125*, 966-972.

[141] C. Yang, M. Nishijima, A. Nakamura, T. Mori, T. Wada, Y. Inoue. A remarkable stereoselectivity switching upon solid-state versus solution-phase enantiodifferentiating photocyclodimerization of 2-anthracenecarboxylic acid mediated by native and 3,6-anhydro-γ-cyclodextrins. *Tetrahedron Lett.* **2007**, *48*, 4357-4360.

[142] C. Yang, A. Nakamura, G. Fukuhara, Y. Origane, T. Mori, T. Wada, Y. Inoue. Pressure and temperature-controlled enantiodifferentiating [4+4] photocyclodimerization of 2-anthracenecarboxylate mediated by secondary face- and skeleton-modified γ-cyclodextrins. *J. Org. Chem.* **2006**, *71*, 3126-3136.

[143] C. F. Ke, C. Yang, T. Mori, T. Wada, Y. Liu, Y. Inoue. Catalytic enantiodifferentiating

photocyclodimerization of 2-anthracenecarboxylic acid mediated by a non-sensitizing chiral metallosupramolecular host. *Angew. Chem. Int. Ed. Engl.* **2009**, *48*, 6675-6677.

[144] C. Yang, G. Fukuhara, A. Nakamura, Y. Origane, K. Fujita, D. Q. Yuan, T. Mori, T. Wada, Y. Inoue. Enantiodifferentiating [4+4] photocyclodimerization of 2-anthracenecarboxylate catalyzed by 6(A),6(X)-diamino-6(A),6(X)-dideoxy-γ-cyclodextrins: Manipulation of product chirality by electrostatic interaction, temperature and solvent in supramolecular photochirogenesis. *J. Photoch. Photobio. A* **2005**, *173*, 375-383.

[145] A. Nakamura, Y. Inoue. Electrostatic manipulation of enantiodifferentiating photocyclodimerization of 2-anthracenecarboxylate within γ-cyclodextrin cavity through chemical modification. Inverted product distribution and enhanced enantioselectivity. *J. Am. Chem. Soc.* **2005**, *127*, 5338-5339.

[146] H. Ikeda, T. Nihei, A. Ueno. Stereoselective photodimerization of 2-anthracenecarboxylic acid using a cation-charged γ-cyclodextrin template. *J. Inclusion Phenom. Macrocyclic Chem.* **2004**, *50*, 63-66.

[147] H. Ikeda, T. Nihei, A. Ueno. Template-assisted stereoselective photocyclodimerization of 2-anthracenecarboxylic acid by bispyridinio-appended γ-cyclodextrin. *J. Org. Chem.* **2005**, *70*, 1237-1242.

[148] C. Yang, A. Nakamura, T. Wada, Y. Inoue. Enantiodifferentiating photocyclodimerization of 2-anthracenecarboxylic acid mediated by γ-cyclodextrins with a flexible or rigid cap. *Org. Lett.* **2006**, *8*, 3005-3008.

[149] C. Yang, T. Mori, Y. Inoue. Supramolecular enantiodifferentiating photocyclodimerization of 2-anthracenecarboxylate mediated by capped γ-cyclodextrins: Critical control of enantioselectivity by cap rigidity. *J. Org. Chem.* **2008**, *73*, 5786-5794.

[150] R. B. Wang, L. N. Yuan, D. H. Macartney. Cucurbit[7]uril mediates the stereoselective [4+4] photodimerization of 2-aminopyridine hydrochloride in aqueous solution. *J. Org. Chem.* **2006**, *71*, 1237-1239.

[151] M. Lubomska, P. Gierycz, M. Rogalski. Enhancement of the anthracene aqueous solubility by a synergistic effect of alcohols and β-cyclodextrin. *Fluid Phase Equilib.* **2005**, *238*, 39-44.

[152] X. Wang, M. L. Brusseau. Cyclopentanol-enhanced solubilization of polycyclic aromatic hydrocarbons by cyclodextrins. *Environ. Sci. Technol.* **1995**, *29*, 2346-2351.

2 Solubilization of Polycyclic Aromatics in Water by *γ*-Cyclodextrin Derivatives

Abstract: A series of hydrophilic per-6-thio-6-deoxy-*γ*-cyclodextrins (CDs) were synthesized from per-6-iodo-6-deoxy-*γ*-CD. These new hosts were able to solubilize polycyclic aromatic guests in aqueous solution to much higher extents than native CDs. Phase-solubility diagrams were mostly linear in accordance with both 1:1 and 1:2 CD-guest complexes in aqueous solution. The stoichiometry of the inclusion complexes was further investigated by fluorescence spectroscopy, which revealed very pronounced Stokes shifts typical for 1:2 complexes. This finding was further consolidated by quantum mechanical calculations of dimer formation of the guests and space-filling considerations by using the cross-sectional areas of the CDs and guests. The calculated dimerization energies correlated well with the binding free energies measured for the 1:2 complexes, and provided the main contribution to the driving force of complexation in the *γ*-CD cavity.

Keywords: cyclodextrin • polycyclic aromatics • dimer formation • inclusion • fluorescence

2.1 Introduction

Comprising a hydrophilic shell and a relatively hydrophobic cavity, CDs solubilize hydrophobic organic compounds through the formation of water-soluble inclusion complexes mainly driven by hydrophobic interaction.[1-3] There are indeed many reports on the solubility enhancements of hydrophobic or amphiphilic guests, including pharmaceutical drugs, by CDs in aqueous solution.[3-4] But, due to the limited water solubilities of native CDs, the solubility enhancements reached by native CDs are generally small. However, modi-

fications on the free hydroxyl groups of native CDs with appropriate function groups[2,5-6] may not only significantly increase the water solubility of CDs, but also greatly increase the ability of CDs to form inclusion complexes with guest molecules. For instance, methylated *β*-CD and 2-hydroxypropyl-*β*-CD are superior in solubilization of drugs compared to native *β*-CD.[2] CD sulfonates[7] perform even better than the neutral derivatives especially for the solubilization of hydrophobic guests like naphthalene (**NAP**) in water.[5] Recently, we found a new class of hydrophilic per-6-deoxy-thioethers of *β*-CD, which showed excellent solubilization ability and exceptionally high binding constants for *p*-disubstituted benzene derivatives and camptothecin in water.[8-9] The higher hydrophobicity of sulphur compared to oxygen, leading to an extension of the hydrophobic cavity, and the additional Coulomb interactions, were attributed to the observed high binding potentials of *β*-CD thioethers.[8,10]

Only few efforts had presently been made to evaluate the capabilities of modified *γ*-CD for solubility enhancements of guest molecules.[11-13] It is known, that *γ*-CD is able to accommodate two aromatic guests simultaneously within its relatively large cavity leading to inclusion compound with 1:2 stoichiometry.[14] Consequently, *γ*-CD and its derivatives are very interesting nano-vessels to carry out various bimolecular reactions especially cycloadditions.[15-25] For instance, Nakamura and Inoue reported that the host–guest ratio in the inclusion complex of *γ*-CD with 2-anthracene carboxylate in water was 1:2 based on the results from ROESY-NMR measurements.[26] Also the ROESY-NMR spectrum of the inclusion system of *γ*-CD with methyl 3-methoxyl-2-naphthoate demonstrated the existence of a complex with 1:2 stoichiometry.[17] Accordingly, regio- and stereoselective photodimerizations between two substrates, both in solution and in the solid state, had been achieved in the presence of *γ*-CD.[15,25]

However, major negative aspects of *γ*-CD that reduces the utility of *γ*-CD are the formation of poorly soluble inclusion complexes between native *γ*-CD and aromatic guests in water. In this work we report on the synthesis of highly water-soluble thioethers of *γ*-CD with flexible neutral or ionic side arms, because

we hoped that this derivatization might lead to a similar enhancement of the binding potential like observed for *β*-CD thioethers.[8-9]

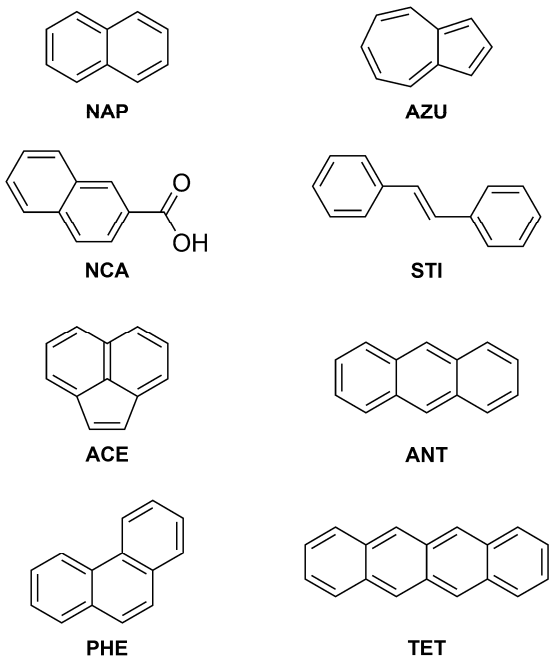

Scheme 2.1 Chemical structures of the selected polycyclic aromatic guests: naphthalene, **NAP**; 2-naphthalenecarboxylic acid, **NCA**; azulene, **AZU**; *trans*-stilbene, **STI**; acenaphthylene, **ACE**; anthracene, **ANT**; phenanthrene, **PHE**; tetracene, **TET**.

Eight polycyclic aromatics of similar size (see **Scheme 2.1**): **NAP**, 2-naphthalenecarboxylic acid (**NCA**), azulene (**AZU**), *trans*-stilbene (**STI**), acenaphthylene (**ACE**), anthracene (**ANT**), phenanthrene (**PHE**), and tetracene (**TET**) were chosen as guests to study solubility enhancements and both stabilities and stoichiometries of the complexes. It should be noted that some of the aromatic guests such as **STI** and **ANT** can serve as candidates for photo-dimerization reactions.

2.2 Results and Discussion

2.2.1 Synthesis and Characterization

Hydrophilic thioethers **1–8** at all primary carbon atoms of *γ*-CD were synthe-

sized from octakis-(6-deoxy-6-iodo)-γ-CD[27] as shown in **Scheme 2.2**. For the purpose of a rigorous purification, the octakis-iodo derivative was completely acetylated, subjected to flash chromatography, and deacetylated again. The target compounds were synthesized by nucleophilic displacement reactions in good yields. The reaction proceeded efficiently, and subsequent selective precipitation of the desired product in proper organic solvent allowed the isolation of the octakis-γ-CD derivative.

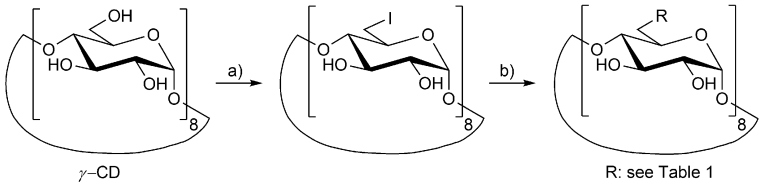

Scheme 2.2 Synthesis of octasubstituted γ-CD thioethers. a) 1. PPh_3, I_2, DMF; 2. Ac_2O, pyridine; 3. NaOMe, MeOH; b) corresponding thiol compound, triethylamine, DMF.

Table 2.1 Substituents R, yields, and solubilities of the synthesized γ-CD derivatives in g/100g water at 25°C.

No.	R	Yield [%]	Solubility [%]
1		71	21
2	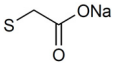	62	40
3	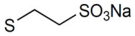	92	49
4	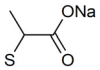	41	42
5	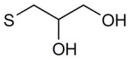	85	22
6	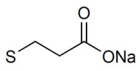	82	24
7	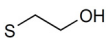	86	0.3
8	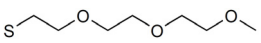	81	48

The structures of γ-CD derivatives were characterized by nuclear magnetic resonance (NMR) spectroscopy and electrospray ionization mass spectrometry (ESI-MS). Further purifications of these compounds were achieved by nanofiltration in water. Except derivative **7**, all other synthesized neutral and ionic γ-CD derivatives showed very high water solubilities. The structures of the substituents R, the obtained yields, and the aqueous solubilities of γ-CD derivatives **1-8** are summarized in **Table 2.1**.

2.2.2 Solubility Studies

Aqueous solubilities of the 8 aromatic guests (shown in **Scheme 2.1**) were measured by uv-vis spectroscopy as functions of the concentrations of hosts. These solubilities in presence of native CDs and γ-CD derivatives for a fixed host concentration 6 mM, as well as the intrinsic water solubilities of the guests, are listed in **Table 2.2**.

Table 2.2 Intrinsic water solubilities of guests and equilibrium solubilities of guests in 6.0 mM solutions of native CDs and γ-CD derivatives **1**–**8**.[a]

Host	Guest [μM]							
	NAP	**NCA**	**AZU**	**STI**	**ACE**	**ANT**	**PHE**	**TET**
water	**189**	**322**	**1.4**	**0.6**	**67**	**0.4**	**0.6**	**0.2**
α-CD	**205**	**913**	**26**	*5.0*	*85*	**2.4**	**1.9**	**0.2**
β-CD	*234*	*1460*	*65*	*17*	*105*	**4.6**	**45**	**0.3**
γ-CD	*196*	*431*	**31**	**1.5**	*103*	**1.6**	**5.9**	**0.5**
1	**2440**	*6180*	**588**	**67**	**898**	**44**	**102**	**8.9**
2	**479**	*11400*	**320**	**13**	**729**	**15**	**60**	**5.5**
3	**1590**	**3570**	**841**	**23**	**1703**	**13**	**100**	**6.8**
4	**481**	**9850**	**149**	**13**	**693**	**6.9**	**64**	**5.0**
5	*258*	**2180**	**390**	**14**	**278**	**7.4**	*56*	**3.2**
6	**1080**	**3420**	**670**	**22**	**1280**	**12**	**132**	**6.2**
7[b]	*199*	**863**	**20**	**2.0**	*95*	**0.8**	**19**	**0.2**
8	**515**	**1200**	**353**	**50**	**162**	**14**	**62**	**3.2**

[a] **Bold** characters: A_L type linear phase-solubility diagram; *italic* characters: non-linear phase-solubility diagram; [b] The concentration of CD derivative **7** was only 1.5 mM due to its low water solubility.

While the solubility enhancements caused by native CDs were quite small, significant enhancements were found for the thioethers, revealing very strong intermolecular interactions between CD derivatives **1**–**8** and these aromatic guests in water. Especially the solubilities enhancements for **NAP**, **AZU**, and **ANT** are much higher than for known CD derivatives like hydroxypropyl-β-CD.[13] The ionic hosts **1**, **3**, and **6** generally performed better than the neutral ones **5**, **7**, and **8**. Most systems show a linear increase of solubility with host concentrations, displayed in bold characters, while a few systems showing non-linear solubility enhancements, displayed in italic characters.

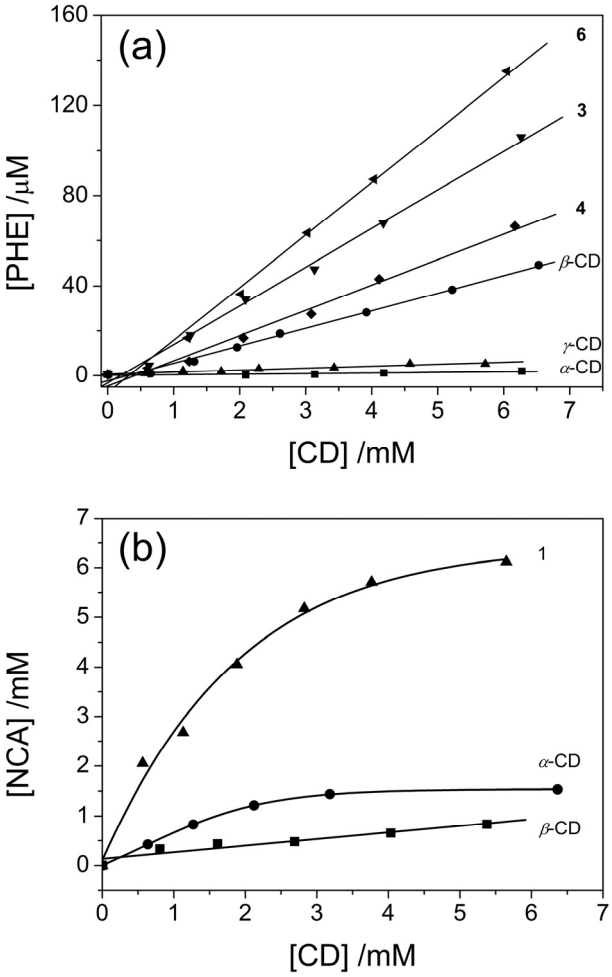

Figure 2.1 Phase-solubility diagrams for a) **PHE** and b) **NCA** in aqueous solution in presence of native CDs and γ-CD derivatives **6**, **3**, **4**, and **1**.

The discussion of so-called phase-solubility diagrams is widely used to inves-

tigate both the complex stoichiometry and binding constants of host–guest complexes. Phase-solubility diagram is obtained by plotting the observed concentration of dissolved guest versus the total concentration of host in solution. According to Higuchi and Connors, they are divided into two main categories, type A and B.[28-30] Type A curves, indicating the formation of soluble inclusion complexes, are obtained when the solubility of the guest increases with increasing CD concentration over the entire concentration range. A linear (A_L type) relationship is distinguished from positively (A_P type) or negatively (A_N type) deviating isotherms. B_s and B_I type phase-solubility diagrams represent the formation of complex with limited solubility and insoluble complex, respectively.

The obtained phase-solubility diagrams are representatively shown in **Figure 2.1**. The solubility of **PHE** increased linearly with the increasing concentrations of native CDs and ionic octasubstituted *γ*-CD derivatives **3**, **4**, and **6**, leading to an A_L type of classification, shown in **Figure 2.1a**. On the other hand, curved phase-solubility diagrams were obtained for the complexes of **NCA** in *α*-CD and *γ*-CD derivative **1** shown in **Figure 2.1b**. **NCA** exhibited a B_S-type diagram with *α*-CD in water, possibly due to a limited solubility of the formed inclusion complex.[29] The diagram of **NCA** with derivative **1** showed A_N-type curvature, which was attributed to electrostatic interaction between the amino groups of **1** and the carboxyl group of **NCA**, which might lead to aggregation of the CD inclusion complex at higher concentrations.[29,31-32] Nevertheless, most complexes in **Table 2.2** are showing the linear A_L type phase solubility diagrams, which can be interpreted by the formation of soluble 1:1, as well as 1:2 host–guest complexes.[28,33] The complex stoichiometry remained still as an open question.

2.2.3 Complex Stoichiometries

The slope *m* of the phase-solubility diagram, equivalent to the average amount of guest per host, called occupancy, gave some rough idea about the

stoichiometry of a complex. These occupancies of γ-CD cavities by the aromatic guests are listed in **Table 2.3**. Initial slopes *m* were taken for the curved phase solubility diagrams.

Table 2.3 Occupancies (in %, equal to slope *m*) of aromatic guests within γ-CD cavity.

Host	Guest[a,b]							
	NAP	**NCA**	**AZU**	**STI**	**ACE**	**ANT**	**PHE**	**TET**
γ-CD	n.d.	*5.4*	**0.5**	**0.03**	n.d.	**0.02**	**0.09**	n.d.
1	**38**	**165**	**9.7**	**1.2**	**13**	**0.7**	**1.5**	**0.1**
2	**3.9**	**167**	**6.5**	**0.2**	**11**	**0.2**	**1.1**	**0.09**
3	**31**	**55**	**16**	**0.4**	**28**	**0.2**	**1.7**	**0.1**
4	**7.7**	**123**	**2.9**	**0.2**	**11**	**0.1**	**1.2**	**0.08**
5	*12*	**30**	**6.9**	**0.3**	**3.4**	**0.1**	*1.9*	**0.05**
6	**18**	**52**	**12**	**0.4**	**21**	**0.2**	**2.3**	**0.1**
7	*30*	**34**	**1.5**	**0.2**	n.d.	**0.06**	**1.2**	n.d.
8	**10**	**15**	**5.7**	**0.9**	**2.5**	**0.2**	**1.1**	**0.05**

[a] For the non-A_L type phase-solubility diagrams, initial slopes *m* are taken, values are given in *italic*. [b] n.d. solubility enhancement of guest is not detectable.

Occupancy values of more than 100% were found for **NCA** included in CD derivatives **1**, **2**, and **4**, providing strong evidence for the existence of complexes with 1:2 stoichiometries. An occupancy of less than 100%, found in the other cases does not necessarily imply a 1:1 stoichiometry, because cooperativity of inclusion has to be taken into account. If there is a strong interaction between two included guests, a mixture of empty CDs and 1:2 CD complexes will prevail. It should be also noted, that several 1:2 complexes with γ-CD or γ-CD derivatives are already known.[16-17,25,34-35]

In order to gain further insight into the host–guest stoichiometries of the complexes, fluorescence spectroscopy was employed, because complexation of two chromophores within a CD cavity is known to cause excimer formation leading to large Stokes shifts. Excimer formation was already observed for CD complexes of **NAP**,[36] **STI**,[37-38] **ANT**,[39] and pyrene.[40-41]

Table 2.4 Absorption (λ_{ab}) and emission (λ_{em}) maxima, and stokes shift values ($\Delta\lambda$) of aromatic guests in water in presence of *β*-CD derivative *β*-**1** and *γ*-CD derivative **1** at 298 K, given in nm.

Guest	*β*-**1**			**1**			$\Delta\Delta\lambda$[a]
	λ_{ab}	λ_{em}	$\Delta\lambda$	λ_{ab}	λ_{em}	$\Delta\lambda$	
NAP	300	325	25	337	424	87	62
NCA	343	374	31	340	412	72	41
AZU	365	377	12	353	424	71	59
STI	310	356	46	351	428	77	31
ACE	354	437	83	284	408	124	41
ANT	361	406	45	294	368	74	29
PHE	357	368	11	290	367	77	66
TET	367	424	57	360	432	72	15

[a] $\Delta\Delta\lambda$ equals to the excess Stokes shift values of guests complexed in *γ*-CD derivatives **1** compared to those complexed in *β*-**1**.

The fluorescence spectra of the inclusion compounds of the aromatic guests in *γ*-CD derivative **1** showed a single emission band in each case with pronounced Stokes shifts of $\Delta\lambda$ = 71 to 124 nm, listed in **Table 2.4**. For comparison, the corresponding heptakis-[6-deoxy-6-(2-amino ethylsulfanyl)]-*β*-CD (*β*-**1**),[8,10] which only accommodates one single guest, showed much smaller Stokes shifts of $\Delta\lambda$ = 26 to 83 nm typical for dilute solutions of the fluorophores in organic solvents. Consequently, the large extra Stokes shifts $\Delta\Delta\lambda$, listed in **Table 2.4**, strongly support our hypothesis of two aromatic guests being included in the large cavity of the *γ*-CD derivative **1**. Only the $\Delta\Delta\lambda$ value for guest **TET** (15 nm) was significantly less than that for the other guests. Therefore 1:2 CD–guest complexes were less likely been formed in this case.

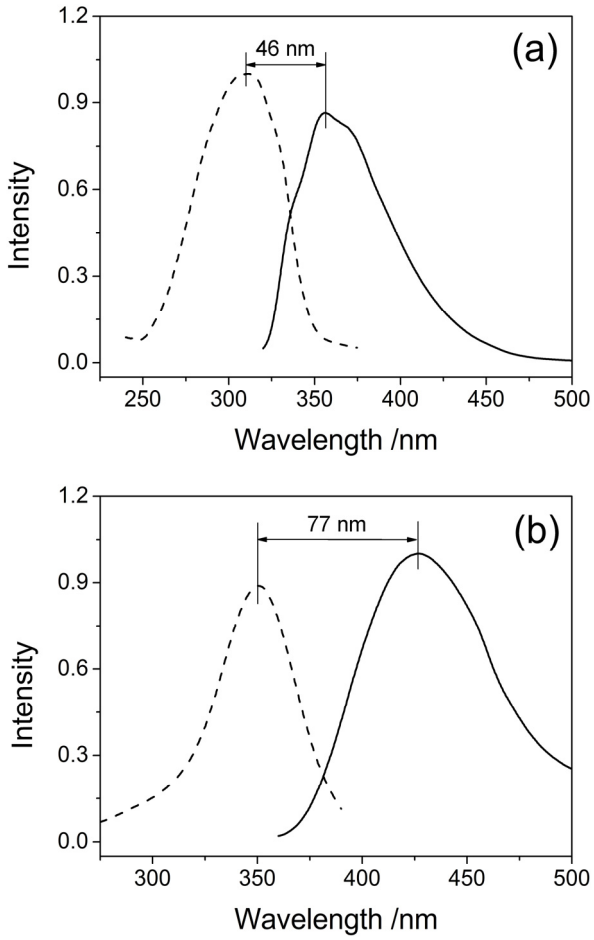

Figure 2.2 Absorption (dashed line) and emission (solid line) spectra of the inclusion system of a) **STI** with *β*-**1** and b) CD **1** in water solution.

Typical absorption and emission spectra of **STI** in presence of CD derivatives in aqueous solution are shown as examples in **Figure 2.2**. A small Stokes shift (Δλ = 46 nm) was found for **STI** complexed in *β*-**1**, while a large Stokes shift (Δλ = 77 nm) was observed for **STI** in *γ*-CD derivative **1**. Both emission bands were narrow and monomodal, demonstrating that only one species of stilbene complex existed in each case, namely the 1:1 and the 1:2 complexes, respectively. This finding was in contrast to the fluorescence spectra obtained for the complex of naphthalene in native *β*-CD, where a broad bimodal fluorescence was found.[36] The formation of a 2:2 complex was discussed for the **NAP**–*β*-CD system. This model appeared implausible for the complexes of aromatic guests in *γ*-CD derivatives described here, because narrow excimer emission bands were already observed for very low concentrations of *γ*-CD derivative **1**. For a

further clarification of the stoichiometries of complexes of γ-CD derivatives **1**–**8** molecular packing was investigated by molecular modeling studies.

2.2.4 Molecular Modeling

Although the modification of γ-CD on the primary rim with side arms changes the height of γ-CD, the internal diameter *d* of the γ-CD should remain unaffected. According to this view, γ-CD was selected as a simple model host throughout the theoretical calculations. Quantum mechanical calculations were employed in order to get the inner surface (electron density map) of γ-CD cavity. The cross-sectional area *A* of the γ-CD cavity was obtained by analysis of the electron density map of γ-CD with the program MolShape,[42] which was already useful for prediction of stoichiometries of polyrotaxanes.[14] Thus, the corresponding profile of the inner width *d* of the γ-CD cavity along the C_8 axis was obtained.

Table 2.5 In plane areas *A* and maximum cross-sectional areas A_{max}, in Å^2 in direction of the long axis and short axis of the molecule of the aromatic guest molecules.

	Guest							
	NAP	**NCA**	**AZU**	**STI**	**ACE**	**ANT**	**PHE**	**TET**
A_{max} long axis	31.4	62.0	40.2	82.3	31.4	64.3	64.3	100.0
A_{max} short axis	20.0	23.4	22.7	19.9	28.5	21.6	24.1	21.6
A in plane	55.0	65.0	55.5	78.4	61.7	62.8	72.0	90.3

The maximum inner diameter (cross-sectional area) at the secondary rim of γ-CD was determined to d_{max} = 10.3 Å (A_{max} = 83.5 Å^2). The minimum internal diameter d_{min} = 8.0 Å (A_{min} = 50.6 Å^2), situated approximately at hydrogens H-5 of γ-CD cavity was found, which was in good accordance with the results of both experimental measurements and other theoretical calculations.[43-44] Similarly, the maximum cross-sectional areas A_{max} of the aromatic guests were calculated, both in direction of the short and the long axis of the molecule, and also the areas *A* in plane of the molecules, summarized in **Table 2.5**. The

dimeric aromatic guest can fit principally in three possible orientations, with long axis, short axis, and both axes perpendicular to the C_8-axis in the γ-CD cavity, depicted in **Scheme 2.3**. From these calculations it became obvious, that all guests can be accommodated in the complete γ-CD cavity as dimers with their short axis oriented perpendicular to the C_8-axis (**Scheme 2.3b**), because twice of the corresponding cross-sectional area A_{max} of the guest is less or equal to the minimum cross-sectional area A_{min} = 50.6 Å^2 of the host. The predominance of this orientation is in accordance with other experimental results.[17-19,25] The other orientations are not possible because of geometrical constraints. The smaller dimensions of the β-CD cavity, A_{min} = 34.6 Å^2 and A_{max} = 60.4 Å^2 explain, why the **NAP** dimer can only protrude partially in it, which leads to the formation of 2:2 complexes, necessary for a complete coverage of the dimer.[36]

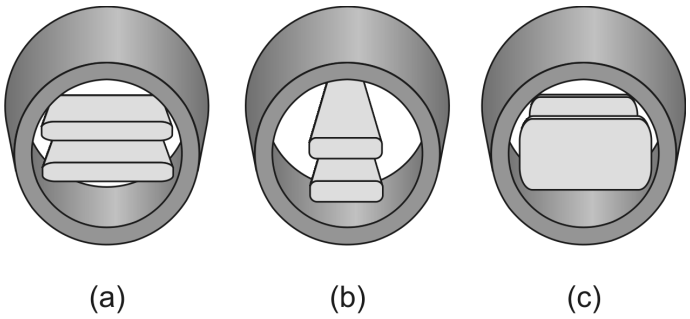

Scheme 2.3 Schematic drawing depicting the top view of 1:2 γ-CD complexes for three possible orientations: (a) long axis, (b) short axis, and (c) both axis perpendicular to the C_8-axis of γ-CD.

Quantum mechanical calculations of the structures and interaction energies ΔE of the aromatic dimers were performed using the Gaussian 03 software package.[45] Former experimental and theoretical investigations on the aromatic dimers indicated that generally the dimers with largest overlapping areas would have the most negative values of intermolecular interaction energy. Accordingly, in this work, two starting orientations of the aromatic dimers were considered, *i.e.*, the parallel ↑↑ and anti-parallel ↑↓ orientations. Given that dispersion forces are known to play an important role in the energetics of

aromatic dimers, it is imperative that the calculation of the energies has to be made at the level of second-order Møller-Plesset perturbation theory MP2.[46] The aromatic dimers were fully optimized at the MP2/6-31G* level without any symmetry restriction during the computation. The resulting interaction energies ΔE, the center of mass distances d, and the maximum cross-sectional areas A_{max} in direction of the short axis are collected in **Table 2.6**.

Table 2.6 The intermolecular interaction energies (ΔE) and the distances d of the mass centers of the two guests within the dimer, and the calculated maximal cross-sectional areas (A_{max}) of the optimized aromatic dimers.

Dimer[a]	ΔE [kJ·mol^{-1}]	d [Å]	A_{max} [Å^2]
NAP	–17.8	3.64	44.8
NCA (dimer ↑↓)	–18.0	3.69	52.3
AZU (dimer ↑↑)	–21.8	3.60	52.0
AZU (dimer ↑↓)	–34.6	3.29	51.0
STI	–22.3	3.91	57.1
ACE (dimer ↑↑)	–20.5	3.54	53.1
ACE (dimer ↑↓)	–29.2	3.18	52.0
ANT	–31.0	3.65	49.6
PHE (dimer ↑↑)	–27.6	3.86	56.8
PHE (dimer ↑↓)	–21.9	3.85	66.7

[a] For **NCA** dimer ↑↑, a T-shaped orientation was obtained after optimization.

The interaction energy ΔE became more negative with increasing size of the molecule, and was in good accordance with the published data reported by Grimme.[46-47] Remarkable differences in ΔE values of the aromatic dimers which possess two stable orientations were clearly observed from **Table 2.6**. For instance, the ΔE value of **NCA** dimer with anti-parallel orientation was found to be significantly more negative than that of the dimer with parallel orientation. This result can be attributed to the additional dipole-dipole interaction between the two monomers in the anti-parallel orientation. Similar phenomena also occurred for the aromatic dimers of **AZU** and **ACE**. The corresponding distances d between two monomers in these parallel-configured

dimers were found to be remarkable larger than those of the monomers with anti-parallel orientation. Contrarily, the interaction energy of the parallel-oriented dimer of **PHE** was more negative than the one of the anti-parallel dimer. It appeared reasonable, that the relative poor overlap between two **PHE** molecules in the anti-parallel dimer caused this result.[48]

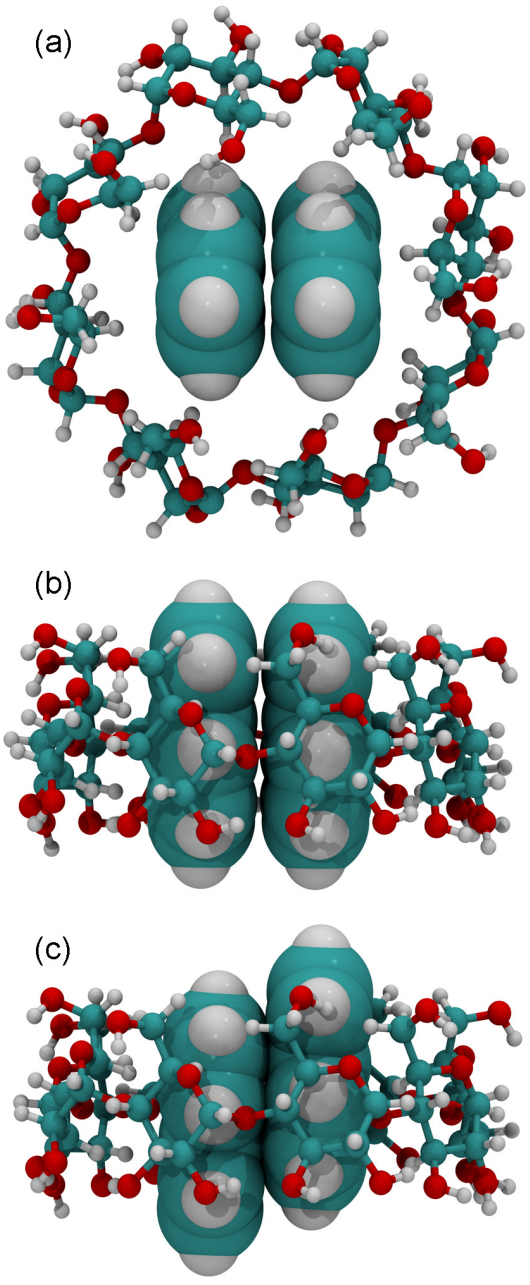

Figure 2.3 Schematic drawing depicting of **AZU** dimer in γ-CD: a) top view, b) side view ↑↑ orientation, and c) side view ↑↓ orientation.

It has to be noted that the cross-sectional areas A_{max} derived from the calculated structures of the dimers are larger than twice of the calculated cross-sectional area of the corresponding monomer. But these more realistic A_{max} values from **Table 2.6** are still small enough to fit in the γ-CD cavity.

The packing of **AZU** dimer in the γ-CD cavity is represented as an example in **Figure 2.3**. This dimer fits well into the cavity of γ-CD without steric hindrance. As can be seen, both orientations within the dimer, parallel (**Figure 2.3b**) and anti-parallel (**Figure 2.3c**) were perfectly accommodated into the cavity of γ-CD. The anti-parallel orientation of **AZU** appears to be more probable, because of its more negative ΔE value. Consequently, taking together all facts like the very good space filling of the γ-CD cavity, the sufficiently large negative values of ΔE and the observed large Stokes shifts the formation of 1:2 host-guest complexes became evident. After determination of the stoichiometry, binding constants and binding free energies could be finally calculated.

2.2.5 Binding Free Energy

Binding constants K and binding free energies ΔG were calculated from the slope m of the solubility isotherm and the solubilities of the free guests in water according to the following equations:

The increase in water solubility of guest molecule is due to the intermolecular interactions between guest molecule and CD to form soluble complexes.[2,29,49] The binding constants ($K_{1:n}$) for the formation of 1:n inclusion complex between CD and guest molecule can be expressed as Equation (2).

$$K_{1:n} = \frac{[\mathrm{HG}]}{[\mathrm{H}]\cdot[\mathrm{G}]^n} \tag{2}$$

where n is the guest–host ratio, [H], [G], and [HG] are the concentrations of the free CD, the free guest and the corresponding inclusion complex, respectively.

Assuming that the concentration of the free guest in CD solution is equal to that in pure water $[G]_0$, the following equations can be obtained:[50]

$$[G] = [G]_0 \quad (3)$$

$$[HG] = (1/n) \cdot ([G]_t - [G]_0) \quad (4)$$

$$[H] = [H]_t - [HG] \quad (5)$$

where $[G]_0$ is the equilibrium solubility of guest in pure water, $[H]_t$ and $[G]_t$ correspond to the total concentrations of CD and guest, respectively.

Substituting Equations (3–5) into Equation (2) affords Equation (6):

$$K_{1:n} = \frac{[G]_t - [G]_0}{[G]_0{}^n \cdot ([H]_t - ([G]_t - [G]_0)/n)} \quad (6)$$

The slope (*m*) of the dependence line is represented by Equation (7) as follows:

$$m = \frac{[G]_t - [G]_0}{[H]_t} \quad (7)$$

A plot of $[G]_t$ against $[H]_t$ yields a straight line. Thus, the binding constant between CD and guest can be calculated from the phase diagrams using Equation (8):

$$K_{1:n} = \frac{m}{[G]_0{}^n \cdot (n - m)} \quad (8)$$

The binding free energy (ΔG) is calculated according to Equation (9):

$$\Delta G = -RT \ln K \quad (9)$$

The calculated ΔG values of the aromatic guests with γ-CD or γ-CD derivatives are summarized in **Table 2.7**. As discussed above, since **TET** is less likely to form an 1:2 inclusion complex with γ-CD or γ-CD derivatives, it was taken off from discussion. Pronounced differences between the ΔG values were observed for the various guests. Guests **AZU**, **ANT**, and **PHE** showed more negative ΔG values (around –55 kJ·mol^{-1}) than **NAP** and **NCA** (around –35 kJ·mol^{-1}) in good correlation with the more negative interaction energies ΔE of **AZU**, **ANT**, and **PHE** dimers (around –31 kJ·mol^{-1}) compared to **NAP** and **NCA** (around –19 kJ·mol^{-1}). This means that the interaction energy of the dimer provides a major contribution to binding free energy. Despite of its strongly

negative ΔE value, **ACE** only shows a moderate ΔG value, which might be due to its large cross-sectional area along its short axis, which might lead to a very tight fit within the *γ*-CD cavity. In previous work we already found out, that a loose fit of a guest in a CD cavity leads to a higher binding constant than a tight fit, possibly due to entropic effects.[42] These entropic effects would also explain why the slim guest **STI** shows a strongly negative ΔG value while its ΔE value is only moderate.

Table 2.7 Binding free energies (ΔG, in kJ·mol^{-1}) for the complexation of aromatic guests in *γ*-CD and *γ*-CD derivatives at 298 K.

Host	Guest[a]						
	NAP	**NCA**	**AZU**	**STI**	**ACE**	**ANT**	**PHE**
γ-CD	–	*–31.0*	**–51.6**	**–48.9**	–	**–50.3**	**–52.1**
1	**–38.9**	–	**–59.3**	**–58.5**	**–40.9**	**–59.1**	**–59.2**
2	**–32.8**	**–43.9**	**–58.3**	**–54.1**	**–40.7**	**–56.4**	**–58.4**
3	**–38.3**	**–37.4**	**–60.7**	**–56.0**	**–43.2**	**–56.1**	**–59.6**
4	**–34.5**	**–41.0**	**–56.3**	**–54.3**	**–40.6**	**–54.4**	**–58.7**
5	*–35.8*	**–35.5**	**–58.5**	**–54.8**	**–37.6**	**–54.6**	*–57.7*
6	**–36.8**	**–37.3**	**–59.9**	**–55.9**	**–42.4**	**–56.0**	**–60.4**
7	*–38.2*	**–35.9**	**–54.6**	**–53.4**	–	**–52.0**	**–53.0**
8	**–35.2**	**–33.7**	**–58.0**	**–57.9**	**–36.8**	**–56.4**	**–58.6**

[a] ΔG values given in *italic* were calculated on the basis of the initial slope *m* of the phase-solubility diagrams.

2.3 Conclusion

In the present work, we have synthesized and characterized a series of octasubstituted *γ*-CD derivatives with various neutral or ionic side arms bound via thioether linkages to the CD scaffold. It was found that these *γ*-CD derivatives showed much higher solubilization abilities for aromatic guests than native CDs or other frequently used derivatives like hydroxypropyl-*β*-CD. The existence of 1:2 host guest complexes was confirmed from the phase-solubility data, the excimer emissions, as well as theoretical investigations. The ΔG values

of the CD–guest complexes obtained from the solubility data are strongly negative, because the interaction energy between the included guests delivers a main contribution to the driving force of complex formation.

These γ-CD derivatives are good candidates as molecular reaction vessels for photodimerization reactions of native polycyclic aromatic molecules in aqueous solution. The significantly enhanced solubilities of the aromatic guests in water would allow photodimerization of these guests under homogenous conditions for the first time. The kinetics as well as the stereo- and region-selectivities[51] of the photodimerizations of these guests mediated by the γ-CD derivatives will be investigated in our future works.

2.4 Experimental Section

2.4.1 General

Unless otherwise stated, all chemicals were used as received. Corresponding thiol compounds for the synthesis of γ-CD derivatives **1–7** were purchased from Sigma Aldrich. The thiol compound for synthesis of **8** was synthesized and purified according to a published procedure.[52]

Solvents were dried as follows: DMF over P_2O_5 and distilled, pyridine over KOH, methanol distilled from iodine and magnesium turnings immediately before use.[53] α-, β-, and γ-CD were dried *in vacuo* at 100°C overnight. γ-CD derivatives were purified by nanofiltration (molecular weight cut-off 1000 Da).

Teflon syringe filters from Roth, Karlsruhe, Germany (0.22 µm) were used to remove insoluble material before ultraviolet-visible (uv-vis) and fluorescence measurements. Thin layer chromatography (TLC) was performed on aluminum sheets coated with silica gel (F254) and developed by charring with 5% H_2SO_4 in ethanol. Electrospray ionization mass spectrometric (ESI-MS) analysis was performed on an ESI single quadrupole mass spectrometer (micromass ZQ 4000, Waters) from solutions in water. The following setting was used: capillary

voltage 3.80 kV, cone voltage 20 V, extractor voltage 5 V. Uv-vis spectra of aqueous samples were performed on a Perkin Elmer Lambda 2 spectrometer (*λ*: 200–600 nm), using quartz cells with a 1 cm or 1 mm optical path at 298 K. Fluorescence spectra were recorded in a JASCO spectrophotometer using quartz cells of 10.0 mm path at 298 K. All NMR spectra were recorded on a Bruker 400 MHz NMR Spectrometer at 298 K using the solvent peaks as internal references and coupling constants (*J*) were measured in Hz. The signals were described as s (singlet), d (doublet), t (triplet), and m (multiplet).

2.4.2 Synthesis

Octakis-[6-deoxy-iodo]-*γ*-CD (9). As shown in **Scheme 2.2**, Ph_3P (104.92 g, 400 mmol) was dissolved in anhydrous DMF (320 mL). Under N_2 atmosphere, I_2 (104.06 g, 410 mmol) was added over 15 min at 0 °C. Dry *γ*-CD (25.94 g, 20 mmol) was then added. The solution was concentrated *in vacuo* to half volume after stirring at 70°C for 24 h. NaOMe in MeOH (3 M, 160 mL) was then added under cooling and stirred for 30 min at r.t. The thick reaction mixture was poured into methanol (2.5 L) under vigorous stirring to form a brownish precipitate, which was filtered, afterwards washed with MeOH (0.5 L) and dried. The brown solid was dissolved in dry pyridine (130 mL). Ac_2O (130 mL) was added and the resulting solution was stirred for 2 d at r.t. Methanol (70 mL) was added and stirred for 1 h to quench the reaction. Using column chromatography on silica gel and EtOAc/*n*-hexane (4:1) as eluent gave a pale-yellow solid (R_f 0.2~0.3). The raw product was then suspended in anhydrous MeOH (200 mL) which contain NaOMe (0.50 g) for 4 d. **9** was recovered as a white powder after suction filtration. Yield: 28.54 g (13.1 mmol, 66%). δ_H (400 MHz, DMSO-d_6) 5.96–5.97 (d, *J* = 2.8 Hz, 8H, OH-2), 5.95 (s, 8H, OH-3), 5.02–5.03 (d, *J* = 3.6 Hz, 8H, H-1), 3.79–3.82 (d, *J* = 9.2 Hz, 8H, H-3), 3.57–3.67 (m, 16H, H-6a,b), 3.44–3.55 (m, 16H, H-4,5), 3.25–3.30 (t, *J* = 9.0 Hz, 8H, H-2). δ_C (100 MHz, DMSO-d_6) 9.25, 71.08, 71.80, 72.37, 85.24, 101.93.

General procedure for the synthesis of neutral octakis-[6-deoxy-6-(alkyl

sulfanyl)]-*γ*-CD. A procedure identical to that described previously was utilized (**Scheme 2.2**).[9] Triethylamine (3.98 mL, 28.57 mmol) and the corresponding thiol compound (28.57 mmol) were added with stirring to a solution of **9** (3.11 g, 1.43 mmol) in DMF (15 mL). After stirring for 3 d at 60°C under N_2, the crude product was diluted with sufficient amount of appropriate organic solvents. The resulting precipitate was filtered off, washed, dried *in vacuo* and then purified by ultrafiltration.

General procedure for the synthesis of ionic octakis-[6-deoxy-6-(alkyl sulfanyl)]-*γ*-CD. Triethylamine (3.98 mL, 28.57 mmol) and the corresponding methyl ester of the thiol compound (28.57 mmol) were added to a solution of compound **9** (3.11 g, 1.43 mmol) in DMF (15 mL). After stirring for 3 d at 60 °C under N_2 atmosphere, the reaction mixture was diluted with sufficient amount of appropriate organic solvents. The resulting precipitate was collected and then stirred in NaOH (1 M) for 18 h and then further purified by ultrafiltration.

Octakis-[6-deoxy-6-(2-aminoethylsulfanyl)]-*γ*-CD (1) was synthesized according to the general procedure. The crude product was precipitated in acetone, dissolved in water, ultrafiltered and lyophilized. Yield: 1.80 g (71 %), white solid. δ_H (400 MHz, D_2O) 5.17–5.18 (d, *J* = 3.6 Hz, 8H, H-1), 3.88–3.97 (m, 16H, H-3,5), 3.65–3.69 (dd, *J* = 10.0 Hz, 8H, H-2), 3.52–3.57 (t, *J* = 9.4 Hz, 8H, H-4), 2.91–3.28 (m, 16H, H-6a,6b), 2.80–2.86 (dd, *J* = 20.0 Hz, 32H, H-7,8). δ_C (100 MHz, D_2O) 35.33, 39.97, 64.56, 71.65, 72.70, 83.32, 100.01. MS (3.80 kV, ESI, water): *m/z* (%): 1769.84 (20) $[M+H]^+$, 884.40 (79) $[M+2H]^{2+}$, 589.57 (100) $[M+3H]^{3+}$.

Octakis-[6-deoxy-6-(2-sulfanyl acetic acid)]-*γ*-CD (2) was synthesized according to the general procedure. The crude product was precipitated in ethanol, stirred in 1 M NaOH for 18 h, ultrafiltered and lyophilized. Yield: 1.82 g (62%), white solid. δ_H (400 MHz, D_2O) 5.13–5.14 (d, *J* = 3.6 Hz, 8H, H-1), 4.01–4.05 (m, 8H, H-5), 3.87–3.92 (t, *J* = 9.6 Hz, 8H, H-3), 3.66–3.70 (t, *J* = 9.4 Hz, 8H, H-2), 3.59–3.62 (dd, *J* = 10.0 Hz, 8H, H-4), 3.30–3.38 (m, 16H, H-7), 2.90–3.12 (m, 16H, H-6a,6b). δ_C (100 MHz, D_2O) 33.73, 38.60, 71.37, 72.31, 72.61,

82.45, 101.19, 177.71. MS (3.80 kV, ESI, water): *m/z* (%): 1912.60 (25) $[M+Na]^+$, 967.84 (100) $[M+2Na]^{2+}$.

Octakis-[6-deoxy-6-(2-sulfanylethanesulfonic acid)]-*γ*-CD (3). 9 (3.11 g, 1.43 mmol), sodium 2-mercapto ethanesulfonate (4.60 g, 28.00 mmol) and triethylamine (3.98 mL, 28.57 mmol) were dissolved in 25 mL of DMSO. After stirring for 3 d at 60°C under N_2, the product was precipitated in acetone, dissolved in water, ultrafiltered and lyophilized; yield: 3.25 g (92%), white solid. δ_H (400 MHz, D_2O) 5.14–5.15 (d, *J* = 3.6 Hz, 8H, H-1), 4.00–4.05 (m, 8H, H-5), 3.88–3.93 (t, *J* = 9.6 Hz, 8H, H-3), 3.58–3.62 (m, 16H, H-2,4), 3.11–3.21 (m, 24H, H-6a,7), 2.91–2.99 (m, 24H, H-6b,8). δ_C (100 MHz, D_2O) 27.27, 33.27, 51.37, 71.32, 72.26, 72.68, 100.01, 100.96. MS (3.80 kV, ESI, water): *m/z* (%): 1257.66 (100) $[M+2Na]^{2+}$.

Octakis-[6-deoxy-6-(2-sulfanylpropanoic acid)]-*γ*-CD (4) was synthesized according to the general procedure. The crude product was precipitated in 2-propanol, stirred in 1 M NaOH for 18 h, ultrafiltered and lyophilized. Yield: 1.27 g (41%), white solid. δ_H (400 MHz, D_2O) 5.21–5.22 (m, 8H, H-1), 3.98–4.09 (m, 16H, H-3,5), 3.50–3.76 (m, 24H, H-2,4,7), 3.11–3.22 (m, 8H, H-6a), 2.96–2.99 (m, 8H, H-6b), 1.43–1.45 (d, *J* = 7.2 Hz, 24H, H-8). MS (3.80 kV, ESI, water): *m/z* (%): 2025.30 (65) $[M+Na]^+$, 1024.57 (100) $[M+2Na]^{2+}$.

Octakis-[6-deoxy-6-(3-sulfanylpropane-1,2-diol)]-*γ*-CD (5) was synthesized according to the general procedure. The crude product was precipitated in ethanol, dissolved in water, ultrafiltered and lyophilized. Yield: 2.44 g (85%), white solid. δ_H (400 MHz, D_2O) 5.18–5.19 (d, *J* = 3.2 Hz, 8H, H-1), 4.00–4.05 (t, *J* = 8.4 Hz, 8H, H-5), 3.90–3.95 (m, 16H, H-3,8), 3.57–3.72 (m, 32H, H-2,4,7), 3.25–3.28 (d, *J* = 12.8 Hz, 8H, H-6a), 3.00–3.03 (m, 8H, H-6b), 2.74–2.92 (m, 16H, H-9). δ_C (100 MHz, D_2O) 34.00, 35.93, 64.54, 71.04, 71.45, 72.26, 72.70, 83.32, 101.33. MS (3.80 kV, ESI, water): *m/z* (%): 2039.63 (29) $[M+Na]^+$, 1030.89 (100) $[M+2Na]^{2+}$.

Octakis-[6-deoxy-6-(3-sulfanylpropanoic acid)]-*γ*-CD (6) was synthesized

according to the general procedure. The crude product was precipitated in ethanol, stirred in 1 M NaOH for 18 h, ultrafiltered and lyophilized. Yield: 2.55 g (82%), white solid. δ_H (400 MHz, D_2O) 5.15–5.14 (d, *J* = 3.2 Hz, 8H, H-1), 4.01–4.04 (t, *J* = 8.4 Hz, 8H, H-5), 3.89–3.93 (t, *J* = 9.4 Hz, 8H, H-3), 3.58–3.64 (m, 16H, H-2,4), 2.93–3.11 (m, 16H, H-6a,b), 2.80–2.84 (t, *J* = 7.4 Hz, 16H, H-7), 2.43–2.47 (m, 16H, H-8). δ_C (100 MHz, D_2O) 29.54, 33.34, 37.75, 64.56, 71.29, 73.01, 83.56, 100.01, 180.73. MS (3.80 kV, ESI, water): *m/z* (%): 2023.63 (20) $[M+Na]^+$, 1023.89 (100) $[M+2Na]^{2+}$.

Octakis-[6-deoxy-6-(2-hydroxyethylsulfanyl)]-*γ*-CD (7) was synthesized according to the general procedure. The reaction mixture was poured into ethanol. The formed precipitate was collected by suction filtration, recrystallized in cold water and dried to give **7** (Yield: 2.19 g, 86%) as a colorless needles. δ_H (400 MHz, DMSO-d_6) 5.91 (s, 16H, OH-2,3), 4.92–4.93 (d, *J* = 3.6 Hz, 8H, H-1), 4.70–4.72 (t, *J* = 5.4 Hz, 8H, OH-9), 3.72–3.76 (m, 8H, H-5), 3.50–3.59 (m, 24H, H-2,3,4), 3.32–3.41 (m, 16H, H-7), 2.79–3.09 (m, 16H, H-6a,b), 2.62–2.67 (m, 16H, H-8). MS (3.80 kV, ESI, water): *m/z* (%): 1799.52 (65) $[M+Na]^+$, 911.37 (100) $[M+2Na]^{2+}$, 1775.88 (100) $[M–H]^–$.

Octakis-[6-deoxy-6-(10-sulfanyl-2,5,8-trioxodecane)]-*γ*-CD (8) was synthesized according to the general procedure. The crude product was precipitated in diethyl ether, ultrafiltered and lyophilized. Yield: 3.02 g (81%), white solid. δ_H (400 MHz, D_2O) 5.03–5.04 (d, *J* = 3.6 Hz, 8H, H-1), 3.71–3.80 (m, 16H, H-3,5), 3.62–3.66 (m, 16H, H-2,4), 3.40–3.59 (m, 80H, H-10), 3.29 (s, 24H, H-9), 2.80–3.25 (m, 32H, H-6,7,8). MS (3.80 kV, ESI, water): *m/z* (%): 1297.63 (35) $[M+2H]^{2+}$, 2593.48 (100) $[M–H]^–$.

2.4.3 Phase-Solubility Investigations

Since the effective polarity of CD cavity was proved to be similar to that of ethanol,[13,54-55] the molar extinction coefficients (*ε*) of **NAP**, **NCA**, **AZU**, **ACE**, **ANT**, and **PHE** were measured in ethanol. However, due to their low solubilities in ethanol, the *ε* values of **STI** and **TET** were measured in 1,4-dioxane and di-

chloromethane, respectively. The observed ε values of the aromatic guests at their absorption maxima (λ) are summarized in **Table 2.8**.

Table 2.8 Molar extinction coefficients (ε, $L \cdot mol^{-1} \cdot cm^{-1}$) of guests at the absorption maxima (λ, nm).

	Guest							
	NAP	**NCA**	**STI**	**AZU**	**ACE**	**ANT**	**PHE**	**TET**
λ	275	280	310	339	322	356	293	277
ε	5590	6950	18570	4370	9090	7350	11710	100700

Solubility measurements of the guests in presence of native CDs and γ-CD derivatives in water were carried out according to the method proposed by Higuchi and Connors.[28-30] In glass vials containing excess amounts of guest molecules, aqueous solutions of native CDs or γ-CD derivatives (concentration of CD: 1.0, 2.0, 3.0, 4.0, and 6.0 mM) were added. The vials were sealed, protected from light, and magnetically stirred at room temperature. After 72 h the solid residues were removed by filtration with syringe filter (0.22 µm). According to Lambert-Beer's law, the concentrations of guests in pure water and in CDs solutions were determined from uv-vis extinctions at the absorption maxima.

2.4.4 Molecular Modeling

All quantum mechanical calculations were carried out with Gaussian 03 software package.[45] The initial geometries of the aromatic guests were built up from their respective crystal structures[56-63] and then fully optimized without any symmetrical restrictions at the MP2/6-31G* level. The input structures of β- and γ-CD were taken from existing crystallographic data[44,64] and fully optimized by PM3 method.[65-66] The glycosidic oxygen atoms of CDs were placed onto the *xy* plane, and the center of the glycosidic oxygen atoms was designated as the origin of the Cartesian coordinate system. The secondary OH rim of CDs was placed pointing toward the positive *z*-axis. The rendering was per-

formed with VMD 1.8.7.[67]

Cross-sectional area. The electron density function was transformed into a discret cubic electron density by using the program Cubegen from Gaussian 03.[45] The cross-sectional diameters and the cross-sectional areas of CD and the guest molecules were then calculated from the cubic electron densities by the program MolShape.[42] An electron density cut-off value of 0.002 au was chosen to define the surface of the molecule.[42]

Aromatic dimer. The aromatic dimers were built up by combining two optimized monomers together, and then used as initial guesses for full geometry optimizations of the gas-phase dimers at the MP2/6-31G* level of theory. The planes of two monomers with a center-to-center distance of 3.5 Å were parallel with each other. In the present case, the geometries of the orientational isomers were fully optimized without any symmetry restriction. Interaction energies (ΔE) corresponding to the optimized aromatic dimers (parallel ↑↑ and anti-parallel ↑↓ orientation) were evaluated by $\Delta E = E_{dimer} - 2E_{monomer}$ at the MP2/6-31G* level, where E_{dimer} and $E_{monomer}$ are energies of the aromatic dimer and the monomer, respectively. ΔE values were corrected for basis set superposition error (BSSE) by means of the counterpoise correction of Boys and Bernardi.[68]

2.5 References

[1] S. Filippone, F. Heimann, A. Rassat. A highly water-soluble 2:1 β-cyclodextrin-fullerene conjugate. *Chem. Commun.* **2002**, 1508-1509.

[2] T. Loftsson, D. Hreinsdottir, M. Masson. Evaluation of cyclodextrin solubilization of drugs. *Int. J. Pharm.* **2005**, *302*, 18-28.

[3] T. Loftsson, M. Brewster. Pharmaceutical applications of cyclodextrins. 1. Drug solubilization and stabilization. *J. Pharm. Sci.* **1996**, *85*, 1017-1025.

[4] T. Loftsson, A. Magnusdottir, M. Masson, J. F. Sigurjonsdottir. Self-association and cyclodextrin solubilization of drugs. *J. Pharm. Sci.* **2002**, *91*, 2307-2316.

[5] G. Wenz, T. Hofler. Synthesis of highly water-soluble cyclodextrin sulfonates by

addition of hydrogen sulfite to cyclodextrin allyl ethers. *Carbohydr. Res.* **1999**, *322*, 153-165.

[6] J. Pitha, J. Milecki, H. Fales, L. Pannell, K. Uekama. Hydroxypropyl-β-cyclodextrin - preparation and characterization - effects on solubility of drugs. *Int. J. Pharm.* **1986**, *29*, 73-82.

[7] V. Zia, R. A. Rajewski, V. J. Stella. Effect of cyclodextrin charge on complexation of neutral and charged substrates: Comparison of (SBE)(7M)-β-CD to HP-β-CD. *Pharm. Res.* **2001**, *18*, 667-673.

[8] G. Wenz, C. Strassnig, C. Thiele, A. Engelke, B. Morgenstern, K. Hegetschweiler. Recognition of ionic guests by ionic β-cyclodextrin derivatives. *Chem. Eur. J.* **2008**, *14*, 7202-7211.

[9] A. Steffen, C. Thiele, S. Tietze, C. Strassnig, A. Kamper, T. Lengauer, G. Wenz, J. Apostolakis. Improved cyclodextrin-based receptors for camptothecin by inverse virtual screening. *Chem. Eur. J.* **2007**, *13*, 6801-6809.

[10] K. Kano, Y. Ishida, K. Kitagawa, M. Yasuda, M. Watanabe. Heat-capacity changes in host-guest complexation by Coulomb interactions in aqueous solution. *Chem. Asian J.* **2007**, *2*, 1305-1313.

[11] M. Lubomska, P. Gierycz, M. Rogalski. Enhancement of the anthracene aqueous solubility by a synergistic effect of alcohols and β-cyclodextrin. *Fluid Phase Equilib.* **2005**, *238*, 39-44.

[12] X. Wang, M. L. Brusseau. Cyclopentanol-enhanced solubilization of polycyclic aromatic hydrocarbons by cyclodextrins. *Environ. Sci. Technol.* **1995**, *29*, 2346-2351.

[13] X. Wang, M. Brusseau. Solubilization of some low-polarity organic compounds by hydroxypropyl-β-cyclodextrin. *Environ. Sci. Technol.* **1993**, *27*, 2821-2825.

[14] G. Wenz, B. H. Han, A. Müller. Cyclodextrin rotaxanes and polyrotaxanes. *Chem. Rev.* **2006**, *106*, 782-817.

[15] K. Takahashi. Organic reactions mediated by cyclodextrins. *Chem. Rev.* **1998**, *98*, 2013-2033.

[16] X. Wu, L. Lei, L. Wu, G. Liao, L. Luo, X. Shan, L. Zhang, C. Tung. Synthesis, structure, and chirality of hydroxyl-and carboxyl-functionalized cubane-like photodimers of 2-naphthalene. *Tetrahedron* **2007**, *63*, 3133-3137.

[17] L. Luo, G. H. Liao, X. L. Wu, L. Lei, C. H. Tung, L. Z. Wu. γ-cyclodextrin-directed enantioselective photocyclodimerization of methyl 3-methoxyl-2-naphthoate. *J. Org. Chem.* **2009**, *74*, 3506-3515.

[18] C. Yang, A. Nakamura, T. Wada, Y. Inoue. Enantiodifferentiating photocyclodimerization of 2-anthracenecarboxylic acid mediated by γ-cyclodextrins with a flexible or rigid cap. *Org. Lett.* **2006**, *8*, 3005-3008.

[19] A. Nakamura, Y. Inoue. Electrostatic manipulation of enantiodifferentiating photocyclodimerization of 2-anthracenecarboxylate within γ-cyclodextrin cavity through chemical modification. Inverted product distribution and enhanced enantioselectivity. *J. Am. Chem. Soc.* **2005**, *127*, 5338-5339.

[20] S. Karthikeyan, V. Ramamurthy. Self-assembled coordination cage as a reaction vessel: Triplet sensitized [2+2] photodimerization of acenaphthylene, and [4+4] photodimerization of 9-anthraldehyde. *Tetrahedron Lett.* **2005**, *46*, 4495-4498.

[21] N. Haga, H. Takayanagi, K. Tokumaru. Mechanism of photodimerization of acenaphthylene. *J. Org. Chem.* **1997**, *62*, 3734-3743.

[22] F. D. Lewis, S. V. Barancyk, E. L. Burch. Photodimerization of phenanthrene-9-carbonitrile and methyl phenanthrene-9-carboxylate. *J. Phys. Chem.* **1992**, *96*, 2548-2553.

[23] K. S. Wei, R. Livingston. Reversible photodimerization of anthracene and tetracene. *Photochem. Photobiol.* **1967**, *6*, 229-232.

[24] J. Reichwagen, H. Hopf, A. Del Guerzo, J. Desvergne, H. Bouas-Laurent. Photodimers of a soluble tetracene derivative. Excimer fluorescence from the head-to-head isomer. *Org. Lett.* **2004**, *6*, 1899-1902.

[25] W. Herrmann, S. Wehrle, G. Wenz. Supramolecular control of the photochemistry of stilbenes by cyclodextrins. *Chem. Commun.* **1997**, 1709-1710.

[26] A. Nakamura, Y. Inoue. Supramolecular catalysis of the enantiodifferentiating [4+4] photocyclodimerization of 2-anthracenecarboxylate by γ-cyclodextrin. *J. Am. Chem. Soc.* **2003**, *125*, 966-972.

[27] P. R. Ashton, R. Koniger, J. F. Stoddart, D. Alker, V. D. Harding. Amino acid derivatives of β-cyclodextrin. *J. Org. Chem.* **1996**, *61*, 903-908.

[28] R. Singh, H. H. Tonnesen, S. B. Vogensen, T. Loftsson, M. Masson. Studies of curcumin and curcuminoids. XXXVI. The stoichiometry and complexation constants of cyclodextrin complexes as determined by the phase-solubility method and uv-vis titration. *J. Inclusion Phenom. Macrocyclic Chem.* **2010**, *66*, 335-348.

[29] T. Higuchi, K. Connors. Phase-solubility techniques. *Adv. Anal. Chem. Instrum.* **1965**, *4*, 117-212.

[30] T. Higuchi, H. Kristiansen. Binding specificity between small organic solutes in

aqueous solution: Classification of some solutes into two groups according to binding tendencies. *J. Pharm. Sci.* **1970**, *59*, 1601-1608.

[31] A. Chauhan, N. Jain, P. Diwan, A. Khopade. Solubility enhancement of indomethacin with poly (amidoamine) dendrimers and targeting to inflammatory regions of arthritic rats. *J. Drug Target.* **2004**, *12*, 575-583.

[32] S. Tenjarla, P. Puranajoti, R. Kasina, T. Mandal. Preparation, characterization, and evaluation of miconazole–cyclodextrin complexes for improved oral and topical delivery. *J. Pharm. Sci.* **1998**, *87*, 425-429.

[33] H. M. Cabral Marques, J. Hadgraft, I. W. Kellaway. Studies of cyclodextrin inclusion complexes. I. The salbutamol-cyclodextrin complex as studied by phase solubility and DSC. *Int. J. Pharm.* **1990**, *63*, 259-266.

[34] T. Tamaki, T. Kokubu, K. Ichimura. Regio- and stereoselective photodimerization of anthracene derivatives included by cyclodextrins. *Tetrahedron* **1987**, *43*, 1485-1494.

[35] K. S. S. P. Rao, S. M. Hubig, J. N. Moorthy, J. K. Kochi. Stereoselective photodimerization of (*E*)-stilbenes in crystalline γ-cyclodextrin inclusion complexes. *J. Org. Chem.* **1999**, *64*, 8098-8104.

[36] G. Grabner, K. Rechthaler, B. Mayer, G. Kohler, K. Rotkiewicz. Solvent influences on the photophysics of naphthalene: Fluorescence and triplet state properties in aqueous solutions and in cyclodextrin complexes. *J. Phys. Chem. A* **2000**, *104*, 1365-1376.

[37] R. A. Agbaria, E. Roberts, I. M. Warner. Excimer fluorescence of trans-stilbene in ternary aqueous-solutions of γ-cyclodextrin. *J. Phys. Chem.* **1995**, *99*, 10056-10060.

[38] Y. Chen, Y. Tao, H. Lin. Novel self-assembled metallo-homopolymers and metallo-alt-copolymer containing terpyridyl zinc (II) moieties. *Macromolecules* **2006**, *39*, 8559-8566.

[39] N. Miyakawa, T. Kiba, S. I. Sato. Self-assembled anthracene dimers formed in aqueous solution in the presence of γ-cyclodextrin. *Mol. Cryst. Liq. Cryst.* **2010**, *520*, 469-476.

[40] K. Kano, H. Matsumoto, S. Hashimoto, M. Sisido, Y. Imanishi. Chiral pyrene excimer in the γ-cyclodextrin cavity. *J. Am. Chem. Soc.* **1985**, *107*, 6117-6118.

[41] T. Yorozu, M. Hoshino, M. Imamura. Fluorescence studies of pyrene inclusion complexes with α-, β-, and γ-cyclodextrins in aqueous solutions. Evidence for formation of pyrene dimer in γ-cyclodextrin cavity. *J. Phys. Chem.* **1982**, *86*, 4426-4429.

[42] A. Müller, G. Wenz. Thickness recognition of bolaamphiphiles by α-cyclodextrin. *Chem. Eur. J.* **2007**, *13*, 2218-2223.

[43] J. Szejtli. Introduction and general overview of cyclodextrin chemistry. *Chem. Rev.* **1998**, *98*, 1743-1753.

[44] K. Harata. The structure of the cyclodextrin complex. 20. Crystal-structure of uncomplexed hydrated γ-cyclodextrin. *Bull. Chem. Soc. Jpn.* **1987**, *60*, 2763-2767.

[45] M. J. Frisch, G. W. Trucks, H. B. Schlegel, G. E. Scuseria, M. A. Robb, J. R. Cheeseman, J. A. Montgomery, T. Vreven, K. N. Kudin, J. C. Burant, J. M. Millam, S. S. Iyengar, J. Tomasi, V. Barone, B. Mennucci, M. Cossi, G. Scalmani, N. Rega, G. A. Petersson, H. Nakatsuji, M. Hada, M. Ehara, K. Toyota, R. Fukuda, J. Hasegawa, M. Ishida, T. Nakajima, Y. Honda, O. Kitao, H. Nakai, M. Klene, X. Li, J. E. Knox, H. P. Hratchian, J. B. Cross, V. Bakken, C. Adamo, J. Jaramillo, R. Gomperts, R. E. Stratmann, O. Yazyev, A. J. Austin, R. Cammi, C. Pomelli, J. W. Ochterski, P. Y. Ayala, K. Morokuma, G. A. Voth, P. Salvador, J. J. Dannenberg, V. G. Zakrzewski, S. Dapprich, A. D. Daniels, M. C. Strain, O. Farkas, D. K. Malick, A. D. Rabuck, K. Raghavachari, J. B. Foresman, J. V. Ortiz, Q. Cui, A. G. Baboul, S. Clifford, J. Cioslowski, B. B. Stefanov, G. Liu, A. Liashenko, P. Piskorz, I. Komaromi, R. L. Martin, D. J. Fox, T. Keith, A. Laham, C. Y. Peng, A. Nanayakkara, M. Challacombe, P. M. W. Gill, B. Johnson, W. Chen, M. W. Wong, C. Gonzalez, J. A. Pople. Gaussian 03, revision E.01. **2004**.

[46] C. Gonzalez, E. C. Lim. Quantum chemistry study of the van der Waals dimers of benzene, naphthalene, and anthracene: Crossed (D_{2d}) and parallel-displaced (C_{2h}) dimers of very similar energies in the linear polyacenes. *J. Phys. Chem. A* **2000**, *104*, 2953-2957.

[47] S. Grimme. Do special noncovalent π–π stacking interactions really exist? *Angew. Chem. Int. Ed. Engl.* **2008**, *47*, 3430-3434.

[48] K. Guckian, B. Schweitzer, X. Rex, C. Sheils, D. Tahmassebi, E. Kool. Factors contributing to aromatic stacking in water: Evaluation in the context of DNA. *J. Am. Chem. Soc.* **2000**, *122*, 2213-2222.

[49] M. E. Brewster, R. Vandecruys, J. Peeters, P. Neeskens, G. Verreck, T. Loftsson. Comparative interaction of 2-hydroxypropyl-β-cyclodextrin and sulfobutylether-β-cyclodextrin with itraconazole: Phase-solubility behavior and stabilization of supersaturated drug solutions. *Eur. J. Pharm. Sci.* **2008**, *34*, 94-103.

[50] H. Takeru, L. L. John. Investigation of some complexes formed in solution by caffeine. IV. Interactions between caffeine and sulfathiazole, sulfadiazine, p-aminobenzoic acid, benzocaine, phenobarbital, and barbital. *J. Am.*

Pharmaceut. Assoc. **1954**, *43*, 349-354.

[51] J. Mizoguchi, Y. Kawanami, T. Wada, K. Kodama, K. Anzai, T. Yanagi, Y. Inoue. Enantiodifferentiating photocyclodimerization of 2-anthracenecarboxylic acid using a chiral n-(2-hydroxymethyl-4-pyrrolidinyl)benzamide template. *Org. Lett.* **2006**, *8*, 6051-6054.

[52] A. W. Snow, E. E. Foos. Conversion of alcohols to thiols via tosylate intermediates. *Synthesis* **2003**, 509-512.

[53] H. Lund, J. Bjerrum. Eine einfache methode zur darstellung wasser-freier alkohole. *Chem. Ber.* **1931**, *64*, 210-213.

[54] S. Nigam, G. Durocher. Spectral and photophysical studies of inclusion complexes of some neutral 3H-indoles and their cations and anions with β-cyclodextrin. *J. Phys. Chem.* **1996**, *100*, 7135-7142.

[55] G. S. Cox, N. J. Turro, N. C. C. Yang, M. J. Chen. Intramolecular exciplex emission from aqueous β-cyclodextrin solutions. *J. Am. Chem. Soc.* **1984**, *106*, 422-424.

[56] D. Holmes, S. Kumaraswamy, A. Matzger, K. Vollhardt. On the nature of nonplanarity in the [n] phenylenes. *Chem. Eur. J.* **1999**, *5*, 3399-3412.

[57] J. Bouwstra, A. Schouten, J. Kroon. Structural studies of the system trans-azobenzene/trans-stilbene. II. A reinvestigation of the disorder in the crystal structure of trans-stilbene, c14h12. *Acta Crystallogr., Sect. C: Cryst. Struct. Commun.* **1984**, *40*, 428-431.

[58] V. Petricek, I. Cisarova, L. Hummel, J. Kroupa, B. Brezina. Orientational disorder in phenanthrene. Structure determination at 248, 295, 339, and 344 k. *Acta Crystallogr., Sect. B: Struct. Sci.* **1990**, *46*, 830-832.

[59] A. C. Blackburn, L. J. Fitzgerald, R. Gerkin. 2-naphthoic acid at 153k. *Acta Crystallogr., Sect. C: Cryst. Struct. Commun.* **1996**, *52*, 2862-2864.

[60] J. Oddershede, S. Larsen. Charge density study of naphthalene based on X-ray diffraction data at four different temperatures and theoretical calculations. *J. Phys. Chem. A* **2004**, *108*, 1057-1063.

[61] J. Robertson, H. Shearer, G. Sim, D. Watson. The crystal and molecular structure of azulene. *Acta Crystallogr.* **1962**, *15*, 1-8.

[62] C. Brock, J. Dunitz. Temperature dependence of thermal motion in crystalline anthracene. *Acta Crystallogr., Sect. B: Struct. Sci.* **1990**, *46*, 795-806.

[63] T. Welberry. Order and disorder in acenaphthylene. *Proc. R. Soc. A* **1973**, *334*, 19-48.

[64] K. Lindner, W. Saenger. Crystal and molecular-structure of cyclohepta-amylose dodecahydrate. *Carbohydr. Res.* **1982**, *99*, 103-115.

[65] J. J. P. Stewart. Optimization of parameters for semiempirical methods. *J. Comput. Chem.* **1989**, *10*, 209-220.

[66] J. J. P. Stewart. Optimization of parameters for semiempirical method Ⅱ. Applications. *J. Comput. Chem.* **1989**, *10*, 221-264.

[67] W. Humphrey, A. Dalke, K. Schulten. VMD: Visual molecular dynamics. *J. Mol. Graph.* **1996**, *14*, 33-38.

[68] S. F. Boys, F. Bernardi. Calculation of small molecular interactions by differences of separate total energies - some procedures with reduced errors. *Mol. Phys.* **1970**, *19*, 553-566.

3 *γ*-Cyclodextrin Thioethers Mediated Solubilization and Dispersal of Fullerene C_{60} in Water

Abstract: In this work, we investigated the solubilization and dispersal of fullerene C_{60} in water. A series of hydrophilic *γ*-cyclodextrin (CD) thioethers, containing neutral and ionic side arms were selected and used as solubilizers. True molecular solutions of C_{60} in water in presence of *γ*-CD thioether were obtained by dissolving C_{60} in aqueous solutions of *γ*-CD thioethers and confirmed by using dynamic light scattering method. The formation of 1:2 complexes between C_{60} and host molecules was demonstrated by phase-solubility diagram and cross-sectional investigations. We also succeed to obtain stable aqueous dispersions of C_{60}, by employing the methods based on solvent exchange in presence of *γ*-CD thioethers. The results of this work provide a platform for further investigating the solubilization and dispersal of fullerene or its hydrophobic derivatives by using host molecules.

Keywords: cyclodextrin • C_{60} • solubilization • dispersion • solvent exchange

3.1 Introduction

Fullerene, the third carbon allotrope, is a classical engineered material with the potential application in biomedicine.[1-4] As the most representative among fullerenes, C_{60} has the shape of an icosahedron, in which every carbon atom is bound to three other adjacent atoms through sp^2 hybridization.[2]

C_{60} and its derivatives have been extensively investigated owing to their potential applications in many different fields both in pharmaceutical chemistry and material sciences.[5-9] C_{60} and its derivatives show enzymatic inhibition of the HIV-1 protease *in vitro*, can be used in photodynamic therapy, have a promising behavior as a neuroprotector, or have antiapoptotic or antibacterial

activity.[5,10]

Major negative aspects of C_{60} that hamper the applications of C_{60} in medicinal chemistry are the very poor solubility of C_{60} in polar solvents and the formation of aggregates in water (solubility 2.6–8.0 ng/L in water).[10-13] To overcome this problem, several approaches for transferring C_{60} into water have been developed, including chemical functionalization of C_{60}, solvent exchange, forming stable colloidal dispersions of C_{60}, and using water soluble supramolecular hosts as solubilizers.[2]

Chemical functionalization of C_{60}, which allows solubilization of C_{60} in water, will lead to a partial loss of its aromatic character. Solvent exchange has been the most common strategy to produce stable dispersion of C_{60} in water without any stabilizing agent. Scrivens *et al.* obtained an aqueous dispersion of C_{60} by dissolving C_{60} in benzene and diluted the solution sequentially with THF, acetone, and water.[14] Deguchi *et al.* obtained stable dispersions of C_{60} as fine clusters only using THF and water. Unfortunately, water suspension obtained by this method reached concentration of C_{60} of only around 10 μM.[13] These preparation methods were very simple and made it possible to evaluate the biological activities of unmodified fullerenes. However, the employment of highly toxic organic solvents such as benzene or toluene limited the application of solvent exchange method since for biological study or medical applications, these solvents should be eliminated from the preparation process.

The most successful strategy to carry the hydrophobic C_{60} into water was to use appropriate water-soluble supramolecular carriers which can form host–guest inclusion complexes such as calixarenes[15-17] and cyclodextrins (CDs).[18-20] Andersson *et al.* firstly reported that *γ*-CD formed a water-soluble 2:1 inclusion complex with C_{60} after reflux in water.[18] Although the cavities of *α*- and *β*-CD seemed to be too small to accommodate the large hydrophobic molecule C_{60}, water-soluble inclusion complexes formed by the smaller sized *α*- and *β*-CD with C_{60} was also reported through use of a mixed organic solution and subsequent addition of water after removal of the organic

solvents.[21-22] The introduction of organic solvents seemed to play an important role in the formation of water-soluble C_{60}–CD inclusion complexes.

However, due to the limited water solubilities of native CDs, the solubility enhancements of C_{60} reached by native CDs were generally low. It was proved that the modifications on the free hydroxyl groups of native CDs with appropriate function groups may greatly increase the ability of CDs to form soluble inclusion complexes with guest molecules.[23-26] Recently, we developed a new class of highly water-soluble per-6-deoxy-thioethers of *β*- and *γ*-CD (> 20% w/w), which showed exceptionally high binding constants and solubilization abilities for several aromatic molecules in water.[27-28]

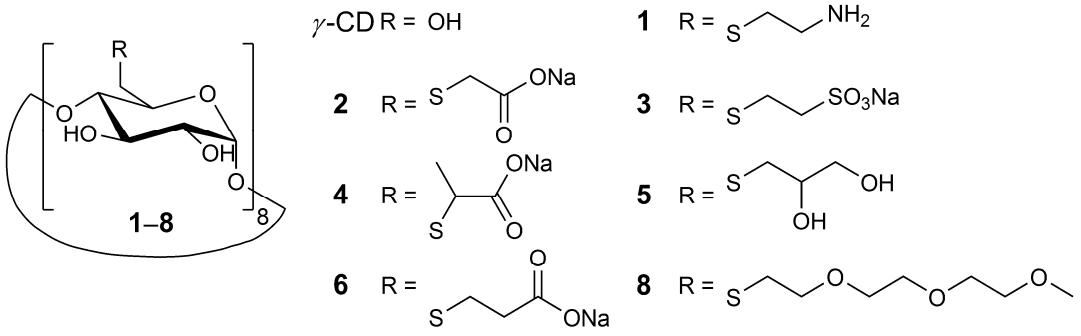

Scheme 3.1 Chemical structures of *γ*-CD and *γ*-CD thioether **1**–**8** used to solubilize C_{60} in water: **1**, octakis-[6-deoxy-6-(2-aminoethylsulfanyl)]-*γ*-CD; **2**, octakis-[6-deoxy-6-(2-sulfanyl acetic acid)]-*γ*-CD; **3**, octakis-[6-deoxy-6-(2-sulfanyl ethanesulfonic acid)]-*γ*-CD; **4**, octakis-[6-deoxy-6-(2-sulfanylpropanoic acid)]-*γ*-CD; **5**, Octakis- [6-deoxy-6-(3-sulfanylpropane-1,2-diol)]-*γ*-CD; **6**, octakis-[6-deoxy-6-(3-sulfanylpropanoic acid)]-*γ*-CD; **8**, octakis-[6-deoxy-6-(10-sulfanyl-2,5,8-trioxodecane)]-*γ*-CD.

In this work, solvent exchange method with different procedures in presence of *γ*-CD and *γ*-CD thioethers (CD **1**–**8**, **Scheme 3.1**) was applied in order to make stable dispersions of C_{60} in aqueous medium. We have also investigated the *γ*-CD thioether induced aqueous solubilization of C_{60} because we hope the derivatization of *γ*-CD into thioethers might also lead to a similar enhancement of the water solubilization abilities like observed for aromatic guests such as anthracene and acenaphthylene, and eventually caused the formation of a true

molecular solution of C_{60} in water.[27,29]

3.2 Results and Discussion

3.2.1 Dissolution Kinetic

Dissolution kinetics of complexation of C_{60} with *γ*-CD thioethers in an aqueous solution at 50°C was investigated in order to examine whether the dissolution process of C_{60} in water had reach the equilibrium state. The result of an isothermal kinetic investigation on the dissolution of C_{60} in water solution of CD **8** is representatively shown in **Figure 3.1**.

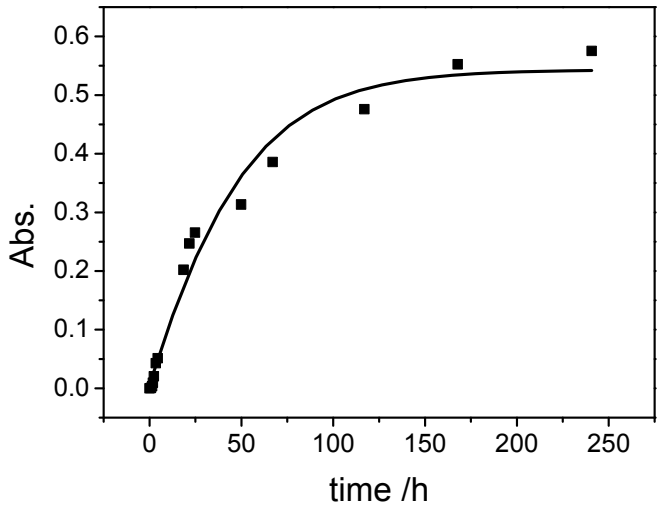

Figure 3.1 Isothermal kinetic run for the dissolution of C_{60} (represented by uv-vis absorbance intensity at 335 nm) in presence of 10 mM CD **8** in water. Curve represented best fit to first order kinetics by using k = 0.021 h^{-1}.

The gradually solubilization of solid C_{60} in presence of CD **8** were monitored by the increase in absorption intensity at 335 nm of C_{60}. The observed first-order kinetic dissolution pattern of C_{60} in water clearly demonstrated that the equilibrium of the inclusion system of CD **8** with C_{60} was approximately reached after stirring for 7 d, in other word, effective water solubilization of C_{60} can be obtained after stirring the CD–C_{60} system for 7 d.

3.2.2 Complexation Induced Aqueous Solubilization of C_{60}

C_{60} concentrations in CD solutions were estimated from uv-vis absorptions at the absorption maxima (λ_{max} = 335 nm). According to the method proposed by Higuchi and Connors,[30] phase-solubility diagrams of C_{60} in presence of *γ*-CD and *γ*-CD thioethers **1**–**8** in water were then obtained by plotting the observed concentration of dissolved C_{60} versus the concentration of CD in water.

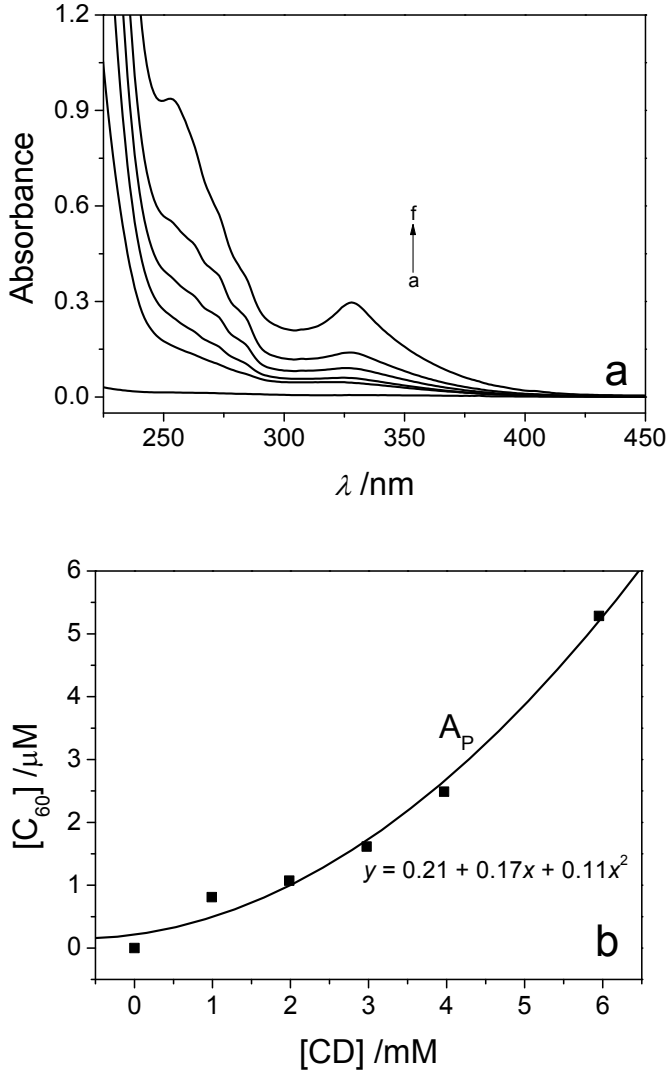

Figure 3.2 (A) Changes in the uv-vis absorption spectra of C_{60} in water containing increasing amounts of CD **3** from 0.0–6.0 mM, using quartz cell with 1 cm optical path at 298 K and (B) the corresponding phase solubility diagram of C_{60} in aqueous solution in presence of CD **3**.

The intermolecular complexation between γ-CD thioether and C_{60} was investigated using uv-vis spectroscopy. Typical uv-vis spectra of C_{60} in water solution of CD **3** with increasing concentrations and the resulting phase-solubility diagram are shown in **Figures 3.2a** and **2b**, respectively. As shown in **Figure 3.2a**, continuous changes in the absorption intensity were observed in the uv-vis spectra of C_{60} with the increasing concentration of CD **3** in water. The uv-vis spectrum of the inclusion complex exhibited absorptions quite similar to that of C_{60} in cyclohexane (λ_{max} = 330 nm).[31] The remarkably increased absorption intensity at approximately 335 nm was not attributable to the added γ-CD derivative **3** in water, since γ-CD derivative **3** did not absorb in this spectral region. Indeed, the intermolecular complexation, *i.e.*, the formation of the water-soluble inclusion complex between CD **3** and C_{60} was made responsible for the phenomenon.[32-33]

In **Figure 3.2b**, positive deviation of the phase-solubility diagram from linearity for C_{60} in presence of γ-CD derivative **3** in aqueous solution was observed at higher CD concentrations. As suggested by Higuchi and Connors, the observed A_P-type phase solubility diagram of CD **3**–C_{60} system indicated the formation of higher order inclusion complexes with respect to CD molecule,[30,34] *i.e.*, in this case, 2:1 stoichiometric ratio host–guest complex was plausibly formed between CD and C_{60}.

Equilibrium solubilities of C_{60} in presence of γ-CD and CD **1**–**8** for a fixed concentration of 6 mM after stirring for 7 d at room temperature (procedure **a**) in water are listed in **Table 3.1**. As shown in **Table 3.1**, the solubility of C_{60} in water was greatly increased in presence of γ-CD thioethers **1**–**8**. The obtained highest concentration of C_{60} in water was 14.9 μM in presence of CD **5**. In **Table 3.1** it was found that neutral γ-CD thioethers (for instance, CD **1**, **5**, and **8**) were able to solubilize C_{60} in water to much higher extends than charged γ-CD derivatives. Since γ-CD was expected to contact with C_{60} at its secondary sites, inhibition of the solubilization due to the modification of γ-CD at primary rim was not expected. Similar phenomena was also reported by Kuroda *et al.*[35]

Table 3.1 C_{60} concentration in 6.0 mM aqueous solutions of *γ*-CD and CD **1**–**8**.

Host	$[C_{60}]$ (μM)[a]			
	Procedure **a**	Procedure **b**	Procedure **c**	Procedure **d**
γ-CD	0.4	7.5	4.0	10.8
1	10.3	21.1	17.6	16.3
2	2.9	3.1	6.9	16.7
3	5.3	12.3	39.9	16.1
4	2.1	3.7	9.6	18.0
5	14.9	21.4	6.3	18.7
6	7.6	11.4	15.3	36.1
8	9.3	24.1	5.2	16.3

[a] Procedures employed for the solubilization of C_{60} by *γ*-CD and CD **1**–**8**. Procedure **a**: stir in water at r.t. for 7 d; procedure **b**: reflux in water/toluene for 3d, dissolve the resulting mixture in water after evaporation of the solvents; procedure **c**: stir in DMF/toluene at r.t. for 7d, dissolve the obtained inclusion complex in water after evaporation of the solvents; procedure **d**: stir in water/CS_2 at r.t. for 7d, dissolve the resulting inclusion complex in water after evaporation of the solvents.

For a further clarification of the stoichiometries of the inclusion complexes, cross-sectional calculations on C_{60} and *γ*-CD were employed. The cross-sectional area *A* of *γ*-CD cavity was obtained by analysis of the electron density map of *γ*-CD (from quantum mechanical calculations using Gaussian 03, E.01 software package[36]) with the program MolShape,[37] which was already useful for prediction of stoichiometries of polyrotaxanes.[38] The maximal and minimum inner diameters of *γ*-CD were determined to be 10.3 and 8.0 Å, respectively. Similarly, the maximal van der Waals diameter of C_{60} was calculated to be 13.0 Å. The calculation results indicated that both 2:1 and 1:1 inclusion complexes between *γ*-CD and C_{60} were believed to exist. The structure of the most stable complex was expected to be a 1:2 inclusion complex between C_{60} and *γ*-CD, in which two *γ*-CD molecules tightly interacted with C_{60} at their secondary rims (see **Figure 3.3**).[18-19,39] Molecular dynamics study also reported that the most stable host-guest complex stoichiometry was 2:1.[10]

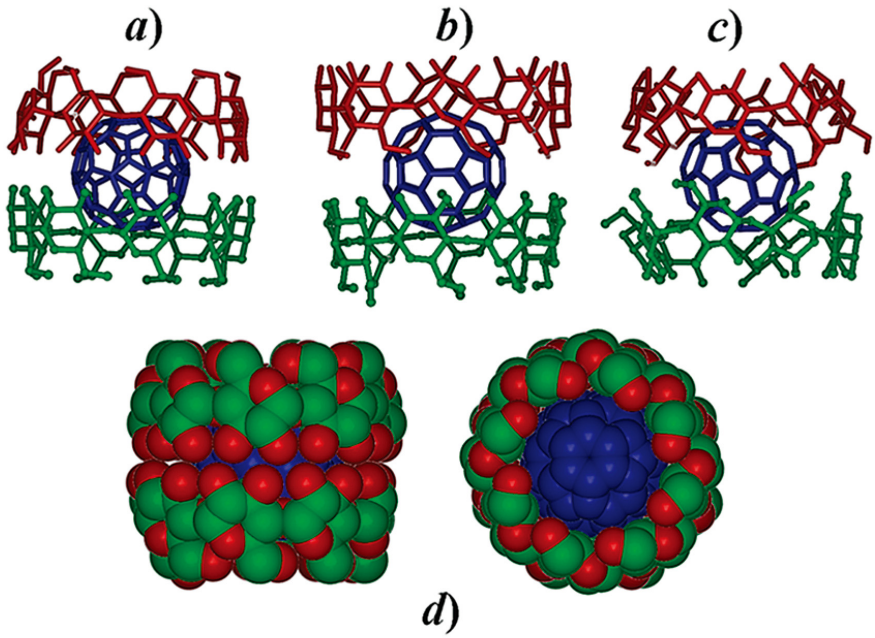

Figure 3.3 Possible inclusion complexes formed by γ-CD with C_{60} in the 2:1 stoichiometry *in vacuo*. The two CDs can interact through the secondary rims (part a, most stable geometry), through one primary and one secondary rim (part b), and through the two primary rims (part c). A space-filling model of the most stable geometry is displayed in part d, where the tight fitting of the whole complex is clearly seen.[10]

3.2.3 Solvent Exchange Investigation

Other than simply dissolve C_{60} in aqueous solutions of γ-CD and γ-CD thioethers (procedure **a**), other procedures **b**–**d** (see **Table 3.1** footnote for definitions) using solvent exchange method in presence of γ-CD or γ-CD thioethers were also applied in order to get a higher concentration of C_{60} in water. **Table 3.1** contains concentration data for all aqueous dispersions generated from procedures **b**–**d** in presence of 6.0 mM γ-CD thioethers.

As can be found from **Table 3.1**, the preparation by the method based on solvent exchange resulted in aqueous dispersions with higher concentrations than those produced by simple mixing C_{60} with γ-CD. Higher concentration of the prepared aqueous dispersion of C_{60} in water was achieved through the use of water/toluene or DMF/toluene or water/CS_2 solution and subsequent addi-

tion of water after removal of the organic solvent. By applying procedures **b**, **c**, and **d**, the acquired maxima concentrations of C_{60} in water were 24.1, 39.9, and 36.1 μM, respectively. Moreover, the reported concentrations of C_{60} aqueous dispersion in presence of *γ*-CD thioethers were higher than those reported for the aqueous dispersions prepared by using solvent exchange method when no host molecules were employed.

A vivid representative example for the significantly enhanced concentration of C_{60} in water by using solvent exchange method in presence of *γ*-CD and modified *γ*-CD **8** is shown in **Figure 3.4**. As shown in **Figure 3.4b**, by applying procedure b, a pale yellow aqueous dispersion with C_{60} concentration of 7.5 μM in presence of *γ*-CD was obtained. When *γ*-CD thioether **8** was used to dissolve C_{60}, a yellowish dispersion of C_{60} (24.1 μM) in water was obtained, shown in **Figure 3.4c**.

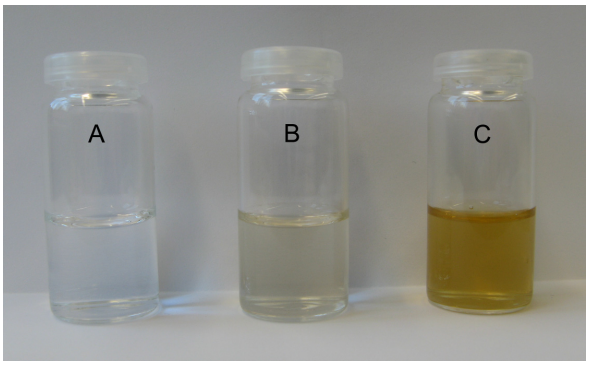

Figure 3.4 Water dispersions of C_{60} obtained according to procedure **b**. (a) blank sample, (b) in presence of *γ*-CD, and (c) in presence of *γ*-CD thioether **8**.

In other attempts to get high concentration of C_{60} in water, refluxing an aqueous solution of *γ*-CD and C_{60}[18] or stirring a methanolic solution of *γ*-CD and C_{60}[40] led to C_{60} dispersion with concentration of *ca*. 80 and 100 μM, respectively. Komatsu *et al.* reported that C_{60} would attained with *γ*-CD by using high-speed vibration milling, a aqueous dispersion with C_{60} concentration up to 1.4 mM can be thus obtained.[31] However, purple crystalline plates appeared after standing the dispersion for two weeks, and thus the concentration of C_{60}

obtained significantly decreased.

However, in present work, by applying procedure **b** in room temperature, C_{60} with concentration as high as 127 μM (with CD **8**, solution were obtained by dissolving the resulting inclusion complex in smallest amount of water) in water was obtained. Furthermore, the dispersions of C_{60} prepared were very stable, no precipitation was observed even after long storage in the dark at room temperature (at least 2 months after preparation). Absorption spectra of the C_{60} dispersion measured immediately after preparation and after storage for 1 month at room temperature in the dark were indistinguishable.

3.2.4 Dynamic Light Scattering Investigation

As discussed above, the concentration of C_{60} in water in presence of *γ*-CD thioether was continually increasing in the course of the approach to the thermodynamic equilibrium state. Since the equilibrium state had been reached, similar concentration of C_{60} in water should be obtained, no matter which kind of procedures was employed.

The observed big differences in the obtained concentration of C_{60} in water by using different procedures might attributed to: (a) the organic solvent molecules might cover a part of C_{60} which was not covered by *γ*-CD, thus avoided direct contact of non-polar C_{60} molecule with water molecules, and consequently increased the apparent concentration of C_{60} in water, or (b) water soluble aggregates were formed when employing the solvent exchange method, which might also significantly increase the apparent solubility of C_{60} in water.

Size distribution profile of the particles in the water solution of C_{60} was then investigated in order to investigate the problem. Dynamic light scattering (DLS) is a relatively fast method that can be used to determine the size distribution profile of small particles including proteins, polymers, micelles, carbohydrates, and nanoparticles.[41-42] It is known that clustering of C_{60} in the polar solvents is

often present.[5] Consequently, in order to evaluate whether a true molecular solution of C_{60} in presence of *γ*-CD thioethers in water was obtained, DLS investigations on the host–guest system were performed since DLS method was able to distinguish between a homogenous solution and an aggregated sample.[42-43]

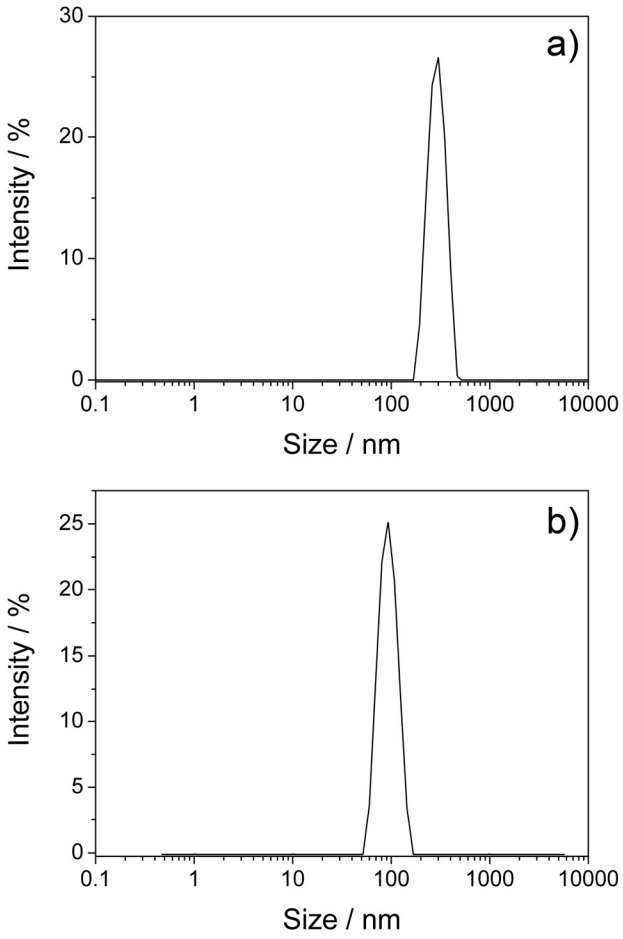

Figure 3.5 Size distribution of nC_{60} in water using dynamic light scattering (DLS): a) before centrifugation and b) after high-speed centrifugation (13,000 rpm) for 60 min. Count rate (kcps) for size distribution measurements of nC_{60} before and after centrifugation is 345.2 and 47.4, respectively.

Figure 3.5 shows representative particle size distribution of nC_{60} determined by using DLS (procedure for preparing nano-particle nC_{60}, see **Section 3.4.5**). As shown in **Figure 3.5a**, particle size distributions of nC_{60} aqueous dispersion in water before centrifugation comprised a sharp peak with a 300 nm average

diameter value was observed with a count rate of 345.2. However, after high-speed centrifugation (13,000 rpm) of the *n*C_{60} aqueous dispersion for 60 min, a different size distribution profile was observed. The average diameter value for the nano-particle and the count rate for the DLS measurement were determined to be 92 and 47.4 nm, respectively, as shown in **Figure 3.5b**. The remarkably decreased count rate observed for the centrifuged mixture clearly demonstrated the efficiency of high-speed centrifugation for removing *n*C_{60} nano-particle from water.

DLS investigation on the CD–C_{60} system in water revealed a completely different size distribution profile compared to that of *n*C_{60} nano-particle. The size characterizations of the inclusion system of C_{60} with 6 mM CD **5** (procedure **a**) in water before and after centrifugation are shown in **Figure 3.6**.

It was found from **Figure 3.6a** that before centrifugation, particle size distribution of C_{60} in presence of CD **5** comprised two peaks. The peak corresponding to smaller size was attributed to the CD–C_{60} inclusion complex. The peak with larger average size was assigned as the aggregates of C_{60} in water.

In **Figure 3.6b**, the inclusion complex with an average diameter of 0.84 nm was observed. After low-speed centrifugation (2,000 rpm) for 30 min, the peak which corresponded to C_{60} aggregates remained but with much lower intensity than that observed for the system before centrifugation.

In **Figure 3.6c**, after high-speed centrifugation (13,000 rpm) for 60 min, only a sharp peak with a 0.96 nm average diameter value was observed. As expect, the peak which corresponded to the remained C_{60} aggregates was completely disappeared after the high-speed centrifugation since high-speed centrifugation was proved to be an effective method to remove C_{60} aggregates from water. It was worth noted that only slight difference in the uv-vis absorption spectra of the freshly prepared water solution of CD–C_{60} inclusion system and the solution after high speed centrifugation for 60 min was observed (less than 8%, see **Figure 3.7**). The finding clearly proved the formation of a true mo-

lecular solution of C_{60} in water in presence of γ-CD thioethers (procedure **a**).

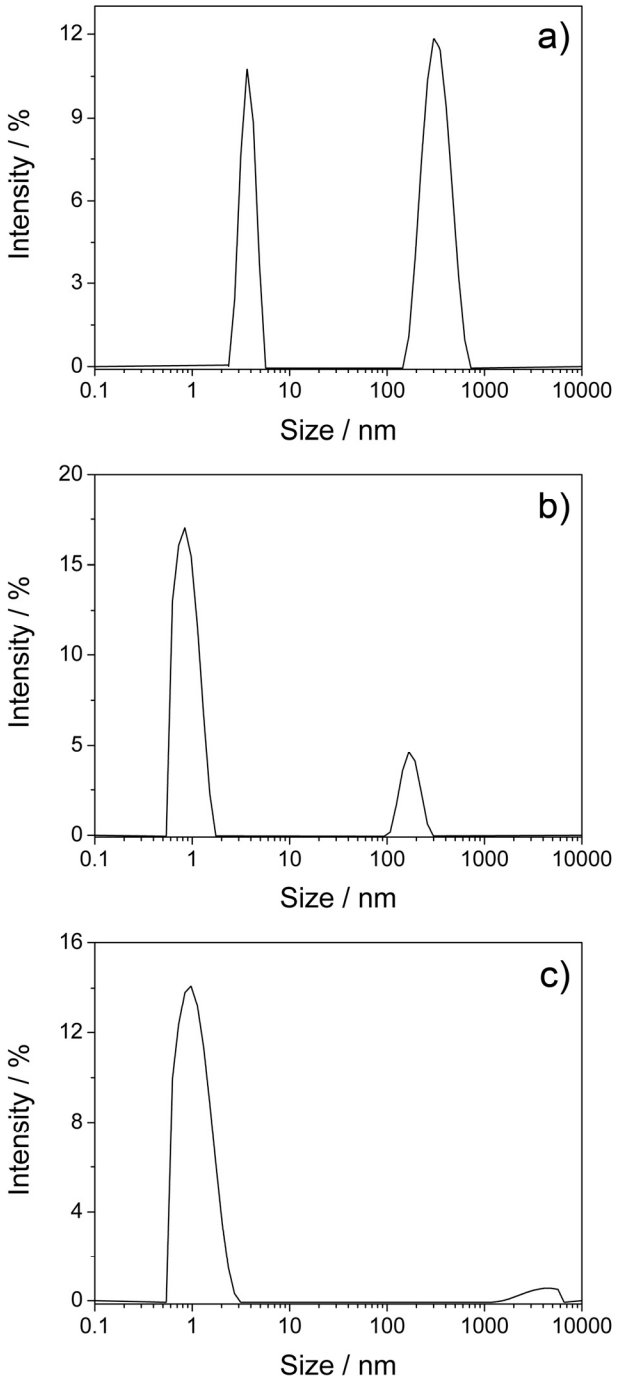

Figure 3.6 Size distribution of the inclusion complex of C_{60} with 6 mM CD **5** (procedure **a**) in water using DLS: a) before centrifugation, b) after low-speed centrifugation (2,000 rpm) for 30 min, and c) after high-speed centrifugation (13,000 rpm) for 60 min. Count rate (kcps) for the size distribution measurements of system a, b, and c were 343.5, 92.6, and 89.1, respectively.

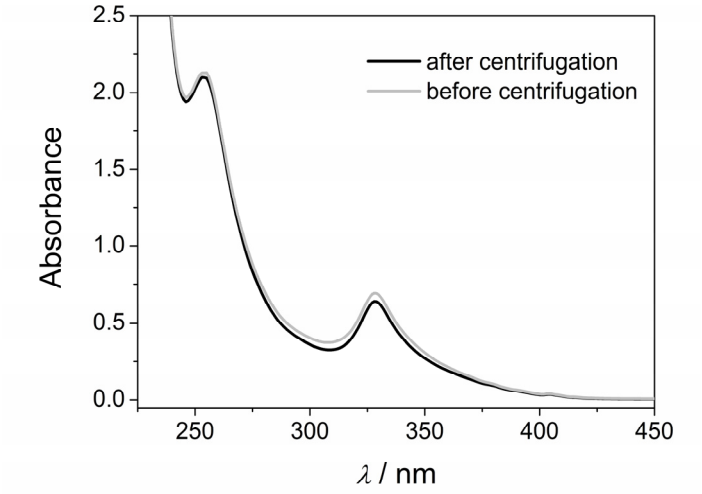

Figure 3.7 Uv-vis absorption spectra of C_{60} in presence of 6 mM CD **5** before and after high speed centrifugation (13,000 rpm) for 60 min.

3.3 Conclusion

In this current study, we used a series of highly water-soluble γ-CD thioethers as solubilizers and gained a true molecular solution of fullerene C_{60} in water with concentration as high as 14.9 μM in presence of 6.0 mM γ-CD thioether. The achieved high aqueous solubilization of C_{60} by complexation with γ-CD thioethers showed that modified CDs were more suitable host molecules for the solubilization of C_{60} than native γ-CD. The A_P -typed phase-solubility diagram and cross-sectional investigations suggested the formation of 1:2 complexes between C_{60} and γ-CD derivatives.

We also succeed to obtain stable aqueous dispersions of C_{60}, by employing the methods based on solvent exchange in presence of γ-CD thioethers. As the procedures employed in this work were easy to perform and use relatively less toxic organic solvents, the prepared dispersions seemed suitable for biological uses and medical applications, and would contribute significantly to the study of the dispersal of fullerenes. The dispersion could also be applied to other water-based applications such as those in food and cosmetics industry.[13] Moreover, in view of the remarkable solubilization abilities of synthesized γ-CD

thioethers to C_{60}, investigations on the separation of C_{60} from C_{60}/C_{70} mixtures are being considered.[44-45]

3.4 Experimental

3.4.1 General

Unless otherwise stated, all chemicals were used as received. Powdered fullerene C_{60} (> 99%) was purchased from Sigma Aldrich. Teflon syringe filters from Roth, Karlsruhe, Germany (0.22 µm) were used to remove insoluble material before ultraviolet-visible (uv-vis) spectrophotometric analysis. Uv-vis spectra of aqueous samples were performed on a Perkin Elmer Lambda 2 spectrometer (λ: 200–600 nm), using quartz cells with a 1 cm or 1 mm optical path at 298 K.

3.4.2 Synthetic Procedures

Hydrophilic thioethers **1**–**8** at all primary carbon atoms of γ-CD were synthesized from octakis-(6-deoxy-6-iodo)-γ-CD by nucleophilic displacement reaction with sulfur nucleophiles by using standard procedures described previously.[46]

3.4.3 Phase-Solubility Investigations

Solubility measurements of C_{60} in presence of γ- and γ-CD derivatives in water were carried out according to the method proposed by Higuchi and Connors.[30] In glass vials containing excess amounts of C_{60}, aqueous solutions of γ-CD or γ-CD derivatives with different concentrations were added. The vials were sealed, protected from light, and magnetically stirred at room temperature for 7 days. The solid residues were removed by filtration with syringe filter (0.22 µm). According to Lambert-Beer's law, the concentrations of C_{60} in pure water and in CDs solutions were determined from uv-vis extinctions at the

absorption maxima ($\log\varepsilon$ = 4.717, λ_{max} = 335 nm).[2]

3.4.4 Kinetic Measurement

A solution of C_{60} in chloroform (*ca*. 0.5mg/ml, 0.5 mL) was carefully evaporated in a 1 cm quartz cell under nitrogen flow. After addition of 3 mL of an aqueous solution containing necessary amount of γ-CD derivative, the cell was sealed, protected from light, and maintained at 50°C with gently shaking. The uv-vis spectra of the resultant solution at appropriate time intervals were directly measured.

3.4.5 Nanoparticle *n*C_{60} Preparation and Characterization

nC_{60} was prepared following a method similar to that reported by Deguchi *et al.*[13] Saturated solution of C_{60} in THF was prepared by adding a small amount of solid C_{60} into THF (20 mL) and stirred overnight under nitrogen atmosphere at room temperature. Excess solid was filtered off with a syringe filter. 500 mL of saturated C_{60}/THF solution was placed in a flask and an equal volume of water was added at a rate of *ca*. 25 mL/min under vigorous stirring. As soon as water was injected into a faint magenta solution of C_{60} in THF, a yellow and visually clear solution formed. The color remained the same even after THF removal. A rotary evaporator was used to remove THF using a stepwise evaporation approach. The start temperature was set at 30°C to reduce the loss of C_{60} in the vapor. When the mixture volume decreased to 500 mL, the temperature was increased at 1°C/min to 70°C and maintained at 70°C until the volume decreased to 250 mL, at which time an additional 250 mL volume of water was added. The last step was repeated once. The resulting *n*C_{60} concentration was *ca*. 12 mg/L and could be diluted by adding water or concentrated by evaporation as needed.

3.4.6 *n*C_{60} Size Measurement

Particle size distribution of the aqueous dispersions of the *n*C_{60} nanoparticles

was determined by dynamic light scattering (DLS) with a ZetaSizer Nano ZS (Malvern Instruments Ltd., Malvern, United Kingdom) from measured diffusion coefficient of the particles according to Stokes-Einstein equation.

Since the scattering intensity is proportional to the particle molecular weight, DLS is very sensitive to aggregation and large impurities, even at low concentrations. For all three methods, *n*C_{60} aqueous dispersions were filtered through a 0.22 μm filter prior to particle size measurements.

According to results from DLS measurements, nano-sized C_{60} cannot be removed completely from the sample after filtration with syringe filter.

3.5 References

[1] S. Bosi, T. Da Ros, G. Spalluto, M. Prato. Fullerene derivatives: An attractive tool for biological applications. *Eur. J. Med. Chem.* **2003**, *38*, 913-923.

[2] V. M. Torres, M. Posa, B. Srdjenovic, A. L. Simplicio. Solubilization of fullerene C_{60} in micellar solutions of different solubilizers. *Colloid Surface. B* **2011**, *82*, 46-53.

[3] M. Horie, K. Nishio, H. Kato, N. Shinohara, A. Nakamura, K. Fujita, S. Kinugasa, S. Endoh, K. Yamamoto, O. Yamamoto, E. Niki, Y. Yoshida, H. Iwahashi. In vitro evaluation of cellular responses induced by stable fullerene C_{60} medium dispersion. *J. Biochem.* **2010**, *148*, 289-298.

[4] S. Endoh, J. Maru, K. Uchida, K. Yamamoto, J. Nakanishi. Preparing samples for fullerene C_{60} hazard tests: Stable dispersion of fullerene crystals in water using a bead mill. *Adv. Powder Technol.* **2009**, *20*, 567-575.

[5] E. Nakamura, H. Isobe. Functionalized fullerenes in water. The first 10 years of their chemistry, biology, and nanoscience. *Acc. Chem. Res.* **2003**, *36*, 807-815.

[6] T. Da Ros, M. Prato. Medicinal chemistry with fullerenes and fullerene derivatives. *Chem. Commun.* **1999**, 663-669.

[7] A. W. Jensen, S. R. Wilson, D. I. Schuster. Biological applications of fullerenes. *Bioorgan. Med. Chem.* **1996**, *4*, 767-779.

[8] F. Diederich, M. Gomez-Lopez. Supramolecular fullerene chemistry. *Chem. Soc. Rev.* **1999**, *28*, 263-277.

[9] A. Hirsch, I. Lamparth, H. R. Karfunkel. Fullerene chemistry in 3 dimensions -

isolation of 7 regioisomeric bisadducts and chiral trisadducts of C_{60} and di(ethoxycarbonyl)methylene. *Angew. Chem. Int. Ed. Engl.* **1994**, *33*, 437-438.

[10] G. Raffaini, F. Ganazzoli. A molecular dynamics study of the inclusion complexes of C_{60} with some cyclodextrins. *J. Phys. Chem. B* **2010**, *114*, 7133-7139.

[11] K. N. Semenov, N. A. Charykov, V. A. Keskinov, A. K. Piartman, A. A. Blokhin, A. A. Kopyrin. Solubility of light fullerenes in organic solvents. *J. Chem. Eng. Data.* **2009**, *55*, 13-36.

[12] N. Sivaraman, R. Dhamodaran, I. Kaliappan, T. G. Srinivasan, P. R. V. Rao, C. K. Mathews. Solubility of C_{60} in organic solvents. *J. Org. Chem.* **1992**, *57*, 6077-6079.

[13] S. Deguchi, R. G. Alargova, K. Tsujii. Stable dispersions of fullerenes, C_{60} and C_{70}, in water. Preparation and characterization. *Langmuir* **2001**, *17*, 6013-6017.

[14] W. A. Scrivens, J. M. Tour, K. E. Creek, L. Pirisi. Synthesis of ^{14}C-labeled C_{60}, its suspension in water, and its uptake by human keratinocytes. *J. Am. Chem. Soc.* **1994**, *116*, 4517-4518.

[15] T. Haino, M. Yanase, C. Fukunaga, Y. Fukazawa. Fullerene encapsulation with calix[5]arenes. *Tetrahedron* **2006**, *62*, 2025-2035.

[16] A. Ikeda, S. Shinkai. Novel cavity design using calix n arene skeletons: Toward molecular recognition and metal binding. *Chem. Rev.* **1997**, *97*, 1713-1734.

[17] A. Ikeda, Y. Suzuki, M. Yoshimura, S. Shinkai. On the prerequisites for the formation of solution complexes from [60]fullerene and calix[n]arenes: A novel allosteric effect between [60]fullerene and metal cations in calix[n] aryl ester complexes. *Tetrahedron* **1998**, *54*, 2497-2508.

[18] T. Andersson, K. Nilsson, M. Sundahl, G. Westman, O. Wennerstrom. C_{60} embedded in γ-cyclodextrin - a water-soluble fullerene. *Chem. Commun.* **1992**, 604-606.

[19] Z. I. Yoshida, H. Takekuma, S. I. Takekuma, Y. Matsubara. Molecular recognition of C_{60} with γ-cyclodextrin. *Angew. Chem. Int. Ed. Engl.* **1994**, *33*, 1597-1599.

[20] Y. Liu, H. Wang, P. Liang, H. Y. Zhang. Water-soluble supramolecular fullerene assembly mediated by metallobridged β-cyclodextrins. *Angew. Chem. Int. Ed. Engl.* **2004**, *43*, 2690-2694.

[21] Y. Zhang, W. Liu, X. Gao, Y. L. Zhao, M. Zheng, F. F. Li, D. L. Ye. The first synthesis of a water-soluble α-cyclodextrin/C_{60} supramolecular complex using anionic C_{60} as a building block. *Tetrahedron Lett.* **2006**, *47*, 8571-8574.

[22] C. N. Murthy, K. E. Geckeler. The water-soluble β-cyclodextrin-[60]fullerene

complex. *Chem. Commun.* **2001**, 1194-1195.

[23] G. Wenz, T. Hofler. Synthesis of highly water-soluble cyclodextrin sulfonates by addition of hydrogen sulfite to cyclodextrin allyl ethers. *Carbohydr. Res.* **1999**, *322*, 153-165.

[24] T. Loftsson, M. Brewster. Pharmaceutical applications of cyclodextrins. 1. Drug solubilization and stabilization. *J. Pharm. Sci.* **1996**, *85*, 1017-1025.

[25] T. Loftsson, D. Hreinsdottir, M. Masson. Evaluation of cyclodextrin solubilization of drugs. *Int. J. Pharm.* **2005**, *302*, 18-28.

[26] V. Zia, R. A. Rajewski, V. J. Stella. Effect of cyclodextrin charge on complexation of neutral and charged substrates: Comparison of (SBE)(7M)-β-CD to HP-β-CD. *Pharm. Res.* **2001**, *18*, 667-673.

[27] G. Wenz, C. Strassnig, C. Thiele, A. Engelke, B. Morgenstern, K. Hegetschweiler. Recognition of ionic guests by ionic β-cyclodextrin derivatives. *Chem. Eur. J.* **2008**, *14*, 7202-7211.

[28] K. Kano, Y. Ishida, K. Kitagawa, M. Yasuda, M. Watanabe. Heat-capacity changes in host-guest complexation by Coulomb interactions in aqueous solution. *Chem. Asian J.* **2007**, *2*, 1305-1313.

[29] A. Steffen, C. Thiele, S. Tietze, C. Strassnig, A. Kamper, T. Lengauer, G. Wenz, J. Apostolakis. Improved cyclodextrin-based receptors for camptothecin by inverse virtual screening. *Chem. Eur. J.* **2007**, *13*, 6801-6809.

[30] T. Higuchi, K. Connors. Phase-solubility techniques. *Adv. Anal. Chem. Instrum.* **1965**, *4*, 117-212.

[31] K. Komatsu, K. Fujiwara, Y. Murata, T. Braun. Aqueous solubilization of crystalline fullerenes by supramolecular complexation with γ-cyclodextrin and sulfocalix 8 arene under mechanochemical high-speed vibration milling. *J. Chem. Soc., Perkin Trans. 1* **1999**, 2963-2966.

[32] Y. Rio, J.-F. Nierengarten. Water soluble supramolecular cyclotriveratrylene-[60]fullerene complexes with potential for biological applications. *Tetrahedron Lett.* **2002**, *43*, 4321-4324.

[33] T. Andersson, G. Westman, O. Wennerstrom, M. Sundahl. NMR and UV-VIS investigation of water-soluble fullerene-60-γ-cyclodextrin complex. *J. Chem. Soc., Perkin Trans. 2* **1994**, 1097-1101.

[34] R. Singh, H. H. Tonnesen, S. B. Vogensen, T. Loftsson, M. Masson. Studies of curcumin and curcuminoids. XXXVI. The stoichiometry and complexation constants of cyclodextrin complexes as determined by the phase-solubility

method and uv-vis titration. *J. Inclusion Phenom. Macrocyclic Chem.* **2010**, *66*, 335-348.

[35] Y. Kuroda, H. Nozawa, H. Ogoshi. Kinetic behaviors of solubilization of C_{60} into water by complexation with γ-cyclodextrin. *Chem. Lett.* **1995**, 47-48.

[36] M. J. Frisch, G. W. Trucks, H. B. Schlegel, G. E. Scuseria, M. A. Robb, J. R. Cheeseman, J. A. Montgomery, T. Vreven, K. N. Kudin, J. C. Burant, J. M. Millam, S. S. Iyengar, J. Tomasi, V. Barone, B. Mennucci, M. Cossi, G. Scalmani, N. Rega, G. A. Petersson, H. Nakatsuji, M. Hada, M. Ehara, K. Toyota, R. Fukuda, J. Hasegawa, M. Ishida, T. Nakajima, Y. Honda, O. Kitao, H. Nakai, M. Klene, X. Li, J. E. Knox, H. P. Hratchian, J. B. Cross, V. Bakken, C. Adamo, J. Jaramillo, R. Gomperts, R. E. Stratmann, O. Yazyev, A. J. Austin, R. Cammi, C. Pomelli, J. W. Ochterski, P. Y. Ayala, K. Morokuma, G. A. Voth, P. Salvador, J. J. Dannenberg, V. G. Zakrzewski, S. Dapprich, A. D. Daniels, M. C. Strain, O. Farkas, D. K. Malick, A. D. Rabuck, K. Raghavachari, J. B. Foresman, J. V. Ortiz, Q. Cui, A. G. Baboul, S. Clifford, J. Cioslowski, B. B. Stefanov, G. Liu, A. Liashenko, P. Piskorz, I. Komaromi, R. L. Martin, D. J. Fox, T. Keith, A. Laham, C. Y. Peng, A. Nanayakkara, M. Challacombe, P. M. W. Gill, B. Johnson, W. Chen, M. W. Wong, C. Gonzalez, J. A. Pople. Gaussian 03, revision E.01. **2004**.

[37] A. Müller, G. Wenz. Thickness recognition of bolaamphiphiles by α-cyclodextrin. *Chem. Eur. J.* **2007**, *13*, 2218-2223.

[38] G. Wenz, B. H. Han, A. Müller. Cyclodextrin rotaxanes and polyrotaxanes. *Chem. Rev.* **2006**, *106*, 782-817.

[39] T. Andersson, G. Westman, G. Stenhagen, M. Sundahl, O. Wennerstrom. A gas-phase container for C_{60} - a γ-cyclodextrin dimer. *Tetrahedron Lett.* **1995**, *36*, 597-600.

[40] K. I. Priyadarsini, H. Mohan, A. K. Tyagi, J. P. Mittal. Inclusion complex of γ-cyclodextrin-C_{60} - formation, characterization, and photophysical properties in aqueous-solutions. *J. Phys. Chem.* **1994**, *98*, 4756-4759.

[41] H. Ruf, Y. Georgalis, E. Grell. Dynamic laser-light scattering to determine size distributions of vesicles. *Method. Enzymol.* **1989**, *172*, 364-390.

[42] M. Alexander, D. G. Dalgleish. Dynamic light scattering techniques and their applications in food science. *Food Biophysics* **2006**, *1*, 2-13.

[43] W. Burchard. Static and dynamic light-scattering from branched polymers and bio-polymers. *Adv. Polym. Sci.* **1983**, *48*, 1-124.

[44] H. Eddaoudi, A. Deratani, S. Tingry, F. Sinan, P. Seta. Fullerene membrane transport mediated by γ-cyclodextrin immobilised in poly(vinyl alcohol) films. *Polym. Int.* **2003**, *52*, 1390-1395.

[45] N. Komatsu. Preferential precipitation of C_{70} over C_{60} with p-halohomooxacalix[3]arenes. *Org. Biomol. Chem.* **2003**, *1*, 204-209.

[46] H. M. Wang, G. Wenz. Solubilization of polycyclic aromatics in water by γ-cyclodextrin derivatives. *Chem. Asian J.* **2011**, *6*, 2390-2399.

4 Template-Induced Selective Photodimerization of Aromatics within *γ*-Cyclodextrin Thioethers in Aqueous Solution

Abstract: A series of hydrophilic *γ*-cyclodextrin (CD) thioethers, containing neutral and ionic side arms, were designed, synthesized, and selected as molecular receptor. *γ*-CD thioethers were selected to form water-soluble 1:2 CD–guest inclusion complexes, in which two guest molecules were held in close proximity within the CD cavity. High quantum yields of the photodimerization reactions of anthracene, *trans*-stilbene, acenaphthylene (**ACE**), and coumarin (**COU**) in presence of *γ*-CD thioethers were obtained when compared to those of the aromatic guests in host-free solutions. *γ*-CD thioether acted as a supramolecular catalytic nano-reaction vessel and facilitated the photodimerization of several aromatic guests. The orientation of two molecules of **ACE** when bound to the template led to the selective formation of the *trans* product upon irradiation in quantitative yield for the first time. Excitation of the 1:2 CD–guest inclusion complex of **COU** in aqueous solution resulted in an increased yield of *syn* head-to-head dimer. Other photoproducts of **COU** which typically produced in the absence of the template were remarkably suppressed by salting out effect.

Keywords: cyclodextrin • photodimerization • regioselectivity • acenaphthylene • coumarin • heavy-atom effect • salting out

4.1 Introduction

Photochemical reactions attract a lot of interests in synthetic chemistry since photo irradiation on the reactants often leads to products virtually inaccessible by thermal reactions because they proceed along the excited-state pathway.[1-2]

However, it is often difficult to predict and manipulate the outcome of photochemical transformations in homogeneous solutions because of the chaotic behavior of the reactant molecules.[1]

Optimizing the selectivity of photochemical reactions is one of the most demanding challenges since photochemical reactions generally tend to give more than one product.[3] The selectivity of chemical transformations is influenced and enhanced by the presence of a molecular flask, *i.e.*, a template molecule which includes the guest or guests, protects substrates from the surrounding environment and thus preorganizing them advantageously for a desired photochemical reaction.[4-5]

With the emphasis to use water as a reaction medium, various template molecules like cyclodextrins (CDs), calixarenes, and cucurbiturils have been explored as green media. These host molecules not only provide an environmentally friendly water soluble medium to perform photochemical transformations, but also offer a constrained environment that helps to manipulate reactive excited-states of organic molecules.[6-8]

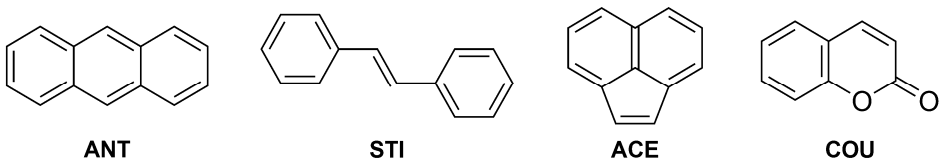

ANT **STI** **ACE** **COU**

Scheme 4.1 Chemical structures of selected aromatic guests: anthracene, **ANT**; *trans*-stilbene, **STI**; acenaphthylene, **ACE**; coumarin, **COU**.

We have investigated the binding and solubilization abilities of a series of highly water-soluble per-6-deoxy-thioethers of *β*- and *γ*-CD for several aromatic molecules in aqueous solution.[9-11] The water solubilities of the guests such like *trans*-stilbene (**STI**) and acenaphthylene (**ACE**) in presence of *γ*-CD thioethers were found to be ten times larger than the intrinsic water solubilities of these guests, and thus allowed the photodimerization of these aromatic guests in aqueous medium.[10]

γ-CD strongly attracted our attention since γ-CD had been proved to be effective in manipulating photodimerization reactions both in solution and in solid state.[1,12-13] Herein, we study the photodimerization of several aromatic guests (**Scheme 4.1**) within a series of highly water-soluble γ-CD thioethers (CD **1–8**, **Scheme 4.2**) in water because we reason that these γ-CD thioethers might be ideal hosts in which two guests can be bring into close proximity with a desirable orientation, thus lead to a better outcome and remarkable selectivity of the photodimerization reaction in aqueous solutions.

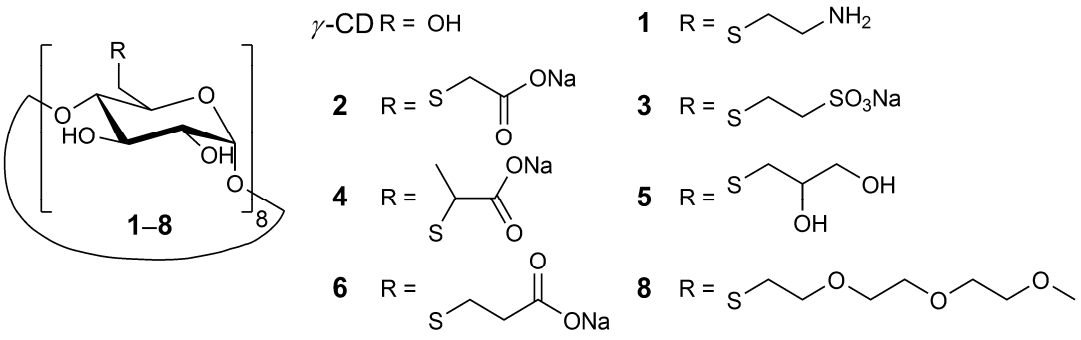

Scheme 4.2 Chemical structures of γ-CD and the synthetic γ-CD thioethers **1**–**8**.

In the present work, several aromatics of similar size: anthracene (**ANT**), **STI**, **ACE**, and coumarin (**COU**), were chosen as guests to study their photodimerization reactivities in presence of γ-CD thioethers.

The best studied photochemical reaction in a molecular flask is probably the photodimerization of anthracene derivatives.[1,8,14-18] We have reported on the influence of the ring size of CDs on the photochemical reactivity of a water-soluble **STI** derivatives.[5] However, to date only limited efforts have been made to systematically examine the quantum yields (Φ) of these photochemical reaction with and without the presence of CDs molecules. Therefore, in this work, we conduct a study on the effects of the presence of γ-CD thioethers on the quantum yield of the photodimerization reaction of these aromatic guests in aqueous medium.

The photochemical reactivities of **ACE** had been studied extensively in the past

few decades as **ACE** dimer can be easily characterized by NMR spectroscopy as the proton resonances of individual dimers were well established in literature.[19-22] Cowan *et al*. reported that the ratio of *cis* to *trans* depends on the nature of the excited state from which the reaction originates.[23-24] Photodimerization of **ACE** in presence of different host molecules were also reported.[19,25-27] However, as far as we are aware, the photodimerization of **ACE** in presence of CDs still lack of investigation, probably because of the low water solubility of the CD–**ACE** inclusion complex. In this regard we study the use of *γ*-CD thioethers to form a better soluble complex and to control the photochemical reactivity of **ACE** in aqueous medium under homogenous conditions for the first time.

COU and its derivatives have attracted considerable interest, in part because of their biological and photobiological importance.[20] Ramamurthy *et al*. reported the micellar pre-orientation effect in the photodimerization of coumarin derivatives.[28-30] Sivaguru *et al*. showed that CB[8] could be very effective in controlling photodimerization of both neutral and cationic coumarins.[21,31] In view of obtaining control over photoproduct selectivity of the photodimerization of **COU**, in this work we investigate whether the introduce of *γ*-CD thioether could promote such product amplification through the geometry or steric confinement of the supramolecular species.

4.2 Results and Discussion

4.2.1 Photodimerization of Anthracene and Stilbene

The quantum yields of photodimerization of **ANT** in presence of *γ*-CD thioether in aqueous solution are measured by potassium ferrioxalate actinometry and listed in **Table 4.1**. Published values for that of **ANT** derivatives in presence of CDs in water are available and also summarized in **Table 4.1**.

The quantum yield of **ANT** in water without the presence of any solubilizer is

not available due to its low intrinsic water solubility. As shown in **Table 4.1**, higher dimerization quantum yields can be achieved in 6.0 mM water solution of *γ*-CD thioether. The highest quantum yield for the photodimerization of **ANT** was determined to be 0.33 in presence of CD **4**.

Table 4.1 The inclusion effects on the quantum yield of the photodimerization of **ANT** and **ANT** derivatives.

Guest[a][b]	Host	Quantum Yield/%	Ref
2AC	none	5	[8]
	β-CD	20	[32]
	γ-CD	40	[32]
1AS	none	4	[32]
	β-CD	4	[32]
	γ-CD	40	[32]
2AS	none	5	[32]
	β-CD	30	[32]
	γ-CD	50	[32]
ANT	**1**	29	this work
	2	16	this work
	3	29	this work
	4	33	this work
	5	25	this work
	6	27	this work
	8	19	this work

[a] **2AC**, **1AS**, and **2AS** are short for 2-anthracenecarboxylate, 1-anthracenesulfonate, and 2-anthracenesulfonate, respectively. [b] The concentration of *γ*-CD thioether aqueous solution is 6.0 mM.

Increased quantum yields were also observed for the photodimerization of **ANT** derivatives. In presence of CDs in water, the photodimerization quantum yields of 2-anthracenecarboxylate, 1-anthracenesulfonate (**1AS**), and 2-anthracenesulfonate (**2AS**) remarkably increased up to 0.5 (**2AS** with *γ*-CD) with the exception of **1AS** with *β*-CD. [8,32] These observations clearly indicated that the existence of CDs would significantly influence the photochemical re-

activities of the guests which might mainly attributed to the intermolecular interactions between CDs and guest molecules.[33]

As reported by Lewis *et al*.,[34] the photodimerization quantum yield of 10 mM **STI** in benzene was determined to be less than 0.01. The quantum yield of **STI** dimerization was found to increase with the increasing concentration of **STI**. However, in the present work, though with low concentration of the reactant in water ([**STI**] < 0.07 mM), irradiation on the 1:2 CD–**STI** inclusion complexes in aqueous solution ultimately resulted in high quantum yields of the photodimerization. For instance, the quantum yields of the photodimerization of **STI** in presence of CD **8** in water were determined to be 0.13. In other word, the quantum yield of the **STI** photodimerization from the 1:2 inclusion complex was an order of magnitude greater than that in the absence of host molecule.

4.2.2 Stereoselective Photodimerization of Acenaphthylene

The solubilities in presence of *γ*-CD and *γ*-CD thioethers for a fixed host concentration of 6 mM as well as the intrinsic water solubilities of the guests, the occupancies of *γ*-CD cavities by **ACE** molecules are listed in **Table 4.2**.

The proved 1:2 stoichiometry of the CD–**ACE** inclusion complex in aqueous solution[10] by using fluorescence spectroscopy and quantum mechanical calculations and the gratefully enhanced water solubility of the resulting inclusion complex of **ACE** with *γ*-CD thioethers **3** and **6** (> 1 mM) allowed us to employ these *γ*-CD thioethers as molecular reaction vessels for the photodimerization of **ACE** and to conduct the photodimerization reactions in aqueous medium under homogenous conditions for the first time.

Quantum yields of the photodimerization reaction of **ACE** in presence of *γ*-CD thioethers **3** and **6** were determined to be 0.28 and 0.12, respectively. The measured quantum yield values from **ACE** inclusion complexes were significantly higher that that of free **ACE** in organic solvents such as toluene (0.05), ethanol (0.04), and methanol/water (20% v/v, 0.03).[35]

Table 4.2 Intrinsic water solubilities of **ACE** and equilibrium solubilities of **ACE** in 6.0 mM solutions of γ-CD and γ-CD thioether **1**–**8**, occupancies of **ACE** within the cavity of γ-CD thioethers.

Host	**ACE**[a]	
	Solubility [μM]	Occupancies [%]
water	67	–
γ-CD	103	n.d.
1	898	13
2	729	11
3	1703	28
4	693	11
5	278	3.4
6	1280	21
8	162	2.5

[a] results taken from chapter 2.[10]

Irradiation of **ACE** in solution leads to two isomeric cyclobutane dimers (*cis* and *trans*, **Scheme 4.3**) and the relative yields of the dimers strongly depend on the reaction medium used.[26,36] The distribution of the *cis* and *trans* dimers of **ACE** upon irradiation as revealed by the peak integrals of ^{1}H NMR spectra, as well as the photodimerization of **ACE** in various media, are comprised in **Table 4.3**.

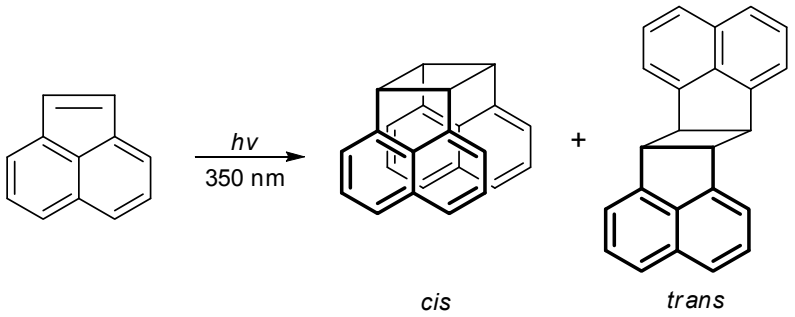

Scheme 4.3 Photodimerization of **ACE**.

A representative ^{1}H-NMR spectrum of the photodimerization product of **ACE** in presence of CD **3** is shown in **Figure 4.1**. As can be found from the NMR spectrum, nearly quantitative conversion of **ACE** into photodimer was ob-

served after the irradiation on the aqueous solution of **ACE** inclusion complex with γ-CD thioether for 12 h at room temperature.

Cyclobutane proton signals (for *cis* photodimer, δ_H = 4.84; for *trans* photodimer, δ_H = 4.10) were monitored for analyzing the isomeric ratios.[19,36] As shown in **Figure 4.1**, only the proton signal at δ_H = 4.10 from the cyclobutane moiety in *trans* configuration was observed in the ^{1}H NMR spectra. Similar phenomenon was also observed for that of **ACE** in presence of CD **6**. These finding showed that excitation of the 1:2 host–guest inclusion complexes of γ-CD thioethers **3** and **6** in aqueous solution only resulted in *trans* cubane-like photocyclodimer in quantitative yields. Several reasons were proposed to be responsible for this extraordinary stereoselectivie photodimerization of **ACE**.

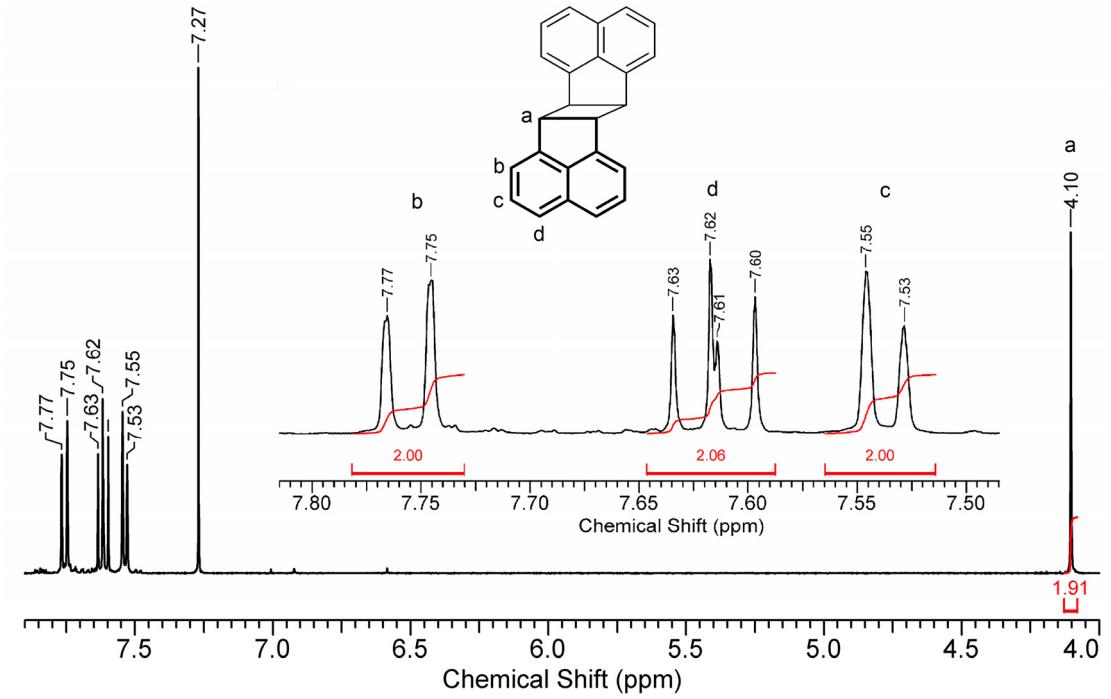

Figure 4.1 ^{1}H-NMR spectrum of the photodimerization product of **ACE** in presence of γ-CD thioether **3** in $CDCl_3$.

First, it is proved that the photodimerization of **ACE** is significantly concentration dependent.[24,37] The *trans* dimer was the dominant species in dilute solutions and the *cis* dimer in concentrated solutions. Previous reports also showed that the ratio of *cis*/*trans* dimers formed was a linear function of **ACE** concen-

tration in solution.[24] In this work, very dilute water solutions of **ACE** (1.7 and 1.3 mM in presence of CD **3** and **6**, respectively) were used for the photodimerization. Accordingly, it was quite reasonable for **ACE** to only form *trans* dimers under such reaction condition.

Table 4.3 Product distribution in the photodimerization of **ACE** in various media.

Reaction Medium	*cis* [%]	*trans* [%]	Ref
Water/suspension	40	60	[25]
Benzene[a]	63	37	[24]
Cyclohexane[a]	79	21	[24]
Octa acid[b]	> 99	0	[25]
Ethyl iodide/cyclohexane[c]	20	80	[23]
Hydrogelators/NaCl solution[d]	8	92	[19]
3	**0**	**100**	this work
6	**0**	**100**	this work

[a] **ACE** concentrations in cyclohexane and benzene were 0.22 M. [b] **ACE** concentration 1 mM. For definition of octa acid, please see ref.[25]. [c] 5% (mol/mol) ethyl iodide in cyclohexane, **ACE** concentration 0.67 M. [d] in 0.5 M NaCl water solution, **ACE** concentration approximately 4 μM.

Second, the product distributions of the **ACE** photodimerization in solution are crucially dependent on the nature of the excited state from which the reaction originates.[23-26] Extensive studies have revealed a mechanism involving two reactive species, a singlet excimer and an **ACE** triplet. The singlet excimer forms only *cis* dimer and the triplet state yields both *cis* and *trans* dimers with the latter being the major product.[26] In this work, the significantly increased yield of **ACE** *trans* dimer and reduced amount of *cis* dimer can be attributed to the existence of heavy atoms in the reaction medium.[23,38] The so-called "heavy-atom effect" accelerates the rate of spin-orbit coupling interaction between states of different spin multiplicity by the presence of an atom of high atomic number, which is either part of, or external to, the excited molecular entity.[39] γ-CD derivatives possessing heavy atoms in the primary rim, sulfur atoms in the present work, can exert the external heavy atom effects on the

ACE aromatic dimer incorporated into its cavity.[38] The reactive singlet state of intersystem crosses to the triplet state or exciplex (indicated by the florescence spectra of the inclusion complex at long wavelength), resulted in the greatly increased *trans* dimer yield.[26] The situation of triplet states had also been largely improved because of the shield of CD thioethers from collisions by the solute impurities, e.g., oxygen, in the inclusion complexes. [4]

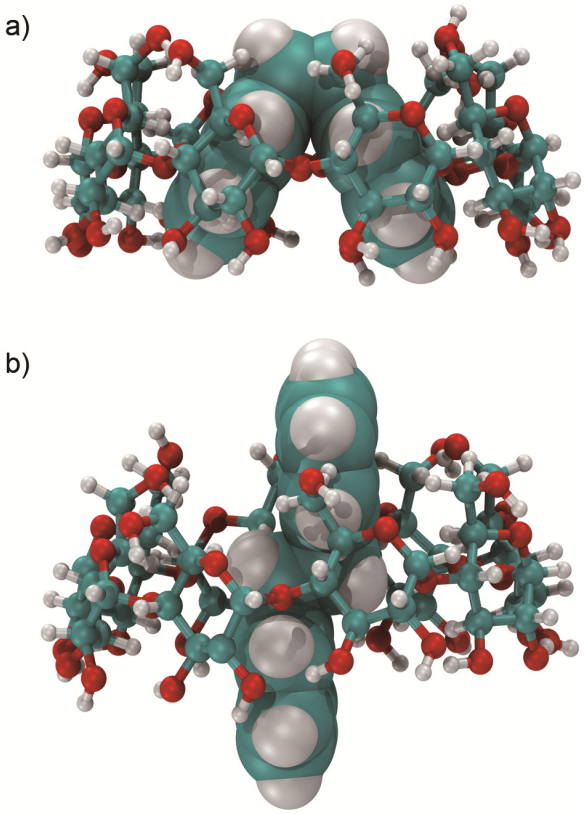

Scheme 4.4 Schematic drawing depicting the **ACE** photodimer in *γ*-CD: side view of the *cis* photodimer a) and the *trans* photodimer b) in *γ*-CD cavity. The rendering was performed with VMD 1.8.7.[40]

It was clear that the environment of **ACE** during irradiation was a major factor in the selectivity of the photodimerization reaction. The cavity of *γ*-CD derivatives accommodated two molecules of **ACE** and aligned them in a geometry that was favorable for the occurrence of photodimerization. As described above, the irradiation of **ACE** in solution resulted in the formation of two cubane-like photodimers, *cis* and *trans*. The size of *trans* photodimer from its

crystal structure suggested that it could tightly fit in the cavity of γ-CD thioether, while that of *cis* dimer was too large to be accommodated into the cavity of γ-CD thioethers for their formation, which also appeared to play an important role in determining the selectivity of the photodimerization.[36] Moreover, according to the results of quantum mechanical calculation (see chapter 2), the preferential anti-parallel alignment of **ACE** dimer in the CD cavity also favored the formation of the *trans* dimer. A schematic drawing which depicting the fitting between **ACE** photodimer in γ-CD cavity is shown in **Scheme 4.4**.

4.2.3 Photodimerization of Coumarin

Photoirradiation of **COU** can potentially lead to four cycloaddition products: *syn* Head-to-Tail (*syn*-HT), *syn*-HH, *anti*-HT, and *anti*-HH photodimers, as shown in **Scheme 4.5**.[20,41] The ratio of **COU** photoproducts can significantly be altered through control of the reaction conditions such as solvent choice and use of host molecules.[21,42]

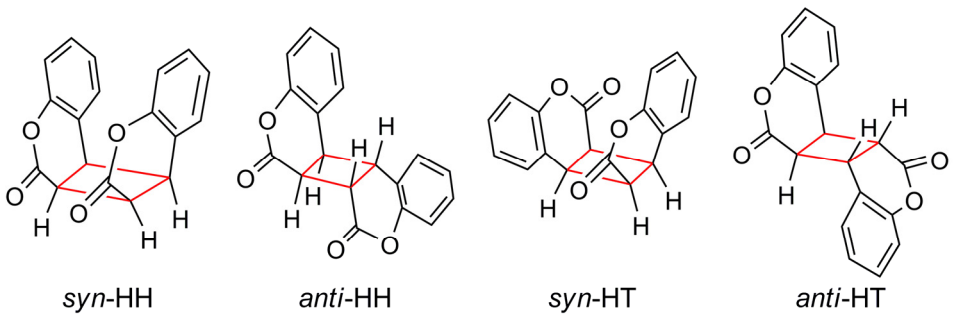

Scheme 4.5 Structures of **COU** photodimers *syn*-HH, *anti*-HH, *syn*-HT, and *anti*-HT.

The structures of four cycloaddition products of **COU** are shown in **Scheme 4.5**. Configurational assignment of the **COU** dimers was based on ^{1}H-NMR spectral data. The chemical shifts and coupling patterns of the cyclobutyl protons of the four coumarin photodimers have been reported elsewhere.[20] **Table 4.4** summarizes the photo product distributions of **COU** in water and in inclusion complexes with γ- and γ-CD thioethers **1**–**8**.

Table 4.4 Product distribution (fractions of photodimers *syn*-HT, *syn*-HH, *anti*-HT, and *anti*-HH) in the photodimerization of **COU** in water and in 6.0 mM solutions of *γ*- and *γ*-CD thioethers **1**–**8**.

Host	Product distribution [%][a,b]			
	syn-HH	*anti*-HH	*syn*-HT	*syn/anti*
water	59.0	9.3	31.7	9.8
γ-CD	52.0	17.4	30.6	4.7
1	57.8	15.7	26.5	5.4
2	86.8	4.8	8.4	19.8
3	56.9	16.5	26.6	5.1
4	71.3	7.8	20.9	11.8
5	71.8	9.1	19.1	10.0
6	71.1	10.4	18.5	8.6
8	50.9	10.5	38.6	8.5

[a] Fractions of dimers based on relative integration of ^{1}H-NMR signals of the photoproducts. The assignments of the dimer were based on previous literature reports. [b] Photoreactions of **COU** in water were carried out under condition similar to that of **COU** in presence of *γ*-CD thioethers.

It makes us able to ascertain the effect of *γ*-CD thioethers on the photodimerization process by performing photodimerization of **COU** in different reaction conditions. Direct irradiation on **COU** in water produced a mixture of *syn*-HH as major product and *anti*-HH as minor product. More specifically, in case of **COU** in water, the photo irradiation resulted in 59.0% *syn*-HH, 9.3% *anti*-HH, and 31.7% *syn*-HT with a *syn*/*anti* dimer distribution of 9.8, as shown in **Table 4.4**.

With regard to **COU** complex with native *γ*-CD, no obvious difference in product distribution was observed when compared to that in host-free solution. Conversely, the yields of *syn*-HH dimer of the photodimerization of **COU** in presence of *γ*-CD thioethers were significantly increased, especially for CD **2**, **4**, **5**, and **6**. For instance, under identical reaction conditions, in presence of CD **2**, *syn*-HH dimer of **COU** was obtained in high yield (86.9%).

From these results, it was clear that the environment of the **COU** in which they

were irradiated was a major factor in both the efficiency and stereochemistry of their photodimerizations.[21,42] The resulting changes in selectivity can be attributed entirely to templating effect of γ-CD thioethers.

Intrinsic water solubility of **COU** (1.7 g/L, 12 mM) at room temperature is quite high, which causes the low extent of complexation between **COU** and γ-CD thioethers. This might be the reason why we only reach 86.9% *syn*-HH selectivity of the photodimerization reaction. Accordingly, lowering the aqueous solubility of **COU** by addition of salt, *i.e.*, the salting-out effect seemed to be a plausible way to enhance the reaction selectivity of *syn*-HH dimer.

Salting-out of **COU** in aqueous salt solutions containing 6 mM CD **2** was performed (Na_2SO_4 concentration: 0, 0.5, 1.0, and 1.5 M). The apparent percentage of complexed **COU** in the total amount of **COU** in CD solution was calculated from the absorbance differences between **COU** in Na_2SO_4 solution and **COU** in the mixed solution of Na_2SO_4 and γ-CD thioether **2**. The effect of salting-out on the product distribution and the apparent percentage of the complexed guest at different concentration of Na_2SO_4 are summarized and listed in **Table 4.5**.

Table 4.5 Salting-out effect on the product distribution in the photodimerization reaction of **COU** in 6.0 mM solution of γ-CD thioether **2**.

$[Na_2SO_4]$ [M]	complexed **COU** [%][a]	Product distribution [%]		
		syn-HH	*anti*-HH	*syn*-HT
0.0	17	86.8	4.8	8.4
0.5	36	88.7	0	11.3
1.0	47	94.9	0	5.1
1.5	68	96.6	0	3.4

[a] Although the complexed amount of **COU** can only be calculated exactly from the binding constant of **COU** in γ-CD thioether at various salt concentrations by using isothermal titration calorimetry, the apparent percentage of the complexed **COU** was approximately estimated from the absorbance differences between **COU** in Na_2SO_4 solution and **COU** in the mixed solution of Na_2SO_4 and γ-CD thioether **2**.

As shown in **Table 4.5**, the apparent percentage of the complexed guest linearly increased with the increasing concentration of Na_2SO_4 in the water solution of CD **2**. In 1.5 M Na_2SO_4 (nearly saturated solution), as high as 68% of **COU** molecules were complexed with host molecules, which meant that the photodimerization reaction of **COU** outside the cavity of CD **2** could be greatly suppressed. Accordingly, high selectivity of **COU** photodimerization can be achieved because of the templating effect of CD on the formation of *syn*-HH dimer.

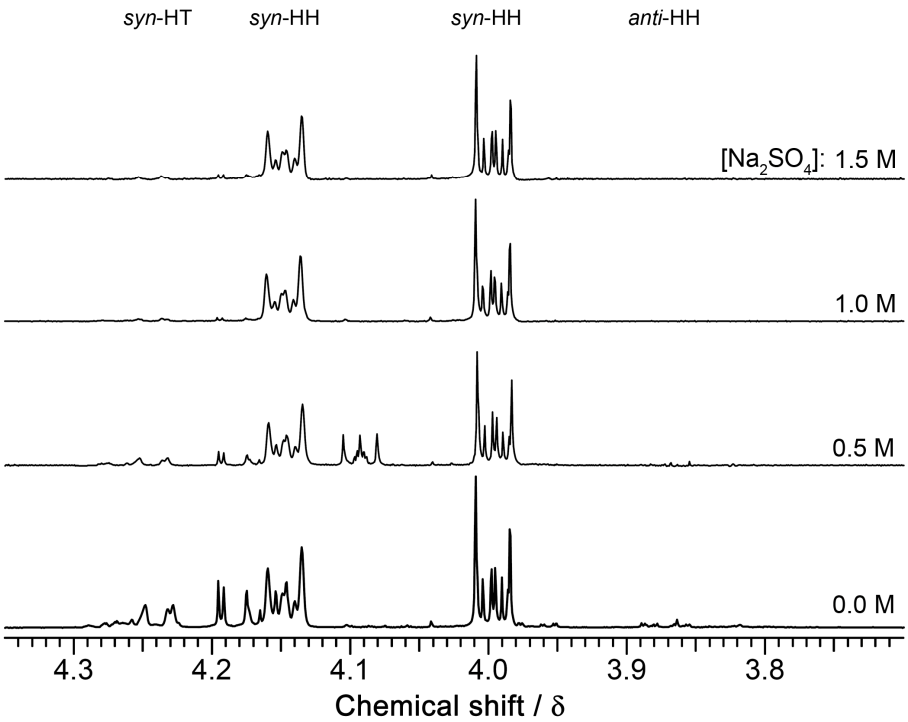

Figure 4.2 Cyclobutyl proton resonances of photodimers formed upon irradiation of **COU** at various concentrations of Na_2SO_4 in presence of γ-CD thioether **2**.

Figure 4.2 highlighted the NMR spectra of the photodimers formed upon irradiation of **COU** at various concentrations of Na_2SO_4 in CD **2** water solution. In **Figure 4.2**, it was clearly observed that without salt in solution, three **COU** dimers were produced simultaneously. In 0.5 M Na_2SO_4 solution, *anti*-HH dimer formed in trace amount after irradiation. The percentage of *syn*-HH dimer (88.7%) in all three products only slightly increased compared to that of

COU in CD **2** solution. In concentrated salt solutions (1.0 M), no proton signal of **COU** *anti*-HH dimer was observed. The formation of the *syn*-HT dimer was also found to be significantly suppressed (< 5.1%). In presence of CD **2** and 1.5 M Na_2SO_4, photodimerization reaction of **COU** was found to be efficient with the *syn*-HH photodimer since *syn*-HH dimer was observed as the nearly exclusive photoproduct (96.6%).

The greatly changed product distributions of **COU** indicated, approximately, the dimerization efficiency and stereoselectivity inside the cavity of *γ*-CD thioether **2**. Since *anti* dimers were not observed upon employing 6 mM CD **2** and high concentration of Na_2SO_4 (> 1.0 M), it was reasonable to assume that the photodimerization likely occurs within the CD cavity. Employing other *γ*-CD thioethers resulted in both *syn* (major) and *anti* (minor) dimers, which might suggested a competitive dimerization both inside and outside the cavity.

It is known that in nonpolar solvents nonreactive self-quenching widely suppresses the formation of **COU** dimers. In polar solvents, the dominant products are *syn*- and *anti*-HH isomers. The *syn*-HH is formed in a singlet-state reaction and *anti*-HH is derived mainly from triplet-state dimerization. Trace amounts of the *anti*-HT dimer possibly formed *via* a triplet diradical intermediate.[20,22,31,43]

The lifetime of the triplet-state of the complexed guest **COU** is proved to be significantly shorter than that of the free guest.[22] Moreover, *anti*-HH products are formed exclusively at low concentrations because of the long lifetime of the triplet state, which allows encounters with ground-state **COU** molecules. Consequently, the suppressed formation of *anti*-HH dimer in concentrated salt solution in presence of CD **2** seemed to be a reasonable result since the high fraction of the complexed guest was significantly due to the salting-out effect.

Quantum mechanical calculations of the structures and interaction energies ΔE of four **COU** dimers were performed using the Gaussian 03 software package.[39] The aromatic dimers were fully optimized at the MP2/6-31G* level without any symmetry restriction during the computation. The interaction energies ΔE of

syn-HH, *anti*-HH, *syn*-HT, and *anti*-HT dimers of **COU** were –32.9, –29.3, –24.0, and –22.5 kJ·mol^{-1}, respectively. The ΔE value of **COU** dimer with *syn*-HH orientation was found to be significantly more negative than that of the dimer with other orientation. This result can be attributed to the relative good overlap between two **COU** molecules in the *syn*-HH dimer than that of the dimer with other orientations.[44] The formation of the inclusion complex of *γ*-CD thioether with *syn*-HH orientation of **COU** dimer appeared to be more probable, because of the more negative ΔE value of the *syn*-HH **COU** dimer and the good space filling of the *γ*-CD cavity.

The quantum yield of the photodimerization of **COU** in water, in 1.5 M Na_2SO_4 solution, in presence of *γ*-CD thioether **2**, and in CD **2** with 1.5 M Na_2SO_4 were also measured in this work. The dimerization quantum yield of COU in water, in Na_2SO_4 water solution, in CD **2**, and in the mixed solution of CD **2** and Na_2SO_4 were 0.11, 0.06, 0.19, and 0.66, respectively. The significantly increased quantum yield value of the photodimerization of **COU** in the mixed solution of CD **2** and Na_2SO_4 were attributed to the increased percentage of the complexed guest by *γ*-CD thioether **2.**

4.3 Conclusion

By employing *γ*-CD thioether as host molecules in the present work, high quantum yields of the photodimerization reactions of **ANT**, **STI**, **ACE**, and **COU** in aqueous medium were obtained when compared to those of the aromatic guests in host-free solutions.

Previously **ACE** photodimerization had been conducted in a number of confined and ordered media. Selectivity of the *trans* dimer of **ACE** obtained in most media was lower than that observed within the cavity of *γ*-CD thioethers **3** and **6**. Quantitative yield of *trans* dimer of **ACE** upon irradiation was achieved for the first time. Selectivity and enhanced reactivity during direct excitation was attributed to the ability of the nano-reaction vessels to localize and pre-

orient the reactant. Heavy atom effect was also supposed to play an important role in the selective photodimerization reaction of **ACE**.

Remarkable selectivity of *syn*-HH dimer obtained in the case of **COU** dimerization in presence of γ-CD thioethers especially for CD **2**, **4**, **5**, and **6** (> 70%), revealed that the non-covalent interactions between the CD cavity and **COU** molecule in water were likely responsible in determining photoproduct distribution during the dimerization process. This work also showed that in concentrated salt solution and in presence of CD **2**, *syn*-HH adduct was exclusively formed upon irradiation as a result of restricted motion of the guest molecules within CD cavity.

Our findings have opened up the possibility of employing γ-CD thioethers as catalytic and green nano-reaction vessels for phototransformations in aqueous medium. This catalyst afforded complete conversions of **ACE** into *trans* **ACE** photodimer upon irradiation in an aqueous solution at room temperature. The productivity and the catalytic activity of γ-CD thioether for the photodimerization of **ACE** under scale-up conditions are being estimated.

4.4 Experimental Section

4.4.1 General

Guest **ANT**, **STI**, **ACE**, and **COU** were purchased from Sigma Aldrich. Potassium ferrioxalte and 1,10-phenanthroline were obtained from Sigma Aldrich. Unless otherwise stated, all chemicals were used as received. γ-CD was donated by Wacker and dried *in vacuo* at 100°C overnight before use. The synthesized γ-CD thioethers were purified by nanofiltration (molecular weight cut-off 1000 Da in Milli-Q water). Teflon syringe filters from Roth, Karlsruhe, Germany (0.22 µm) were used to remove insoluble material before uv-vis and fluorescence measurements as well as the photoirradiation experiments. Uv-vis spectra of aqueous samples were performed on a Perkin Elmer Lambda 2 spectrometer (λ:

200–600 nm), using quartz cells with a 1 cm or 1 mm optical path at 298 K. Fluorescence spectra were recorded in a JASCO spectrophotometer using quartz cells of 10.0 mm path at 298 K. All NMR spectra were recorded on a Bruker 400 MHz NMR Spectrometer at 298 K using the solvent peaks as internal references and coupling constants (*J*) were measured in Hz.

4.4.2 Synthetic Procedures

Hydrophilic thioethers **1–8** at all primary carbon atoms of *γ*-CD were synthesized from octakis-(6-deoxy-6-iodo)-*γ*-CD[9-10,45] by nucleophilic displacement reaction with sulfur nucleophiles, by using standard procedures described in chapter 2.[10]

4.4.3 Photoreaction Procedures

In glass vials containing excess amounts of guest molecules, aqueous solutions of native CDs or *γ*-CD thioethers (25 mL, 6.0 mM) were added. In order to evaluate the salting-out effect on the photo product distribution of **COU**, different amount of sodium sulfate was added to the vial to obtain the desired final salt concentration (Na_2SO_4 concentration: 0, 0.5, 1.0, and 1.5 M). Sample solutions were thoroughly degassed using sonication. The vials were tightly sealed, protected from light, and magnetically stirred at room temperature. After 72 h the resulting suspensions were filtered through syringe filter. The concentrations of the reactants in CDs solutions were determined from uv-vis extinctions at the absorption maxima.

The aqueous solutions of the inclusion complexes were taken in a 50 mL quartz round-bottomed flask and bubbled with nitrogen gas for 20 min with stirring before photo-irradiation. Photodimerization of the samples were carried out using a medium pressure mercury lamp (166.5 W, Heraeus Noblelight GmbH, UVB) as a light source. After irradiation for 12 h at room temperature under nitrogen atmosphere, the photo products formed were extracted with chloroform and then analyzed by ^{1}H NMR.[36] It was worth of note that, precipitate

was formed after irradiation on the aqueous solution of the inclusion complex of **ACE** with γ-CD thioether. This precipitate was assigned to the *trans* dimer of **ACE** according to the ^{1}H NMR measurement.

4.4.4 Quantum Yield Measurement

The definition of a quantum yield (Φ) for a photochemical reaction at a given irradiation wavelength (λ) can be expressed as Equation (1):[46-49]

$$\Phi = n_r / n_p \quad (1)$$

where n_r is the amount of the molecules that reacted and n_p is the amount of photons at the irradiation wavelength λ that were absorbed by the reactant.

n_r was determined as follows: Exactly 3 mL of the water solution of host-guest complex (γ-CD thioether concentration 6 mM) was added into a 1 cm depth quartz cuvette and exposed to UV light radiation from the monochromatic filter for different intervals of time. The irradiation wavelengths used for **ANT**, **STI**, **ACE**, and **COU** were 350, 300, 300, and 300 nm, respectively. The amount of the reacted guest molecules was determined by quantitative uv spectrophotometric analysis on the absorption of the guests before and after irradiation, using the reported extinction coefficients of the guest molecules (molar extinction coefficients in $L \cdot mol^{-1} \cdot cm^{-1}$ of **ANT**, **STI**, **ACE**, and **COU** are 7350, 18570, 9090, and 5650, respectively).[10]

n_p was determined as follows: The 6 mM actinometer (potassium ferrioxalte) solution was prepared by dissolving 2.95g of potassium ferrioxalte in *ca.* 800 mL of water. 100 mL of 0.5 M Sulfuric acid was then added, the solution diluted to 1 L and mixed. Cuvette containing 6 mM solution of actinometer in water was irradiated simultaneously during the determination of quantum yields of dimerization reactions in order to produce ferrous iron. The amount of the formed Fe^{2+} was determined by titration with phenanthroline. A 1 cm depth of 0.006 M solution of potassium ferrioxalte absorbs 99% or more of the light of the wavelength up to 390 nm. Accordingly, in present work, the absorption of

the incident light was complete.

During irradiation of the actinometer, the solution was stirred with a magnetic bar. After photoirradiation, an aliquot (0.2 mL) of the solution was pipetted into a 10 mL calibrated flask. 0.1 mL of buffer (600 mL of 1 M sodium acetate and 360 mL of 0.5 M sulfuric acid diluted to 1 L) and 0.2 mL of phenanthroline solution (0.1% w/v, so that the formed ferrous ion converted to its 1,10-phenanthroline complex) were added into the flask. Water was then added to made the solution with a volume of 10 mL. The absorbance of the resulting solution and the unexposed actinometer solution at 510 nm was measured. The quantity of ferrous iron was calculated from the absorbance difference using a extinction coefficient of 11050 $L \cdot mol^{-1} \cdot cm^{-1}$. Convert the quantity of ferrous iron to a radiation dose using the recommended quantum yield of potassium ferrioxalte at given wavelength ($\Phi_{(\text{potassium ferrioxalte})}$ = 1.24 at 313 nm).[49]

4.4.5 Molecular Modeling

A procedure identical to that described in chapter 2 was utilized.[10] The geometries of the orientational isomers of **COU** gas-phase dimer were fully optimized without any symmetry restriction at the MP2/6-31G* level of theory by using Gaussian 03 (E.01) software package.[39] Corrected interaction energies (ΔE) corresponding to the optimized aromatic dimers were evaluated by $\Delta E = E_{\text{dimer}} - 2E_{\text{monomer}}$ at the MP2/6-31G* level, where E_{dimer} and E_{monomer} are energies of the aromatic dimer and the monomer, respectively.[50]

4.5 References

[1] J. Svoboda, B. Konig. Templated photochemistry: Toward catalysts enhancing the efficiency and selectivity of photoreactions in homogeneous solutions. *Chem. Rev.* **2006**, *106*, 5413-5430.

[2] G. Schmidt. Photodimerization in the solid state. *Pure Appl. Chem.* **1971**, *27*, 647–678.

[3] B. Chen, S. F. Cheng, G. H. Liao, X. W. Li, L. P. Zhang, C. H. Tung, L. Z. Wu. Efficient and selective photodimerization of 2-naphthalenecarbonitrile mediated by cucurbit[8]uril in an aqueous solution. *Photochem. Photobiol. Sci.* **2011**, *10*, 1441-1444.

[4] A. Douhal, *Cyclodextrin materials photochemistry, photophysics and photobiology, Vol. 1*, Elsevier Science, **2006**.

[5] W. Herrmann, S. Wehrle, G. Wenz. Supramolecular control of the photochemistry of stilbenes by cyclodextrins. *Chem. Commun.* **1997**, 1709-1710.

[6] S. Y. Jon, Y. H. Ko, S. H. Park, H. J. Kim, K. Kim. A facile, stereoselective [2+2] photoreaction mediated by cucurbit[8]uril. *Chem. Commun.* **2001**, 1938-1939.

[7] L. Luo, G. H. Liao, X. L. Wu, L. Lei, C. H. Tung, L. Z. Wu. γ-cyclodextrin-directed enantioselective photocyclodimerization of methyl 3-methoxyl-2-naphthoate. *J. Org. Chem.* **2009**, *74*, 3506-3515.

[8] A. Nakamura, Y. Inoue. Supramolecular catalysis of the enantiodifferentiating [4+4] photocyclodimerization of 2-anthracenecarboxylate by γ-cyclodextrin. *J. Am. Chem. Soc.* **2003**, *125*, 966-972.

[9] A. Steffen, C. Thiele, S. Tietze, C. Strassnig, A. Kamper, T. Lengauer, G. Wenz, J. Apostolakis. Improved cyclodextrin-based receptors for camptothecin by inverse virtual screening. *Chem. Eur. J.* **2007**, *13*, 6801-6809.

[10] H. M. Wang, G. Wenz. Solubilization of polycyclic aromatics in water by γ-cyclodextrin derivatives. *Chem. Asian J.* **2011**, *6*, 2390-2399.

[11] G. Wenz, C. Strassnig, C. Thiele, A. Engelke, B. Morgenstern, K. Hegetschweiler. Recognition of ionic guests by ionic β-cyclodextrin derivatives. *Chem. Eur. J.* **2008**, *14*, 7202-7211.

[12] L. Luo, S. F. Cheng, B. Chen, C. H. Tung, L. Z. Wu. Stepwise photochemical-chiral delivery in γ-cyclodextrin-directed enantioselective photocyclodimerization of methyl 3-methoxyl-2-naphthoate in aqueous solution. *Langmuir* **2010**, *26*, 782-785.

[13] K. S. S. P. Rao, S. M. Hubig, J. N. Moorthy, J. K. Kochi. Stereoselective photodimerization of (*E*)-stilbenes in crystalline γ-cyclodextrin inclusion complexes. *J. Org. Chem.* **1999**, *64*, 8098-8104.

[14] T. Tamaki, Y. Kawanishi, T. Seki, M. Sakuragi. Triplet sensitization of anthracene photodimerization in γ-cyclodextrin. *J. Photoch. Photobio. A* **1992**, *65*, 313-320.

[15] C. Yang, G. Fukuhara, A. Nakamura, Y. Origane, K. Fujita, D. Q. Yuan, T. Mori, T. Wada, Y. Inoue. Enantiodifferentiating [4+4] photocyclodimerization of

2-anthracenecarboxylate catalyzed by 6(A),6(X)-diamino-6(A),6(X)-dideoxy-γ-cyclodextrins: Manipulation of product chirality by electrostatic interaction, temperature and solvent in supramolecular photochirogenesis. *J. Photoch. Photobio. A* **2005**, *173*, 375-383.

[16] A. Nakamura, Y. Inoue. Electrostatic manipulation of enantiodifferentiating photocyclodimerization of 2-anthracenecarboxylate within γ-cyclodextrin cavity through chemical modification. Inverted product distribution and enhanced enantioselectivity. *J. Am. Chem. Soc.* **2005**, *127*, 5338-5339.

[17] C. Yang, A. Nakamura, G. Fukuhara, Y. Origane, T. Mori, T. Wada, Y. Inoue. Pressure and temperature-controlled enantiodifferentiating [4+4] photocyclodimerization of 2-anthracenecarboxylate mediated by secondary face- and skeleton-modified γ-cyclodextrins. *J. Org. Chem.* **2006**, *71*, 3126-3136.

[18] H. Ikeda, T. Nihei, A. Ueno. Template-assisted stereoselective photocyclodimerization of 2-anthracenecarboxylic acid by bispyridinio-appended γ-cyclodextrin. *J. Org. Chem.* **2005**, *70*, 1237-1242.

[19] S. Bhat, U. Maitra. Hydrogels as reaction vessels: Acenaphthylene dimerization in hydrogels derived from bile acid analogues. *Molecules* **2007**, *12*, 2181-2189.

[20] X. L. Yu, D. Scheller, O. Rademacher, T. Wolff. Selectivity in the photodimerization of 6-alkylcoumarins. *J. Org. Chem.* **2003**, *68*, 7386-7399.

[21] N. Barooah, B. C. Pemberton, A. C. Johnson, J. Sivaguru. Photodimerization and complexation dynamics of coumarins in the presence of cucurbit[8]urils. *Photochem. Photobiol. Sci.* **2008**, *7*, 1473-1479.

[22] B. C. Pemberton, R. K. Singh, A. C. Johnson, S. Jockusch, J. P. Da Silva, A. Ugrinov, N. J. Turro, D. K. Srivastava, J. Sivaguru. Supramolecular photocatalysis: Insights into cucurbit[8]uril catalyzed photodimerization of 6-methylcoumarin. *Chem. Commun.* **2011**, *47*, 6323-6325.

[23] D. O. Cowan, R. L. E. Drisko. Photochemical reaction. 5. Photodimerization of acenaphthylene - heavy-atom solvent effects. *J. Am. Chem. Soc.* **1970**, *92*, 6281-6285.

[24] D. O. Cowan, R. L. E. Drisko. Photochimical reactions. 4. Photodimerization of acenaphthylene - mechanistic studies. *J. Am. Chem. Soc.* **1970**, *92*, 6286-6291.

[25] L. S. Kaanumalle, V. Ramamurthy. Photodimerization of acenaphthylene within a nanocapsule: Excited state lifetime dependent dimer selectivity. *Chem. Commun.* **2007**, 1062-1064.

[26] V. Ramamurthy, S. Arumugam, L. S. Kaanumalle. Alkali ion exchanged nafion as a confining medium for photochemical reactions. *Photochem. Photobiol.* **2006**, *82*,

139-145.

[27] S. Karthikeyan, V. Ramamurthy. Self-assembled coordination cage as a reaction vessel: Triplet sensitized [2+2] photodimerization of acenaphthylene, and [4+4] photodimerization of 9-anthraldehyde. *Tetrahedron Lett.* **2005**, *46*, 4495-4498.

[28] K. Muthuramu, V. Ramamurthy. Selectivity in chemical-reactions in micellar media - photodimerization of substituted coumarins in micelles. *Indian J. Chem., Sect B* **1984**, *23*, 502-508.

[29] K. Muthuramu, N. Ramnath, V. Ramamurthy. Photo-dimerization of coumarins in micelles - limitations of alignment effect. *J. Org. Chem.* **1983**, *48*, 1872-1876.

[30] K. Muthuramu, V. Ramamurthy. Photo-dimerization of coumarin in aqueous and micellar media. *J. Org. Chem.* **1982**, *47*, 3976-3979.

[31] N. Barooah, B. C. Pemberton, J. Sivaguru. Manipulating photochemical reactivity of coumarins within cucurbituril nanocavities. *Org. Lett.* **2008**, *10*, 3339-3342.

[32] T. Tamaki, T. Kokubu, K. Ichimura. Regioselective and stereoselective photodimerization of anthracene-derivatives included by cyclodextrins. *Tetrahedron* **1987**, *43*, 1485-1494.

[33] T. Wolff, N. Muller, G. Vonbunau. Regioselective photo-dimerization of 9-methylanthracene in homogeneous and micellar solutions. *J. Photochem.* **1983**, *22*, 61-70.

[34] F. D. Lewis, D. E. Johnson. Self-quenching and dimerization of singlet trans-stilbene. *J. Photochem.* **1977**, *7*, 421-423.

[35] R. Livingston, K. S. Wei. Reversible photochemical dimerization of acenaphthylene. I. Reaction in liquid solutions. *J. Phys. Chem.* **1967**, *71*, 541-&.

[36] R. C. Santos, C. E. S. Bernardes, H. P. Diogo, A. F. M. Piedade, J. N. C. Lopes, M. E. M. da Piedade. Energetics of the thermal dimerization of acenaphthylene to heptacyclene. *J. Phys. Chem. A* **2006**, *110*, 2299-2307.

[37] Livingst.R, K. S. Wei. Reversible photochemical dimerization of acenaphthylene. I. Reaction in liquid solutions. *J. Phys. Chem.* **1967**, *71*, 541-547.

[38] S. Hamai, T. Kudou. External heavy atom effects of 6-deoxy-6-iodo-α-cyclodextrin on the room-temperature phosphorescence of 6-bromo-2-naphthol and 3-bromoquinoline in aqueous solutions. *J. Photoch. Photobio. A* **1998**, *113*, 135-140.

[39] M. J. Frisch, G. W. Trucks, H. B. Schlegel, G. E. Scuseria, M. A. Robb, J. R. Cheeseman, J. A. Montgomery, T. Vreven, K. N. Kudin, J. C. Burant, J. M. Millam, S.

S. Iyengar, J. Tomasi, V. Barone, B. Mennucci, M. Cossi, G. Scalmani, N. Rega, G. A. Petersson, H. Nakatsuji, M. Hada, M. Ehara, K. Toyota, R. Fukuda, J. Hasegawa, M. Ishida, T. Nakajima, Y. Honda, O. Kitao, H. Nakai, M. Klene, X. Li, J. E. Knox, H. P. Hratchian, J. B. Cross, V. Bakken, C. Adamo, J. Jaramillo, R. Gomperts, R. E. Stratmann, O. Yazyev, A. J. Austin, R. Cammi, C. Pomelli, J. W. Ochterski, P. Y. Ayala, K. Morokuma, G. A. Voth, P. Salvador, J. J. Dannenberg, V. G. Zakrzewski, S. Dapprich, A. D. Daniels, M. C. Strain, O. Farkas, D. K. Malick, A. D. Rabuck, K. Raghavachari, J. B. Foresman, J. V. Ortiz, Q. Cui, A. G. Baboul, S. Clifford, J. Cioslowski, B. B. Stefanov, G. Liu, A. Liashenko, P. Piskorz, I. Komaromi, R. L. Martin, D. J. Fox, T. Keith, A. Laham, C. Y. Peng, A. Nanayakkara, M. Challacombe, P. M. W. Gill, B. Johnson, W. Chen, M. W. Wong, C. Gonzalez, J. A. Pople. Gaussian 03, revision E.01. **2004**.

[40] W. Humphrey, A. Dalke, K. Schulten. VMD: Visual molecular dynamics. *J. Mol. Graph.* **1996**, *14*, 33-38.

[41] W. G. Skene, E. Couzigne, J. M. Lehn. Supramolecular control of the template-induced selective photodimerization of 4-methyl-7-O-hexylcoumarin. *Chem. Eur. J.* **2003**, *9*, 5560-5566.

[42] J. N. Moorthy, K. Venkatesan, R. G. Weiss. Photodimerization of coumarins in solid cyclodextrin inclusion complexes. *J. Org. Chem.* **1992**, *57*, 3292-3297.

[43] B. C. Pemberton, N. Barooah, D. K. Srivatsava, J. Sivaguru. Supramolecular photocatalysis by confinement-photodimerization of coumarins within cucurbit[8]urils. *Chem. Commun.* **2010**, *46*, 225-227.

[44] K. Guckian, B. Schweitzer, X. Rex, C. Sheils, D. Tahmassebi, E. Kool. Factors contributing to aromatic stacking in water: Evaluation in the context of DNA. *J. Am. Chem. Soc.* **2000**, *122*, 2213-2222.

[45] P. R. Ashton, R. Koniger, J. F. Stoddart, D. Alker, V. D. Harding. Amino acid derivatives of β-cyclodextrin. *J. Org. Chem.* **1996**, *61*, 903-908.

[46] J. Tonne, H. Prinzbach, J. Michl. Double actinometry for rigorous evaluation of quantum yields of clean photoreversible photochemical reactions. *Photochem. Photobiol. Sci.* **2002**, *1*, 105-110.

[47] L. Z. Sun, J. R. Bolton. Determination of the quantum yield for the photochemical generation of hydroxyl radicals in TiO2 suspensions. *J. Phys. Chem.* **1996**, *100*, 4127-4134.

[48] D. N. Harpp, C. Heitner. Photodimerization of thianaphthene 1,1-dioxide - mechanism. *J. Am. Chem. Soc.* **1972**, *94*, 8179-8184.

[49] C. G. Hatchard, C. A. Parker. A new sensitive chemical actinometer. 2. Potassium ferrioxalate as a standard chemical actinometer. *Proc. R. Soc. A* **1956**, *235*,

518-536.

[50] S. F. Boys, F. Bernardi. Calculation of small molecular interactions by differences of separate total energies - some procedures with reduced errors. *Mol. Phys.* **1970**, *19*, 553-566.

5 Appendix

5.1 Abbreviations

A	cross-sectional area
Å	Angstrom, 10^{-10} m
Ac_2O	Acetic anhydride
A_{max}	maximum cross-sectional areas
br	broad signal (NMR spectroscopy)
ca.	Latin *Circa*, meaning "approximately"
CDs	Cyclodextrins
[CD]	Concentration of cyclodextrin in water
$CDCl_3$	Deuterochloroform
CH_3Cl	Chloroform
d	day
d	doublet (NMR spectroscopy)
d	diameter
DLS	Dynamic light scattering
DMF	*N*, *N*'-Dimethylformamide
DMSO	Dimethyl sulfoxide
DMSO-d_6	Hexadeuterodimethyl sulfoxide
δ	Chemical shift
$\Delta\delta$	Chemical shift change
D_2O	Deuterium oxide
ε	extinction coefficient, $L \cdot mol^{-1} \cdot cm^{-1}$
ESI-MS	Electrospray ionisation mass spectrometry
et al.	Latin *et alii,* meaning "and others"
EtOAc	Ethyl acetate
EtOH	Ethanol
Et_2O	Diethyl ether

Φ	Quantum yield
g	gram
h	hour
HP-	Hydroxypropyl ($CH_2CH(OH)CH_3$)
i.e.	Latin *id est*, meaning “that is; in other words”
λ	wavelength
L	liter
m	multiplet (NMR spectroscopy)
min	minute
M	molar ($mol \cdot L^{-1}$)
Me	Methyl
MeOH	Methanol
NaOMe	Sodium methoxide
NMR	Nuclear magnetic resonance
NEt_3	Triethylamine
ppm	Parts per million
PPh_3	Triphenylphosphin
p-TSA	p-Toluenesulphonic acid monohydrate
ROESY	Rotating-frame Overhauser spectroscopy (NMR spectroscopy)
r.p.m	revolutions per minute
r.t.	room temperature
s	singlet (NMR spectroscopy)
t	triplet (NMR spectroscopy)
TMS	Tetramethylsilane (NMR standard)
THF	Tetrahydrofuran
UV/Vis	Ultraviolet-visible spectroscopy

5.2 List of Figures

5.3 List of Schemes

5.4 List of Tables

Acknowledgements

I would like to gratefully and sincerely thank Prof. Dr. Gerhard Wenz for his guidance, understanding, and patience during my graduate studies at Universität des Saarlandes. His kindness, help, stimulating suggestions, and constant encouragements helped me in all the time of research for and writing of this dissertation.

I am very thankful to Prof. Dr. Gerhard Wenz and Lisa Becker for the correction of the early version of this thesis. Thanks are also due to Zhong Ren for his kindly translating the summary from English into German, to Yong Pang and Dr. Melanie Schnabel for their corrections of the German.

My special appreciation goes to all of my colleagues from the research group: Jennifer Ax, Lisa Becker, Dr. Prajaktar Dandekar, Michael Hahn, Daniela Hausen, Dr. Masayuki Hirosue, Manuel Keil, Andreas Lippach, Lisa Markenstein, Dr. Christoph Michel, Dr. Melanie Schnabel, Dr. Thomas Stauner, Dr. Thomas Stöhr, Christian Teuchert, Dr. Carolin Thiele and Sebastian Witti. I really enjoy the time with them. I have learned many from them as well.

Thanks also goes out to those who provided me with a lot of technical supports, including: Blandine Boßmann, Annegret Engelke, Jutta Ganz, Dr. Matthias Großer, Ronny Heisel, Devid Hero, Thomas Scherer and Tanja Seibert. Many thanks also to our secretaries Ms. Gerti Radünz and Ms. Petra Thinnes.

I must also acknowledge Dagmar Auerbach, Prof. Dr. Gregor Jung, and Christian Spies, for their assistance in fluorescence spectroscopy measurements and helpful discussions. I would like to extend my thanks to Dr. Yi Dong and Prof. Dr. Michael Springborg from Saarland University for helpful discussions concerning molecular modeling.

I also owe my sincere gratitude to my closest friends Jia Nan Ma, Yong Pang,

Xiang Jun Pang, Li Xing, Yan Nan Zang and Jian Guo Zhao, who gave me their help and time in listening to me and played essential roles in helping me work out my problems.

My special thanks would also goes to my beloved parents for their loving considerations and great confidence in me all through these years. Especially, I would like to give my special thanks to my fiancée Wen Hui Liu whose patient love enabled me to complete this work.

Finally, financial supports from Universität des Saarlandes and China Scholarship Council are gratefully acknowledged.

Hai Ming Wang

Saarbrücken

23 April 2012

Hosts Used in the Present Work

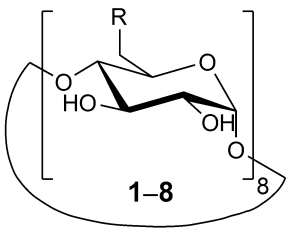

No.	R
1	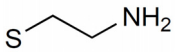
2	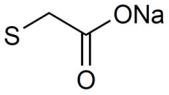
3	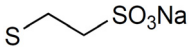
4	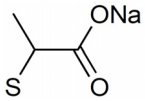
5	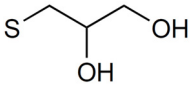
6	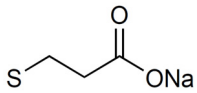
7	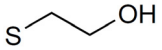
8